

Recommendations for the Formulation of Grazing in Marine Biogeochemical and Ecosystem Models

Tyler Rohr^{1,1,1}, Anthony Richardson^{2,2,2}, Andrew Lenton^{3,3,3}, and Elizabeth Shadwick^{1,1,1}

¹Australian Antarctic Partnership Program, Hobart, TAS, Australia

²Commonwealth Scientific and Industrial Research Organisation (CSIRO) Oceans and Atmosphere, BioSciences Precinct (QBP), St Lucia, Queensland, Australia

³Commonwealth Scientific and Industrial Research Organisation (CSIRO) Oceans and Atmosphere, Hobart, TAS, Australia

November 30, 2022

Abstract

For nearly a century, the functional response curves, which describe how predation rates vary with prey density, have been a mainstay of ecological modelling. While originally derived to describe terrestrial interactions, they have been adopted to characterize aquatic systems in marine biogeochemical, size-spectrum, and population models. However, marine ecological modellers disagree over the qualitative shape of the curve (e.g. Type II vs. III), whether its parameters should be mechanistically or empirically defined (e.g. disk vs. Michaelis-Menten scheme), and the most representative value of those parameters. As a case study, we focus on marine biogeochemical models, providing a comprehensive theoretical, empirical, and numerical road-map for interpreting, formulating, and parameterizing the functional response when used to prescribe zooplankton specific grazing rates on a single prey source. After providing a detailed derivation of each of the canonical functional response types explicitly for aquatic systems, we review the literature describing their parameterization. Empirical estimates of each parameter vary by over three orders of magnitude across 10 orders of magnitude in zooplankton size. However, the strength and direction of the allometric relationship between each parameter and size differs depending on the range of sizes being considered. In models, which must represent the mean state of different functional groups, size spectra or in many cases the entire ocean's zooplankton population, the range of parameter values is smaller, but still varies by two to three orders of magnitude. Next, we conduct a suite of 0-D NPZ simulations to isolate the sensitivity of phytoplankton population size and stability to the grazing formulation. We find that the disk parameterizations scheme is much less sensitive to its parameterization than the Michaelis-Menten scheme, and quantify the range of parameters over which the Type II response, long known to have destabilizing properties, introduces dynamic instabilities. Finally, we use a simple theoretical model to show how the mean apparent functional response, averaged across sufficient sub-grid scale heterogeneity diverges from the local response. Collectively, we recommend using a type II disk response for models with smaller scales and finer resolutions but suggest that a type III Michaelis-Menten response may do a better job of capturing the complexity of all processes being averaged across in larger scale and coarser resolution modal, not just local consumption and capture rates. While we focus specifically on the grazing formulation in marine biogeochemical models, we believe these recommendations are robust across a much broader range of ecosystem models.

Recommendations for the Formulation of Grazing in Marine Biogeochemical and Ecosystem Models

Tyler Rohr¹, Anthony J. Richardson^{2,3}, Andrew Lenton^{4,5}, Elizabeth
Shadwick^{1,4,5}

¹Australian Antarctic Partnership Program, Hobart, TAS, Australia

²School of Mathematics and Physics, The University of Queensland, St Lucia, Queensland, Australia

³Commonwealth Scientific and Industrial Research Organisation (CSIRO) Oceans and Atmosphere,

BioSciences Precinct (QBP), St Lucia, Queensland, Australia

⁴Commonwealth Scientific and Industrial Research Organisation (CSIRO) Oceans and Atmosphere,

Hobart, TAS, Australia

⁵Centre for Southern Hemisphere Oceans Research, Hobart, TAS, Australia

Key Points:

- We review the derivation of the functional response equations, unified across all common response types and parameter schemes, which should benefit a range of marine models.
- Zooplankton grazing parameter values vary by 3 to 4 orders of magnitude with inconsistent allometric relationships, both in models and experiments.
- The apparent mean functional response, averaged across sufficient sub-grid scale heterogeneity, begins to resemble the shape and parameter sensitivity of a type III Michaelis-Menten response even when a local type II disk response is prescribed.
- We recommend a type II disk response in smaller scale, finer resolution models but a type III Michaelis-Menten response in larger scale, coarser resolution models.
- We recommend considering a wide range of $K_{1/2}$ values, particularly low ones.

Corresponding author: Tyler Rohr, tyler.rohr@csiro.au

Abstract

For nearly a century, functional response curves, which describe how predation rates vary with prey density, have been a mainstay of ecological modelling. While originally derived to describe terrestrial interactions, they have been adopted to characterize aquatic systems in marine biogeochemical, size-spectrum, and population models. However, marine ecological modellers disagree over the qualitative shape of the curve (e.g. Type II vs. III), whether its parameters should be mechanistically or empirically defined (e.g. disk vs. Michaelis-Menten scheme), and the most representative value of those parameters. As a case study, we focus on marine biogeochemical models, providing a comprehensive theoretical, empirical, and numerical road-map for interpreting, formulating, and parameterizing the functional response when used to prescribe zooplankton specific grazing rates on a single prey source. After providing a detailed derivation of each of the canonical functional response types explicitly for aquatic systems, we review the literature describing their parameterization. Empirical estimates of each parameter vary by over three orders of magnitude across 10 orders of magnitude in zooplankton size. However, the strength and direction of the allometric relationship between each parameter and size differs depending on the range of sizes considered. In models, which must represent the mean state of different functional groups, size spectra or in many cases the entire zooplankton community, the range of parameter values is smaller, but still varies by two to three orders of magnitude. Next, we conduct a suite of 0-D NPZ simulations to isolate the sensitivity of phytoplankton population size and stability to the grazing formulation. We find that the disk parameterizations scheme is less sensitive to its parameterization than the Michaelis-Menten scheme, and quantify the range of parameters over which the Type II response, long known to have destabilizing properties, introduces dynamic instabilities. Finally, we use a simple theoretical model to show how the mean apparent functional response, averaged across sufficient sub-grid scale heterogeneity, diverges from the local response. Collectively, we recommend using a type II disk response for models with smaller scales and finer resolutions but suggest that a type III Michaelis-Menten response may do a better job of capturing the complexity of all processes being averaged across in larger-scale and coarser-resolution models, not just local consumption and capture rates. While we focus specifically on the grazing formulation in marine biogeochemical models, we believe these recommendations are robust across a much broader range of population and ecosystem models that use functional response curves.

1 Introduction

In the late 1950s, Buzz Holling began studying the predation of sawfly cocoons by small mammals (Holling, 1959a) to better understand how predation rates varied with prey density, a relationship coined a decade earlier as the functional response (Solomon, 1949). Holling observed that individual predators consumed more prey at higher prey densities, but found that this relationship was not necessarily linear or consistent across species. Over the course of three seminal papers, Holling developed a theoretical framework to describe how different assumptions about the rates at which predators captured and consumed their prey could explain observed nonlinearities and variability in the shape of functional response curve (Holling, 1959a, 1959b, 1965). Using this mechanistic approach, Holling derived three qualitatively distinct response types to describe differences in predator-prey interactions and their associated rates. In the ensuing decades, these equations have been further generalized (Real, 1977, 1979) and cemented into the bedrock of ecological modelling (Beardsell et al., 2021; Denny, 2014).

Although the functional response was originally developed for terrestrial applications (Holling, 1959a), the equations are also common in marine ecological modelling (Evans & Parslow, 1985; Fasham, 1995; Franks, Wroblewski, & Flierl, 1986). In the ocean, the functional response equations are now routinely used to link trophic dynamics in ma-

77 rine biogeochemical (Law et al., 2017; Moore, Lindsay, Doney, Long, & Misumi, 2013),
78 size spectrum (Heneghan et al., 2020), and population models (Alver, Broch, Melle, Bagøien,
79 & Slagstad, 2016). They are used to simulate both the rate at which heterotrophic zoo-
80 plankton graze on autotrophic phytoplankton (Evans & Parslow, 1985; Franks et al., 1986)
81 as well as the transfer of mass and energy further up the food chain in ecosystem (Buten-
82 schön et al., 2016) and fisheries models (Maury, 2010; Tittensor et al., 2018, 2021).

83 However, there remains a great deal of uncertainty surrounding the formulation of
84 the functional response. For example, trade offs between the ecological veracity and nu-
85 merical stability of different response types (Gismervik, 2005; Morozov, 2010; Morozov,
86 Arashkevich, Reigstad, & Falk-Petersen, 2008) have led to disagreement over which is
87 best suited for rapidly growing, easily perturbed, microbial systems common in marine
88 ecology (Fasham, 1995; Flynn & Mitra, 2016; Gentleman & Neuheimer, 2008). Even amongst
89 mathematically identical curves, there is not a consensus on how to define their param-
90 eters, no less prescribe them. While some modellers opt for a parameter scheme that mir-
91 rors the Michaelis–Menten (Michaelis & Menten, 1913) and Monod (Monod, 1949) equa-
92 tions developed to describe enzyme kinetics and bacterial growth rates (Aumont & Bopp,
93 2006; Dutkiewicz et al., 2015; Moore et al., 2013; Vichi, Pinardi, & Masina, 2007), oth-
94 ers use a parameter scheme that mirrors the disk equation (Holling, 1959b, 1965) devel-
95 oped by Holling to describe terrestrial interactions (Fasham, 1995; Laws, Falkowski, Smith,
96 Ducklow, & McCarthy, 2000; Oke et al., 2013; Schartau & Oschlies, 2003b). While the
97 parameters used in the Michaelis–Menten scheme are overtly empirical, those used in the
98 disk scheme are theoretically mechanistic. Disagreement over which parameter set to use
99 can confuse inter-model comparisons and influence the parameter space considered in
100 optimization schemes, especially when there are no robust observations to bound them.

101 Here, we focus on the formulation of grazing in marine biogeochemical models, which
102 are a critical component of coupled earth system models used to simulate climate (Eyring
103 et al., 2016; Flato et al., 2013; Taylor, Stouffer, & Meehl, 2012) and are often used to
104 drive fisheries models (Maury, 2010; Tittensor et al., 2018, 2021). These models are in-
105 creasingly under constrained and over parameterized (Doney, 1999; Matear, 1995; Schar-
106 tau et al., 2017; Ward, Friedrichs, Anderson, & Oschlies, 2010). Accurately represent-
107 ing grazing is critical to both climate and ecosystem models, as it mediates the biolog-
108 ical transport of carbon fixed via net primary production (Behrenfeld, Doney, Lima, Boss,
109 & Siegel, 2013; Laufkötter et al., 2015) and transported to higher trophic levels via sec-
110 ondary production (Brander, 2007; Scherrer et al., 2020). Still, despite the growing recog-
111 nition that biogeochemical models are highly sensitive to the grazing formulation (Ad-
112 jou, Bendtsen, & Richardson, 2012; T. Anderson, Gentleman, & Sinha, 2010; Chenillat,
113 Rivière, & Ohman, 2021; Fasham, 1995; Flynn & Mitra, 2016; Fussmann & Blasius, 2005;
114 Gentleman & Neuheimer, 2008; Gross, Ebenhöf, & Feudel, 2004), it remains challeng-
115 ing to constrain global zooplankton dynamics using a limited number of simplified equa-
116 tions, state variables, and parameters. Most biogeochemical models represent only 1-2
117 zooplankton functional groups, but parameters inferred empirically vary considerably
118 across zooplankton species, size and age (Hansen, Bjørnsen, & Hansen, 1997; Hirst &
119 Bunker, 2003). Allometric models can vary parameters across size classes, but measured
120 allometric relationships are not always robust (Hansen et al., 1997). Even once param-
121 eters are chosen, global simulations cannot be easily validated because we lack the re-
122 quired spatial resolution in observed distributions of zooplankton biomass and their as-
123 sociated grazing parameters (but see Moriarty, Buitenhuis, Le Quéré, and Gosselin (2013);
124 Moriarty and O’Brien (2012)). Moreover, equations modellers must parameterize are em-
125 pirical and theoretical simplifications and may not be adequate to represent the mean-
126 state of diverse communities grazing in fundamentally different ways distributed hetero-
127 geneously across a patchy ocean.

128 Depending on the model, zooplankton diets range from a single generic phytoplankton
129 to a complex portfolio of multiple phytoplankton, smaller zooplankton, and detri-

130 tus. When multiple prey are available, the distribution of grazing across them is deter-
 131 mined by one of many multiple-prey response functions, which can take into account both
 132 the relative distribution of prey options and their intrinsic desirability (Fasham, Duck-
 133 low, & McKelvie, 1990). These equations, which are typically extensions of the single-
 134 prey response functions, have been reviewed in detail by Gentleman, Leising, Frost, Strom,
 135 and Murray (2003). Here, we focus on the single-prey response functions, which are a
 136 prerequisite for understanding the multiple-prey response functions and often describe
 137 their implied behavior when only one prey option is available. While many modern mod-
 138 els use a multiple-prey response (Aumont, Ethé, Tagliabue, Bopp, & Gehlen, 2015; Stock
 139 et al., 2020; Totterdell, 2019; Yool et al., 2021), zooplankton grazing with a single-prey
 140 response remains common in many state-of-the-art CMIP6-class earth system models
 141 (Christian et al., 2021; Hajima et al., 2020; Law et al., 2017; Long et al., 2021; Tjipu-
 142 tra et al., 2020)

143 By combining theory, empirical data, and numerical models, we consolidate exist-
 144 ing information and new results to develop a comprehensive guide for how the single-
 145 prey functional response is employed in marine ecological models to represent grazing.
 146 We begin by presenting a unified review of how each functional response and its asso-
 147 ciated parameter schemes are derived, providing detailed insights into how they relate
 148 to each other from first principles (**Section 2**). Next we review the mathematical in-
 149 fluence of different grazing formulations on population stability (**Section 3**) and sur-
 150 vey the literature to assess the range of parameter values that have been estimated em-
 151 pirically and used prescriptively in models (**Section 4**). Then we conduct a suite of sim-
 152 ulations to isolate the sensitivity of phytoplankton population size and stability to the
 153 parameterization of the functional response using four different combinations of response
 154 type (i.e. II vs. III) and parameter scheme (i.e. disk vs. Michaelis-Menten; **Section 5**).
 155 Finally, we use a simple theoretical model to examine the influence of sub-grid scale het-
 156 erogeneity on the shape of the functional response (**Section 6**). This work culminates
 157 with a set of recommendations for the formulation of grazing based on the evidence pre-
 158 sented (**Section 7**). These recommendations are tailored to the single-prey representa-
 159 tion of grazing in marine biogeochemical models, but are broadly applicable to much wider
 160 usage of the functional response across marine and terrestrial applications.

161 2 Derivation of the grazing formulation

162 The rate at which prey is grazed by zooplankton is generally expressed as the graz-
 163 ing rate (G) in units of prey concentration lost per unit time (e.g. $\frac{mmolC}{m^3d}$). Here, we gen-
 164 erally refer to prey as phytoplankton, but all results are relevant to grazing on any generic
 165 single prey (e.g. bacteria, detritus, or other zooplankton). The grazing rate is equal to
 166 the product of the ambient zooplankton concentration, $[Z]$, and the zooplankton spe-
 167 cific grazing rate (g), often referred to as the ingestion rate (Franks et al., 1986; Gen-
 168 tleman & Neuheimer, 2008), which describes the concentration of phytoplankton grazed
 169 per unit zooplankton per unit time, reducing to units of one over time (e.g. $1/d$), such
 170 that

$$G = g[Z]. \quad (1)$$

171 To account for the intuitive fact that grazing is less successful when phytoplank-
 172 ton are scarce, the zooplankton specific grazing rate, g , must vary with the ambient phy-
 173 toplankton concentration, $[P]$, particularly when $[P]$ is low. The mathematical formula
 174 that describes these relationships is known as the functional response.

175 Buzz Holling originally derived the functional response by assuming there was a
 176 fixed time interval, T , over which predator and prey were exposed (e.g. same location,
 177 same time, predator is awake), and that predators were assumed to exclusively be cap-

178 turing (e.g. searching, encountering, hunting, attacking) (T_{cap}) or consuming (e.g. killing,
 179 handling, processing, eating, digesting) prey (T_{con}) during this interval (Holling, 1959a),
 180 such that

$$T = T_{cap} + T_{con}. \quad (2)$$

181 The canonical type I, II, and III functional responses (**Fig. 1a**) were consequently
 182 derived (**Fig. 1b**) from different assumptions (**Fig. 1c**) about the efficiency of the cap-
 183 ture and consumption processes, the associated total time needed to capture and con-
 184 sume a given amount of prey, and how those rates and times vary with prey density (see
 185 **Table 1** for a catalogue of terms). However, prey density was originally expressed in dis-
 186 crete units of prey over a given circular area (or disk). Here, we instead provide a deriva-
 187 tion of the type I (**Section 2.2**), II (**Section 2.3**), and III (**Section 2.4**) responses ex-
 188 plicitly for aquatic systems, with units of concentration ($mmolC/m^3$) for phytoplank-
 189 ton and zooplankton communities and days (d) for time. Further, we show how each func-
 190 tional response can be described by two sets of parameters: the disk scheme in which
 191 the consumption and capture processes are explicitly prescribed and mechanistically de-
 192 fined, and the Michaelis-Menten scheme, in which the maximum grazing rate and half
 193 saturation concentration of the curve are explicitly prescribed and empirically defined.
 194 Note, many of these equations have been derived in various forms and various contexts
 195 before (Aksnes & EGGE, 1991; Caperon, 1967). Here, we present them together, specif-
 196 ically in the context of zooplankton grazing, with careful attention to how they relate
 197 theoretically and mathematically to each other and first principles.

198 For each derivation, consider some concentration of phytoplankton, $[P_G]$ ($mmolC/m^3$),
 199 that is grazed (i.e. captured and consumed) by the ambient zooplankton community, $[Z]$
 200 ($mmolC/m^3$), over the fixed grazing (or exposure) interval, T (d), at a grazing rate of
 201 $G = \frac{[P_G]}{T}$ and a zooplankton specific (i.e. considering the amount of predator present)
 202 grazing rate of $g = \frac{[P_G]}{[Z]T}$. To derive each functional response type, $g([P])$, we must solve
 203 for g ($1/d$) in terms of the ambient phytoplankton population, $[P]$ ($mmolC/m^3$), con-
 204 sidering their respective assumptions regarding capture and consumption rates.

205 2.1 Type 0 response

206 A type 0 functional response is described by a straight horizontal line in which a
 207 zooplankton specific grazing rate is invariant to the ambient phytoplankton population
 208 ($g([P]) = constant$, **Fig. 1**; magenta). A type 0 response is not ecologically realistic
 209 for any species, nor does it appear in any models, but for pedagogical purposes assumes
 210 that the capture process is unaffected by prey scarcity and that the consumption pro-
 211 cess is negligible.

212 2.2 Type I response

213 A type I functional response is described by a straight line (Holling, 1959b), in which
 214 the zooplankton specific grazing rate ($g([P])$) increases linearly with the ambient phy-
 215 toplankton concentration (**See Fig. 1**; black). Ecologically, a type I response assumes
 216 that zooplankton capture prey faster when it is more abundant and that the time needed
 217 to consume it is negligible compared with the time needed to capture it ($T_{cap} \gg T_{con}$).
 218 Accordingly, zooplankton can spend all of their time capturing prey, such that

$$T = T_{cap}. \quad (3)$$

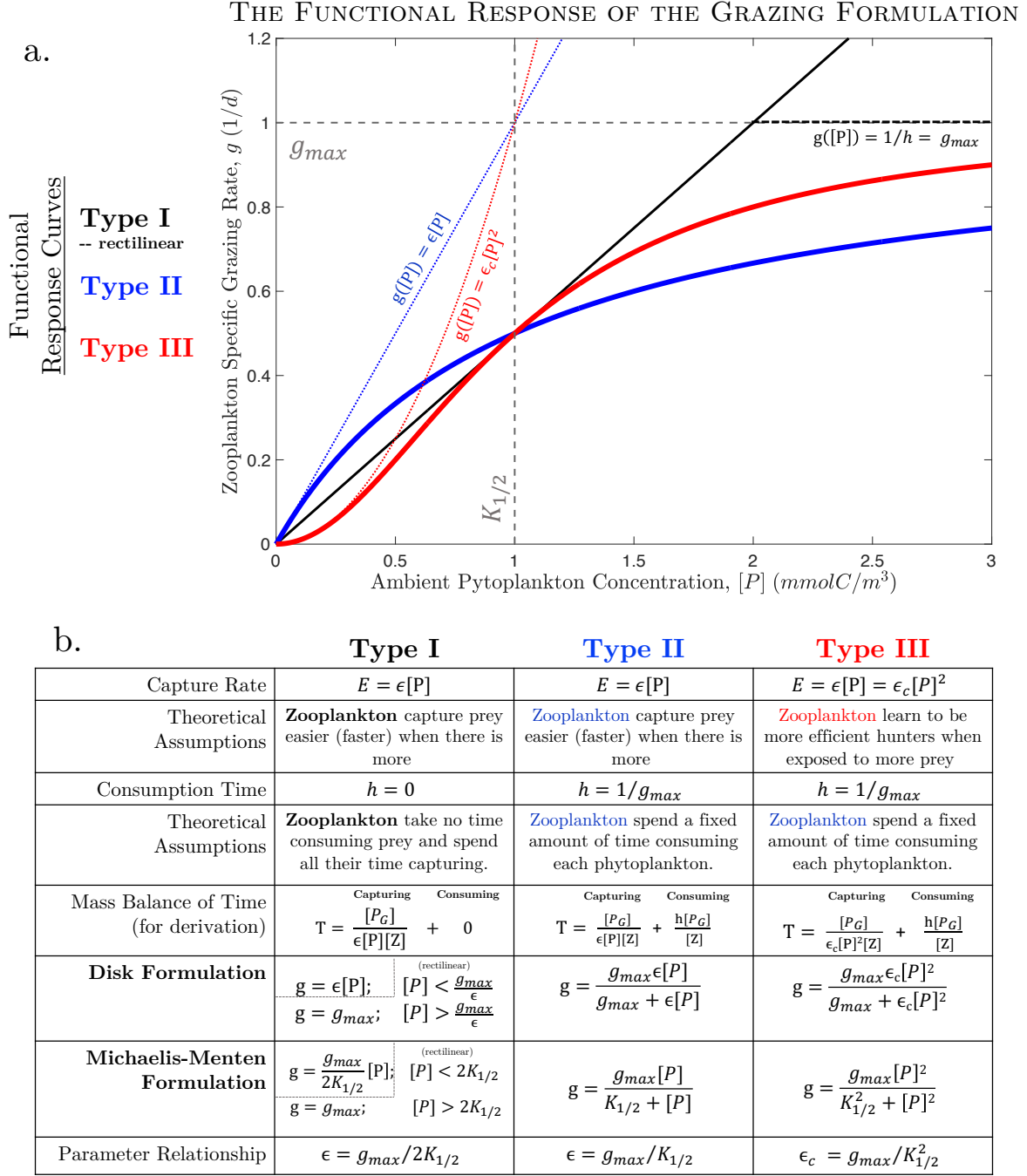


Figure 1. The functional response of the grazing formulation. **a.** The zooplankton specific grazing rate (or ingestion rate) as a function of prey density, known as the the functional response curve is plotted for a type I, II, and III response, along with **b.** a description of their associated attributes, assumptions, and formulations. Each response type is parameterized such that the maximum specific grazing rate, g_{max} , and the half saturation concentration, $K_{1/2}$, are equal to one. Note, this requires different parameters for the disk parameter scheme. Dashed lines in **a.** show what each response reduces to at low and high prey densities.

Variable	Notation	Conceptual Units	Reduced Units	Relevant Relationships	Description
Phytoplankton concentrations	$[P], [P_G], [P_{Cap}], [P_{Con}]$	$[P]$	$\frac{mmolC}{m^3}$	$[P_G] = GT = g[Z]T$ $[P_G] = [P_{Cap}] = [P_{Con}]$	Concentration of ambient, grazed (i.e. captured and consumed), captured, and consumed phytoplankton over the exposure period, respectively
Zooplankton concentration	$[Z]$	$[Z]$	$\frac{mmolC}{m^3}$	-	Concentration of zooplankton biomass
Functional response	$g([P])$	$\frac{[P]}{[Z]time}$	$\frac{1}{d}$	$g([P]) = \epsilon[P]$ (I) $= \frac{g_{max}}{2K_{1/2}}[P]$ (I-Rect) $g([P]) = \frac{g_{max}\epsilon[P]}{g_{max} + \epsilon[P]}$ (II) $= \frac{g_{max}[P]}{K_{1/2} + [P]}$ $g([P]) = g_{max}(1 - e^{-\lambda[P]})$ (II-IV) $g([P]) = \frac{g_{max}\epsilon_c[P]^2}{g_{max} + \epsilon_c[P]^2}$ (III) $= \frac{g_{max}[P]^2}{K_{1/2}^2 + [P]^2}$	Functional description of how the zooplankton specific grazing rate varies with the phytoplankton concentration
Half saturation concentration	$K_{1/2}$	$[P]$	$\frac{mmolC}{m^3}$	$K_{1/2} = \frac{g_{max}}{2\epsilon}$ (II-R) $K_{1/2} = \frac{g_{max}}{\epsilon}$ (II) $K_{1/2} = \frac{\epsilon}{-\ln(0.5)}$ (II-IV) $K_{1/2} = \sqrt{\frac{g_{max}}{\epsilon_c}}$ (III)	Phytoplankton concentration where $g = \frac{g_{max}}{2}$
Maximum grazing rate	g_{max}	$\frac{[P]}{[Z]time}$	$\frac{1}{d}$	$g_{max} = \frac{1}{h}$	Rate of phytoplankton consumption per unit zooplankton when food replete
Grazing rate	G	$\frac{[P]}{time}$	$\frac{mmolC}{m^3d}$	$G = \frac{[P_G]}{T}$ $G = g[Z]$	Rate at which phytoplankton are grazed by zooplankton
Phytoplankton specific grazing loss rate	l	$\frac{[P]}{[P]time}$	$\frac{1}{d}$	$l = \frac{G}{[P]}$	Phytoplankton specific rate at which phytoplankton are lost to grazing
Zooplankton specific grazing rate (i.e. ingestion rate)	g	$\frac{[P]}{[Z]time}$	$\frac{1}{d}$	$g = \frac{G}{[Z]}$	Zooplankton specific rate at which phytoplankton are grazed. The way in which g varies with $[P]$ is the functional response
Clearance rate	Cl	$\frac{[P]}{[P][Z]time}$	$\frac{m^3}{mmolCd}$	$Cl = \frac{G}{[P][Z]}$ $Cl = \frac{g}{[P]}$	Phytoplankton specific rate at which phytoplankton are grazed per unit zooplankton
Exposure period	T	<i>time</i>	<i>d</i>	$T = T_{cap} + T_{con}$	Fixed period over which zooplankton and phytoplankton are exposed
Capture period	T_{cap}	<i>time</i>	<i>d</i>	$T_{cap} = \frac{[P_G]}{[Z]\epsilon[P]}$	Time spent capturing phytoplankton
Consumption period	T_{con}	<i>time</i>	<i>d</i>	$T_{con} = 0$ (I) $T_{con} = \frac{h[P_G]}{[Z]}$ (II,III)	Time spent consuming phytoplankton
Capture rate	C	$\frac{[P]}{time}$	$\frac{mmolC}{m^3d}$	$C = \frac{[P_{cap}]}{T_{cap}}$ $C = E[Z]$ (II) $C = \epsilon_c[Z]^2$ (III)	Rate at which phytoplankton are captured by the zooplankton
Zooplankton specific capture rate	E	$\frac{[P]}{[Z]time}$	$\frac{1}{d}$	$E = \frac{C}{[Z]}$ $E = \epsilon[P]$	Specific rate at which phytoplankton are captured per unit zooplankton
Prey capture efficiency	ϵ	$\frac{[P]}{[P][Z]time}$	$\frac{m^3}{mmolCd}$	$\epsilon = \epsilon_c[P]$ (III) $\epsilon = \lambda g_{max}$ (II-IV)	Rate at which the zooplankton specific capture rate increases with the ambient phytoplankton concentration
Prey capture efficiency coefficient	ϵ_c	$\frac{[P]}{[P]^2[Z]time}$	$\frac{m^6}{mmolC^2d}$	-	Rate at which the prey capture efficiency increases with the ambient phytoplankton concentration
Consumption time	h	$\frac{[Z]time}{[P]}$	<i>d</i>	-	Time it takes for one unit of zooplankton to eat one unit of phytoplankton
Consumption rate	$\frac{1}{h}$	$\frac{[P]}{[Z]time}$	$\frac{1}{d}$	-	Rate of phytoplankton consumption per unit zooplankton
Ivlev parameter	λ	$\frac{1}{[P]}$	$\frac{m^3}{mmolCd}$	-	Used to parameterize Ivlev equation, which is qualitatively similar to a type II

Table 1. List of terms relevant to the derivation, parameterization and context of the functional response. Conceptual units distinguish between phytoplankton and zooplankton concentration and are not reduced.

219 The time, T_{cap} (d), that it takes to capture some concentration of phytoplankton,
 220 $[P_{Cap}]$ ($mmolC/m^3$), can be related to the capture rate, C ($\frac{mmolC}{m^3d}$), or the concen-
 221 tration of phytoplankton captured per unit time, by the equation

$$T_{cap} = \frac{[P_{Cap}]}{C}. \quad (4)$$

222 The capture rate can then be decomposed into the product of the ambient zooplank-
 223 ton concentration, $[Z]$ ($mmolC/m^3$), and the zooplankton specific capture rate, E ($1/d$),
 224 which describes the concentration of phytoplankton captured per unit zooplankton per
 225 unit time, such that

$$C = E[Z]. \quad (5)$$

226 Depending on the zooplankton in question, the zooplankton specific capture rate,
 227 E ($1/d$), can represent a passive encounter rate (e.g. filter feeding) or an active search
 228 and attack rate (e.g. hunting), but does not include the time required to consume phy-
 229 toplankton once captured. Either way, E ($1/d$) is assumed to increase linearly with the
 230 ambient phytoplankton concentration, $[P]$ ($mmolC/m^3$), to account for the fact that zoo-
 231 plankton are stochastically more likely to encounter and capture phytoplankton at higher
 232 ambient phytoplankton concentrations. The rate (per unit phytoplankton) at which the
 233 zooplankton specific capture rate increases with the ambient phytoplankton concentra-
 234 tion can be considered the prey capture efficiency, ϵ ($\frac{1}{(mmolC/m^3)d}$), such that

$$E = \epsilon[P]. \quad (6)$$

235 The prey capture efficiency can be thought of as the fraction of the ambient phytoplank-
 236 ton concentration captured per unit zooplankton per unit time, in which units of $\frac{(mmolC/m^3)}{(mmolC/m^3)^2d}$
 237 reduce to $\frac{1}{(mmolC/m^3)d}$, and reflects the efficiency with which zooplankton can capture
 238 their prey. Note that the prey capture efficiency is variously referred to as the prey cap-
 239 ture rate (Schartau & Oschlies, 2003b), attack rate (Gentleman & Neuheimer, 2008), affin-
 240 ity, and maximum clearance rate. It is also qualitatively similar to the search area de-
 241 fined by Holling (1959b), but not identical for concentration-based rates.

242 Substituting **eqs. 5 & 6** into **eq. 4** yields,

$$T_{cap} = \frac{[P_{Cap}]}{\epsilon[P][Z]}. \quad (7)$$

243 Next, we can substitute T_{cap} for T because of our assumption that no time is needed
 244 for zooplankton to consume phytoplankton (i.e. $T_{con} = 0$), and substitute $[P_{Cap}]$ for
 245 $[P_G]$ because the entire concentration of phytoplankton lost to grazing, $[P_G]$, must first
 246 be captured, $[P_{Cap}]$. Finally, we solve for the rate at which phytoplankton are grazed
 247 by the zooplankton community ($G = gZ = \frac{[P_G]}{T}$) as a function of $[P]$,

$$G([P]) = \frac{[P_G]}{T} = \epsilon[P][Z], \quad (8)$$

248 and divide by $[Z]$ to yield the zooplankton specific grazing rate, g ($1/d$), as a function
 249 of the ambient phytoplankton concentration $[P]$, such that,

$$g([P]) = \frac{[P_G]}{T[Z]} = \epsilon[P]. \quad (9)$$

250 **Eq. 9** is the type I functional response, wherein $g([P])$ increases linearly with the
 251 ambient phytoplankton concentration, $[P]$, at a rate described by the prey capture ef-
 252 ficiency, ϵ . This type of response is akin to a food-limited system in which it takes much
 253 longer to find and capture prey than it takes to consume it, and is analogous to the clas-
 254 sic Lotka-Volterra equations (Lotka, 1910; Volterra, 1927) used to describe simple predator-
 255 prey dynamics. Note that here the grazing rate is identical to the capture rate ($G = C$)
 256 and the zooplankton specific grazing rate is identical to the zooplankton specific capture
 257 rate ($g = E = \epsilon[P]$). This is because the entire grazing process is assumed to be de-
 258 scribed by the capture process; however, this is not the case for higher order functional
 259 responses, in which zooplankton are assumed to spend a non-trivial amount of time con-
 260 suming phytoplankton in addition to capturing them.

261 A standard type I response may be characteristic of passive filter feeders (Jeschke,
 262 Kopp, & Tollrian, 2004), but can overestimate the zooplankton specific grazing rate of
 263 mesozooplankton such as copepods (Gentleman & Neuheimer, 2008) by over an order
 264 of magnitude compared to observations (Frost, 1972; Hansen et al., 1997) because it does
 265 not account for predator satiation at high prey densities. To account for predator sati-
 266 ation, the type I response can be extended to a rectilinear response (Chen, Laws, Liu,
 267 & Huang, 2014; Frost, 1972; Hansen, Bjørnsen, & Hansen, 2014; Mayzaud, Tirelli, Bernard,
 268 & Roche-Mayzaud, 1998), in which $g([P])$ reaches some maximum rate, g_{max} (d^{-1}) such
 269 that

$$\begin{aligned} g([P]) &= \epsilon[P] & \text{if } [P] < \frac{g_{max}}{\epsilon} \\ g([P]) &= g_{max} & \text{if } [P] > \frac{g_{max}}{\epsilon}, \end{aligned} \quad (10)$$

270 where $\frac{g_{max}}{\epsilon}$ ($\frac{mmolC}{m^3}$) describes the prey concentration required to reach the maximum
 271 zooplankton specific grazing rate, g_{max} , for a given prey capture efficiency, ϵ .

272 Solving for $[P]$ when $g([P]) = \frac{g_{max}}{2}$ returns the half saturation concentration, $K_{1/2} =$
 273 $\frac{g_{max}}{2\epsilon}$. Note that parameterizing **eq. 10** with $K_{1/2}$ allows one to explicitly define the lo-
 274 cation of satiation using a single variable (as opposed to $\frac{g_{max}}{2\epsilon}$); however, changing $K_{1/2}$
 275 with a fixed g_{max} necessarily alters the slope of the response, ϵ , and therefore implicitly
 276 alters assumptions about the prey capture efficiency.

277 2.3 Type II response

278 A type II functional response assumes a more gradual transition to satiation by em-
 279 ploying a rectangular hyperbola with downward concavity (Holling, 1959b), in which the
 280 zooplankton specific grazing rate ($g([P])$) saturates towards a maximum asymptote at
 281 high phytoplankton concentrations (**See Fig. 1**; blue). Ecologically, a type II response
 282 assumes that zooplankton capture prey faster when it is more abundant and that a fixed,
 283 non-trivial, amount of time is needed to consume it ($T_{con} > 0$), allowing for gradual
 284 predator satiation as the prey density increases and more time is needed to consume it
 285 (Jeschke et al., 2004). Note, all assumptions about the capture process and zooplank-
 286 ton specific capture rate ($E = \epsilon[P]$) from the type I response are held.

287 The time it takes to consume the captured phytoplankton is parameterized by the
 288 consumption time, h (d), also commonly referred to as the handling time (Holling, 1959b,
 289 1965), which is assumed to be equal to the fixed amount of time it takes for one unit of
 290 zooplankton to eat one unit of phytoplankton. The total time, T_{con} (d), needed for con-
 291 sumption of the entire captured phytoplankton concentration, $[P_{Cap}]$ ($mmolC/m^3$), by
 292 the ambient zooplankton concentration, $[Z]$ ($mmolC/m^3$), can then be expressed as the
 293 consumption time, h , multiplied by the ratio of the concentration of phytoplankton cap-

294 tured relative to the ambient concentration of zooplankton capturing them ($\frac{[P_{Cap}]}{[Z]}$), such
 295 that

$$T_{con} = \frac{h[P_{Cap}]}{[Z]}. \quad (11)$$

296 Remembering that all phytoplankton grazed must first be captured (i.e. $[P_G] = [P_{Cap}]$)
 297 and substituting T_{cap} and T_{con} into **eq. 2** yields

$$T = T_{cap} + T_{con} = \frac{[P_G]}{\epsilon[P][Z]} + \frac{h[P_G]}{[Z]}. \quad (12)$$

298 Solving for the concentration of phytoplankton lost to grazing, $[P_G]$, yields the aquatic
 299 analogue to the familiar disk equation, originally derived by Holling (1959b) for terres-
 300 trial predation on a planar disk,

$$[P_G] = \frac{\epsilon[P][Z]T}{1 + \epsilon h[P]}, \quad (13)$$

301 where dividing by T returns the grazing rate,

$$G = \frac{[P_G]}{T} = \frac{\epsilon[P][Z]}{1 + \epsilon h[P]}, \quad (14)$$

302 and dividing again by Z returns the zooplankton specific grazing rate, which is the type
 303 II functional response,

$$g([P]) = \frac{[P_G]}{[Z]T} = \frac{\epsilon[P]}{1 + \epsilon h[P]}. \quad (15)$$

304 Note that by factoring out $\epsilon[P]$ from the denominator and rearranging **eq. 15** as

$$g([P]) = \frac{1}{\frac{1}{\epsilon[P]} + h}, \quad (16)$$

305 it becomes clear that when food is limiting the type II disk equation reduces to a type
 306 I linear Lotka-Volterra functional response with a slope equal to the prey capture efficiency
 307 (**Fig. 1a**; dashed blue line). If the consumption rate ($\frac{1}{h}$) is much faster than the zoo-
 308 plankton specific capture rate ($E = \epsilon[P]$), such that $\frac{1}{h} \gg \epsilon[P]$ or equivalently $h \ll$
 309 $\frac{1}{\epsilon[P]}$, then **eqs. 15 & 16** reduce to $g([P]) = \epsilon[P]$ (i.e. **eq. 9**). This occurs when the
 310 consumption time, h , is very fast (i.e. type I, **Section 2.1.1**), or the phytoplankton con-
 311 centration, $[P]$, is very low (i.e. a food-limited system).

312 Alternatively, we see that **eqs. 15 & 16** saturate towards $g([P]) = 1/h$ when the
 313 consumption rate ($\frac{1}{h}$) is much slower than the zooplankton specific capture rate ($E =$
 314 $\epsilon[P]$), such that $\frac{1}{h} \ll \epsilon[P]$ or equivalently $h \gg \frac{1}{\epsilon[P]}$ (**Fig. 1a**; dashed black line).
 315 This is typical of a food replete system (high $[P]$), where more food is captured as soon
 316 as the previous prey item has been consumed. The maximum grazing rate, g_{max} ($1/d$),
 317 can now be defined by the consumption rate, or one over the consumption time, such
 318 that $g_{max} = \frac{1}{h}$. Note, however, g_{max} is approached slowly in a type II response, and
 319 $g([P])$ is still only 80% of g_{max} even when $[P] > 4K_{1/2}$.

320 The disk equation (**eq. 13**) can be simplified by substituting the parameter $g_{max} =$
 321 $\frac{1}{h}$ into **eq. 15** and multiplying by $\frac{g_{max}}{g_{max}}$ to arrive at

Type II (disk)

$$g([P]) = \frac{g_{max}\epsilon[P]}{g_{max} + \epsilon[P]}. \quad (17)$$

Henceforth, this will be referred to as the disk parameter scheme. Note, the formulation of the disk equation used here differs from the traditional form (eq. 14) because we replaced the handling time with its reciprocal (g_{max}), making it easier to compare with the Michaelis–Menten form of the equation (see below).

Equation 17 can be rewritten as the familiar Michaelis–Menten equation originally derived for enzyme kinetics (Michaelis & Menten, 1913) (or Monod equation derived for bacterial growth (Monod, 1949)) by defining the half-saturation concentration, $K_{1/2}$ ($mmolC/m^3$), in terms of parameters g_{max} and ϵ . Setting $g([P]) = \frac{g_{max}}{2}$ and solving for $[P]$, we find,

$$[P] = K_{1/2} = \frac{g_{max}}{\epsilon}. \quad (18)$$

Substituting $\epsilon = \frac{g_{max}}{K_{1/2}}$ into eq. 17 and rearranging yields the familiar form,

Type II (Michaelis–Menten)

$$g([P]) = \frac{g_{max}[P]}{K_{1/2} + [P]}. \quad (19)$$

Henceforth, this will be referred to as the Michaelis–Menten parameter scheme. Note, that in the Michaelis–Menten formulation $g([P])$ still reduces to g_{max} , or $\frac{1}{h}$, when $[P] \gg K_{1/2}$ and to $\frac{g_{max}}{K_{1/2}}$, or (eq. 18), when $[P] \ll K_{1/2}$.

Eq. 19 is mathematically identical to eq. 17. That is, for all parameter sets $\{g_{max}, \epsilon\}$, there exists a parameter set $\{g_{max}, K_{1/2}\}$ that can identically describe $g([P])$. As with the type I response (eq. 10), the difference is that $\{g_{max}, \epsilon\}$ are ecologically independent, while $\{g_{max}, K_{1/2}\}$ more directly define the shape of the curve. For example, increasing g_{max} in eq. 17 does not affect the prey capture efficiency, ϵ , but it does increase the half-saturation concentration. This makes sense ecologically, as it should require a higher phytoplankton concentration for a faster consumption time (i.e. higher g_{max}) to become limiting, given a constant prey capture efficiency. On the other hand, increasing g_{max} in eq. 19 does not change the location of $K_{1/2}$, but implicitly assumes that the prey capture efficiency, ϵ , increases in order to maintain a constant $K_{1/2}$.

Note, another common formulation that is qualitatively similar to the type II response is the Ivlev equation (Ivlev, 1961), where

$$g([P]) = g_{max}(1 - e^{-\lambda[P]}) \quad (20)$$

(T. Anderson et al., 2010; C. A. Edwards, Batchelder, & Powell, 2000; Franks & Chen, 2001; Shigemitsu et al., 2012). However, the Ivlev formulation is strictly empirical and cannot be derived mechanistically, but is qualitatively similar to the type II response (See Fig. 1a; cyan). All else being equal, the Ivlev equation will yield slower grazing rates below the half saturation concentration and faster grazing rates above the half saturation concentration. As noted elsewhere (Aldebert & Stouffer, 2018; T. Anderson et al., 2010; Gentleman et al., 2003), the half saturation point and prey capture efficiency can be related to the Ivlev parameter, λ ($\frac{1}{mmolC/m^3}$), as

$$K_{1/2} = \frac{-\ln(0.5)}{\lambda} \quad (21)$$

$$\epsilon = \lambda g_{max}$$

355 **2.4 Type III response**

356 A type III functional response is described by a sigmoidal curve (Jeschke et al., 2004),
 357 in which the zooplankton specific grazing rate ($g([P])$) increases quadratically at low phy-
 358 toplankton concentrations and approaches saturation much faster at high ones (**Fig. 1**;
 359 red). Ecologically, a type III response further assumes that the prey capture efficiency,
 360 ϵ ($\frac{1}{(mmolC/m^3)d}$), increases with prey density. That is, the zooplankton specific capture
 361 rate, $E = \epsilon[P]$, does not just increase due to a stochastic increase in the likelihood of
 362 encountering phytoplankton as the ambient phytoplankton concentration increases, but
 363 zooplankton additionally become more efficient grazers as well, capturing an increasing
 364 fraction of the ambient phytoplankton concentration. Consequently, specific grazing rates
 365 increases quadratically at low $[P]$ and approach saturation much faster than at high $[P]$.

366 Mathematically, this change in behavior can be represented by assuming the prey
 367 capture efficiency, ϵ ($\frac{1}{(mmolC/m^3)d}$), is a function of the ambient phytoplankton concen-
 368 tration, $[P]$. In a type III response this function is assumed to be linearly proportional
 369 to some prey capture efficiency coefficient, ϵ_c ($\frac{1}{(mmolC/m^3)d}$), such that,

$$\epsilon = \epsilon_c[P], \quad (22)$$

370 and

$$E = \epsilon_c[P]^2. \quad (23)$$

371 By assuming that the prey capture efficiency, ϵ , increases linearly with the phyto-
 372 plankton concentration at a rate described by the prey capture efficiency coefficient, ϵ_c ,
 373 we are in turn assuming that the zooplankton specific grazing rate, E , increases quadrat-
 374 ically with the phytoplankton population (i.e. $E = \epsilon_c[P]^2$). Note that higher order func-
 375 tional responses can be achieved by modifying the relationship between the prey cap-
 376 ture efficiency and the phytoplankton concentration (e.g. $\epsilon = \epsilon_c[P]^2$).

377 Following the same derivation as **Section 2.3**, but now using **eq. 23** instead of
 378 **eq. 6** to define the specific capture rate, yields the disk parameterization of the type III
 379 functional response,

Type III (disk)

$$g([P]) = \frac{g_{max}\epsilon_c[P]^2}{g_{max} + \epsilon_c[P]^2}. \quad (24)$$

380 As for the type II response, $g([P])$ reduces to the zooplankton specific capture rate ($E =$
 381 $\epsilon_c[P]^2$) at low phytoplankton densities (**Fig. 1a**; dashed red line) and saturates towards
 382 the consumption rate ($1/h$) at very high phytoplankton densities (**Fig. 1a**; dashed black
 383 line). Now, however, because the zooplankton specific capture rate, E , is described by
 384 a quadratic function of $[P]$, the functional response, $g(P)$, is sigmoidal in shape (**Fig.**
 385 **1a**).

386 The prey capture efficiency, ϵ , in **eq. 17** has been replaced with the prey capture
 387 efficiency coefficient, ϵ_c , in **eq. 24**, which describes how ϵ varies with $[P]$. Units of ϵ_c are

388 non-intuitive, but can be considered as the fraction of the phytoplankton population cap-
 389 tured per unit zooplankton, per unit phytoplankton, per unit time, which reduces to $\frac{1}{(mmolC/m^3)^2d}$.

390 Finally, following identical logic to the type II response, **eq. 24** can be transformed
 391 to the Michaelis–Menten function by setting $g([P])$ equal to $\frac{g_{max}}{2}$, solving for $[P]$ to find
 392 $K_{1/2}$, and substituting the ensuing value of $K_{1/2}$ into **eq. 24**. The result is the Michaelis–Menten
 393 parameterization of the type III functional response,

Type III (Michaelis–Menten)

$$g([P]) = \frac{g_{max}[P]^2}{K_{1/2}^2 + [P]^2}, \quad (25)$$

394 where,

$$K_{1/2} = \sqrt{\frac{g_{max}}{\epsilon_c}}. \quad (26)$$

395 Note that the Michaelis–Menten parameter scheme employs the same parameters in each
 396 response type ($K_{1,2}, g_{max}$), while the disk scheme requires a slightly different parame-
 397 ter set in a type II (ϵ, g_{max}) and III (ϵ_c, g_{max}) response.

398 Finally, note that where we refer to the disk and Michaelis–Menten parameteriza-
 399 tion of the type III response, throughout the literature they are often referred to as the
 400 ‘Holling Type III’ and ‘Sigmoidal Type III’ response, respectively. We use the former
 401 nomenclature to clarify that both functions are sigmoidal in shape and because it allows
 402 us to refer to the parameter scheme generically without specifying the response type. Through-
 403 out the review, this is semantically useful for comparisons between parameter schemes
 404 that are agnostic to response type.

3 Stability of the grazing formulation

405
 406 Past studies have shown that the shape of these theoretical relationships, when em-
 407 bedded into models and integrated forward in time, influences the dynamical stability
 408 of the system, and in turn the propensity for phytoplankton extinction (Adjou et al., 2012;
 409 Dunn & Hovel, 2020; J. Steele, 1974) and excitation (i.e. blooms) (Hernández-García &
 410 López, 2004; Malchow, Hilker, Sarkar, & Brauer, 2005; Truscott & Brindley, 1994; Tr-
 411 uscott, Brindley, Brindley, & Gray, 1994). In particular, Gentleman and Neuheimer (2008)
 412 have shown how the stabilizing influence of the grazing formulation is determined by the
 413 sign of the first derivative of the clearance rate ($\frac{dCl}{d[P]}$). The clearance rate (Cl) is equal
 414 to the the functional response ($g([P])$) normalized by the ambient phytoplankton con-
 415 centration (i.e. $Cl = g([P])/[P]$). This is equivalent to the phytoplankton specific loss
 416 rate to grazing per unit zooplankton (see **Table 1**) or in other words, the volume of wa-
 417 ter completely cleared of phytoplankton per unit time, per unit zooplankton (Gentle-
 418 man & Neuheimer, 2008). Ecologically, higher clearance rates imply individual zooplank-
 419 ton are either spending less time consuming their prey or more efficiently capturing it.

420 Gentleman and Neuheimer (2008) showed how clearance rates vary with prey den-
 421 sity in different functional response types (see their **Fig. 2**). In a type I functional re-
 422 sponse, clearance rates are constant because it is assumed that the prey capture efficiency
 423 (ϵ) is constant and the consumption time is negligible (thus constant). In a type II re-
 424 sponse, clearance rates decrease with increasing prey density because the consumption
 425 rate is no longer assumed negligible, meaning the more zooplankton graze, the more time
 426 they need to consume their food, leaving less time to capture it. In a type III response
 427 clearance rates first increase, then decrease with prey density based on the balance be-
 428 tween increasing consumption time and increasing prey capture efficiency.

429 The stabilizing influence of the functional response is negative, or destabilizing, when
 430 clearance rates decrease with increasing prey density ($\frac{dCl}{d[P]} < 0$). In turn, growing (de-
 431 caying) phytoplankton populations are subject to decreasing (increasing) per capita graz-
 432 ing pressure, creating a destabilizing feedback that amplifies changes in phytoplankton
 433 growth (decay) and increases the likelihood of excitation (extinction). This occurs when
 434 the functional response has downward concavity, such that a type II response has a desta-
 435 bilizing influence at all prey densities, while a type III response has a destabilizing in-
 436 fluence only above $K_{1/2}$ (Gentleman & Neuheimer, 2008). The stabilizing influence of
 437 the functional response is positive, or stabilizing when clearance rates increase with in-
 438 creasing prey density ($\frac{dCl}{d[P]} > 0$). In turn, growing (decaying) phytoplankton popula-
 439 tions are subject to increasing (decreasing) per capita grazing pressure, creating a sta-
 440 bilizing feedback that buffers changes in phytoplankton growth (decay) and decreases
 441 the likelihood of excitation (extinction). This occurs when the functional response has
 442 upward concavity, such that a type III response has stabilizing influence below $K_{1/2}$ (Gen-
 443 tleman & Neuheimer, 2008). A type I response, in which clearance rates are constant
 444 ($\frac{dCl}{d[P]} = 0$), has no first order influence on stability.

445 The parameterization of the functional response can influence stability in two ways.
 446 First, increasing g_{max} or decreasing $K_{1/2}$ both increase the curvature of the response,
 447 which directly increases its stabilizing or destabilizing influence. Thus, a type II response
 448 with a higher g_{max} or lower $K_{1/2}$ is more destabilizing at all prey densities. However,
 449 a type III response is more destabilizing above $K_{1/2}$ but more stabilizing below $K_{1/2}$.
 450 This is illustrated clearly in Figure 5 of Gentleman and Neuheimer (2008), which tracks
 451 the first derivative of clearance rates ($\frac{dCl}{d[P]}$). Second, the parameterization of the func-
 452 tional response can influence stability indirectly by applying stronger or weaker grazing
 453 pressure, which in turn drives the size of the phytoplankton population and thus the po-
 454 sition on the curve at which $\frac{dCl}{d[P]}$ is considered. For example, if using a type III response
 455 with a lower $K_{1/2}$, the functional response will have a more destabilizing influence on
 456 all phytoplankton populations above $K_{1/2}$, but faster grazing rates associated with the
 457 lower $K_{1/2}$ value make it more difficult for population levels to exceed $K_{1/2}$, such that
 458 the overall outcome may be increasing the stabilizing influence of the response. Note,
 459 in a disk scheme, $K_{1/2}$ is not parameterized directly and its location varies with both
 460 parameters.

461 4 Parameters of the grazing formulation

462 Constrained by computational resources and parsimony, biogeochemical models are
 463 limited in the number of zooplankton functional groups they can include, making it dif-
 464 ficult to select parameters that accurately represent the mean state of natural variabil-
 465 ity across the diverse zooplankton they are trying to simulate. We combine data from
 466 two extensive reviews by Hansen et al. (1997) and Hirst and Bunker (2003) to show how
 467 the values of 119 empirically estimated sets of grazing parameters vary across zooplank-
 468 ton size and species (**Fig. 2**; filled markers; **Fig. 3a-c**). We then compare them to the
 469 values used in 40 modelling studies that have over 70 unique grazing formulations (**Table**
 470 **2**; **Fig. 2**; empty markers; **Fig. 3d-f**). Of the 40 models surveyed, 28 include only one
 471 zooplankton group, meaning they must represent the mean behavior of all global zoo-
 472 plankton with a single set of parameters. Those that include multiple zooplankton have
 473 the flexibility to imply different traits for different functional groups by selecting differ-
 474 ent parameters. However, functional group resolution is still very limited, with only one
 475 model including more than three (Stock, Powell, & Levin, 2008). To determine if the val-
 476 ues used in models are ecologically realistic approximations of the mean state, it is es-
 477 sential to understand how empirical estimates vary and how models attempt to either
 478 capture or average out this variability.

479 The most common partitioning of zooplankton functional groups in models is al-
 480 lometric (i.e. by size). Accordingly, we have binned all observed and modelled zooplank-

481 ton based on body volume, with nanozooplankton defined as $< 10^3 \mu\text{m}^3$ (\sim nanoflag-
 482 ellates), microzooplankton defined as $10^3 - 10^6 \mu\text{m}^3$ (\sim dinoflagellates, rotifers and cil-
 483 iates), mesozooplankton defined as $10^6 - 10^9 \mu\text{m}^3$ (\sim copepods, meroplankton larvae and
 484 cladocerans) and macrozooplankton as $> 10^9 \mu\text{m}^3$ (none reported). In the models the
 485 same size classes are assigned based on the relative prey portfolio or other specified de-
 486 scriptions of each zooplankton functional group. For example, in a model with 2 zoo-
 487 plankton functional groups nominally called ‘small’ and ‘large’ and prescribed to pref-
 488 erentially graze on small phytoplankton and diatoms, we would categorize these as ‘mi-
 489 cro’ and ‘meso’, respectively. The ‘nano-’ and ‘macro-’ designations were only given when
 490 more than two zooplankton were included or they were classified explicitly as such in the
 491 study. Models with one generic, unspecified zooplankton were left unclassified.

492 For consistent comparison between models and empirical studies, we converted all
 493 units to mmolC/m^3 for prey density and $1/d$ for rates. In Hirst and Bunker (2003) $K_{1/2}$
 494 was reported in chlorophyll units and converted with a C:Chl ratio of 50:1 (T. Ander-
 495 son et al., 2010). In Hansen et al. (1997), $K_{1/2}$ was reported in ppm, and converted as-
 496 suming a carbon density of $0.12 \text{ gC}/\text{cm}^3$, consistent with the range of carbon densities
 497 in phytoplankton (Menden-Deuer & Lessard, 2000). Different conversion factors would
 498 shift the absolute values of $K_{1/2}$ reported here, but not the size of their range or strength
 499 of their correlations with size. In modelling studies that used a currency other than car-
 500 bon, units were converted assuming a fixed Redfield ratio of 106:16:1, unless otherwise
 501 stated in the study. Finally, eqs. 18 & 26 were used to convert between Michaelis-Menten
 502 and disk parameters and eq. 21 was used to determine the initial slope (i.e. ϵ) and half
 503 saturation concentration (i.e. $K_{1/2}$) of Ivlev responses. Note, the maximum clearance
 504 rates reported in Hansen et al. (1997) are synonymous with ϵ once units have been con-
 505 verted.

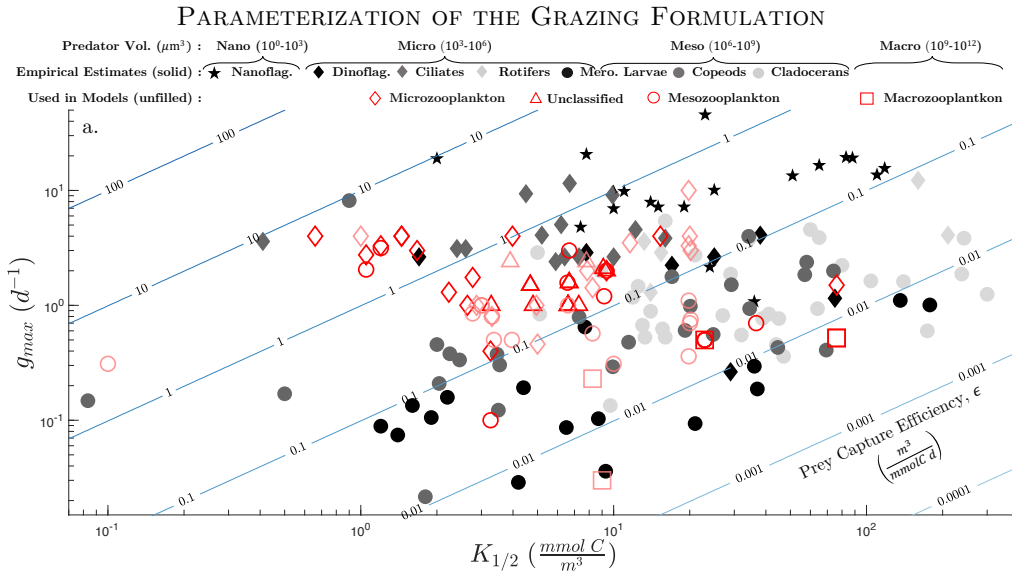


Figure 2. Parameters of the grazing formulation. **a.** Empirical estimates of parameters for >60 zooplankton species (Hansen et al., 1997; Hirst & Bunker, 2003) are plotted with filled markers. Parameters for different zooplankton functional groups from 40 modelling studies (Table 2) are plotted with red empty markers. Light red markers denote formulations with a multiple-prey response and parameters refer to the implied single-prey response when grazing exclusively on their most preferred prey. Contours for the corresponding prey capture efficiency (assuming type-II response) are overlaid.

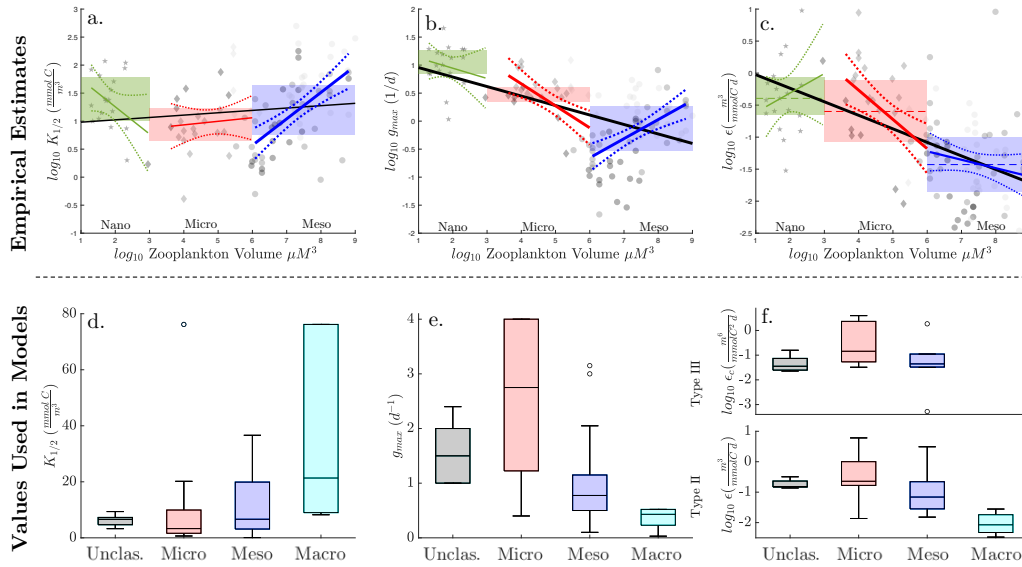


Figure 3. Allometric Relationships. **a-c.** Empirical estimates of all grazing parameters are plotted against zooplankton size and subdivided into size classes. Marker shapes are consistent with species in **Fig. 2**. The interquartile range (IQR) is overlaid for each size class along with a log-linear regression and 95% confidence intervals. A log-linear regression is shown for the complete data set as well (black). Statistically significant correlations have thicker line widths and detailed statistical information is provided in **Table 3a**. **d-f.** Box plots of each grazing parameter in models for each size class. Note, macrozooplankton and nanozooplankton are not included for empirical and model plots, respectively, because less than two of each were surveyed. Additionally, ϵ_c is not shown for the empirical values because all empirical estimates were fit to a type II response.

506

4.1 Empirical estimates

507

508

509

510

511

512

513

514

515

516

517

518

Grazing parameters for a myriad of different zooplankton have been estimated empirically via laboratory incubation and dilution experiments. In these studies, specific grazing rates were measured at different prey concentrations and then fit to a type II response function. Together, reviews by Hansen et al. (1997) and Hirst and Bunker (2003) describe 119 empirical estimates of over 20 functional groups, derived from data on over 200 species. Looking across all surveyed zooplankton, the values of each grazing parameter vary by over three orders magnitude, with $K_{1/2}$ ranging from .08-499 $mmolC/m^3$, g_{max} ranging from 0.02-45.6 d^{-1} , and ϵ ranging from .003-9.5 $\frac{m^3}{mmolCd}$ (**Fig. 2**). While some of this variability can be explained statistically by the large variability in zooplankton size ($10-10^9 \mu m^3$), the strength of the allometric relationship differs with both the parameter in question and whether you are considering all samples or just a subset within a certain size class (**Fig. 3; Table 3**).

519

520

521

522

523

524

525

526

Consistent with Hansen et al. (1997), when considering the entire, combined data set there is a statistically significant allometric relationship between zooplankton size and both g_{max} (**Fig. 3b**; black regression) and ϵ (**Fig. 3c**; black regression). This decrease in the parameters that describe consumption and capture rates, respectively, is consistent with the conventional wisdom that grazing rates decrease with predator size (Moloney & Field, 1989; Peters & Downing, 1984; Saiz & Calbet, 2007; Wirtz, 2013). However, as in Hansen et al. (1997), $K_{1/2}$ values from the combined data set do not exhibit a statistically significant allometric relationship (**Fig. 3a**; black regression), contradicting the

527 notion that $K_{1/2}$ should increase with increasing predator size (Ray et al., 2011). This
 528 can be explained because $K_{1/2}$ is not an independent, physiological parameter, but rather
 529 a mathematical description of the curve, relating the other two parameters that mech-
 530 anistically describe consumption (i.e. g_{max}) and capture (i.e. ϵ) rates (see **Section 2**).
 531 While all parameters are estimated here empirically, only ϵ and g_{max} reflect independent
 532 trait-based differences in grazing behaviour. Therefore, if g_{max} and ϵ both decrease with
 533 zooplankton size, grazing rates will decrease at low and high concentrations such that
 534 the half-saturation concentration may increase, decrease, or remain largely unaltered,
 535 depending of the relative changes. The net effect when considered across all zooplankton
 536 sizes is a flat and not statistically significant (**Table 3a**).

537 Similarly, when grouped into discrete size classes, the mean, median and interquar-
 538 tile range (IQR) of g_{max} and ϵ decrease monotonically from nanozooplankton (**Fig. 3;**
 539 **green**) to microzooplankton (red) to mesozooplankton (blue), while those of $K_{1/2}$ do
 540 not (**Table 3b**). Instead the median value of $K_{1/2}$ decreases from $23 \text{ mmolC}/\text{m}^3$ in nanozoo-
 541 plankton to $8.9 \text{ mmolC}/\text{m}^3$ in microzooplankton but then increases to $18.1 \text{ mmolC}/\text{m}^3$
 542 in mesozooplankton. Of the three parameters, binning by size class does the best job of
 543 explaining variability in distributions of g_{max} , which has the smallest coefficient of vari-
 544 ability (i.e. std/mean) of all parameters in all size classes. Moreover, using a two sam-
 545 ple t-test at the 95% confidence level, g_{max} is the only parameter in which the mean value
 546 in adjoining size classes are statistically different from one another. For ϵ , only nano- and
 547 mesozooplankton have statistically different means, although the difference between micro-
 548 and mesozooplankton is nearly significant ($p=0.1$) and may become so if the binning bounds
 549 were adjusted. For $K_{1/2}$, the range of values in each size class varies by over two order
 550 of magnitude and largely overlaps. In turn, there is no statistically significant difference
 551 between the mean $K_{1/2}$ value within any two size classes, even nano- and microzooplank-
 552 ton which differ by ~ 6 orders of magnitude in volume. Together, empirical estimates
 553 of g_{max} appear better constrained by size class than $K_{1/2}$, or even ϵ , suggesting that con-
 554 sumption rates are better correlated than capture rates with zooplankton size class.

555 However, these trait-based correlations become more complex when looking at vari-
 556 ability within a given size class, rather than across them (**Fig. 3a-c; Table 3a**). Nanozoo-
 557 plankton parameter values are the most poorly constrained by size. When considered
 558 in isolation, there is no statistically significant relationship between any of their empir-
 559 ically derived grazing parameters and size (**Fig. 3a-c; green**). Microzooplankton pa-
 560 rameter values, on the other hand, are the best constrained by size. Both g_{max} (**Fig. 3b;**
 561 **red**) and ϵ (**Fig. 3c; red**) exhibit a robust, statistically significant, inverse relationship
 562 with size, with a higher coefficient of determination (r^2) than in any other size class. In
 563 turn, the correlation between $K_{1/2}$ and size is flat and not statistically significant (**Fig.**
 564 **3b; red**). This is consistent with decreasing capture and consumption rates that com-
 565 bine to lower mean grazing rates but not systematically modify $K_{1/2}$. Mesozooplank-
 566 ton parameter values are also fairly well constrained by size, but in a qualitatively dif-
 567 ferent way. When exclusively considering mesozooplankton (**Fig. 3a-c; blue**), $K_{1/2}$ and
 568 g_{max} both exhibit a statistically significant positive relationship with size, while the re-
 569 lationship with ϵ is flatter and not statistically significant. This suggests that consump-
 570 tion rates in mesozooplankton actually increase with size while capture rates are invari-
 571 ant, leading to an apparent increase in the $K_{1/2}$ (see **eq. 18**). Critically though, this in-
 572 crease in $K_{1/2}$ is associated with faster, not slower, grazing on average.

573 The most common partitioning in models with multiple zooplankton is into two
 574 micro- and mesozooplankton groups (**Table 2**). Nanozooplankton on the other hand only
 575 appear in one surveyed (**Table 2**). When considering exclusively empirical variability
 576 in micro- and mesozooplankton, ignoring nanozooplankton, there is a statistically sig-
 577 nificant correlation with size for all three parameters. Similar to when considering all
 578 zooplankton, g_{max} and ϵ both decrease with size; however, with nanozooplankton removed,
 579 the decline in g_{max} is flatter and less significant (i.e. lower p-value) while the decline in

580 ϵ is steeper and more significant (**Table 3a**). In turn, there is now also a statistically
 581 significant increase in $K_{1/2}$ with size. Additionally, if only considering the IQR of $K_{1/2}$,
 582 there is statistically significant difference in the means value in micro- and mesozooplank-
 583 ton.

584 Accordingly, in biogeochemical models using two discrete zooplankton state vari-
 585 ables to simulate the mean state of micro- and mesozooplankton, it appears the meso-
 586 zooplankton class should have slower consumption (i.e. g_{max}) and capture rates (i.e. ϵ)
 587 than microzooplankton. Further, the empirically observed increase in $K_{1/2}$ means that
 588 the decrease in ϵ should be disproportionately larger than that of g_{max} . However, in dif-
 589 ferent model configurations one may wish to vary different parameters in different ways,
 590 depending on the range and resolution of what you are simulating. For example, a size-
 591 spectrum model of exclusively microzooplankton may wish to decrease both capture and
 592 consumption rates with size, whereas a size spectrum model of exclusively mesozooplank-
 593 ton may wish to increase consumption rates with size and leave capture rates constant.

594 Finally, it is important to note that the way in which these trait-based correlations
 595 can be prescribed depends on the parameter scheme. For example, to increase consump-
 596 tion rates without increasing capture rates in a Michaelis-Menten scheme one must in-
 597 crease g_{max} and $K_{1/2}$ or else otherwise increase ϵ implicitly as well. This would inad-
 598 vertently overestimate grazing rates at low prey densities. However, to increase consump-
 599 tion and capture rates in a Michaelis-Menten scheme one must still increase g_{max} but
 600 the change in $K_{1/2}$ depends on the intended relative difference in the two properties. In
 601 any scenario, all parameters should be computed and considered explicitly to confirm
 602 if the correct behavior is being implied at low and high prey densities.

603 4.2 Values used in models

604 Over 70 independent grazing formulations from 40 modelling studies were surveyed
 605 (**Table 2**, **Fig. 2**; empty markers) to gauge the range of commonly prescribed param-
 606 eter values and investigate if they vary in a manner consistent with the natural variabil-
 607 ity measured empirically (**Sec. 4.1**). A large sampling of prominent modelling studies,
 608 from canonical 0-dimensional theoretical work (Evans & Parslow, 1985; Franks et al., 1986),
 609 through slightly more sophisticated NPZD models (Fasham, 1995; Fasham et al., 1990),
 610 to state-of-the-art CMIP6 earth system models (Aumont et al., 2015; Christian et al.,
 611 2021; Hajima et al., 2020; Law et al., 2017; Long et al., 2021; Stock et al., 2020; Tjipu-
 612 tra et al., 2020; Totterdell, 2019; Yool et al., 2021) were included. Surveyed models were
 613 assessed to determine if their selection of parameter values is representative of the mean
 614 state of empirically estimated values and if variability therein is consistent with the ob-
 615 served allometric variability (**Fig. 3d-f**; **Table 3c**) or varies with other aspects of the
 616 grazing formulation (**Table 3d**).

617 Of the 40 models surveyed, 26 include a zooplankton group that grazes with a single-
 618 prey response, including 5 of 9 IPCC CMIP6 earth system models. This amounts to 40
 619 of the 70 unique grazing formulations. The others graze on multiple prey (**Table 2**; grey
 620 rows & **Figure 3**; light red markers) and use a $K_{1/2}$ parameter that is fundamentally
 621 different from that of the single-prey response (Gentleman et al., 2003). In multiple-prey
 622 response functions, $K_{1/2}$ refers to the half saturation ‘concentration’ of the total, preference-
 623 weighted prey pool, which is not a one-to-one function of the prey distribution. In **Ta-**
 624 **ble 2**, we report this value in parenthesis, but focus our analysis on the implied $K_{1/2}$
 625 for the single-prey response for each zooplankton group when grazing exclusively on their
 626 preferred prey. Gentleman et al. (2003) describe in detail how this value can be calcu-
 627 lated algebraically from the reduced multiple-prey response based on both innate prey
 628 preferences (i.e. constants) and assumptions about whether preferences can vary with
 629 the relative distribution of prey (i.e. switching vs. no switching; Fasham et al. (1990)).
 630 Although the apparent $K_{1/2}$ for a given prey item will increase in the presence of other

Reference	Dimensions (# Z, P tracers)	Location	Zooplankton Functional Group	Grazing Formulation (Single Prey Response)			
				Resp. Type	Parameter Scheme	$K_{1/2}$ ($mmolC/m^3$)	g_{max} ($1/d$)
Wroblewski (1977)	2 (1P1Z) ^N	coastal upwelling	macro	II	Ivlev	76.18	.52
Evans and Parslow (1985)	0 (1P1Z) ^N	N. Atlantic	-	II th	M-M	7.28	
Franks et al. (1986)	0 (1P1Z) ^N	-	meso	II	Ivlev	2.25-45.7	0.16-1.5
Fasham et al. (1990)	0 (1P1Z) ^N	Bermuda	meso	II	M-M	6.6 (6.6)	1
Frost (1993)	1 (1P1Z) ^C	Station P	micro	II th	M-M	2.23	1.01-1.6
Truscott and Brindley (1994)	0 (1P1Z) ^N	coastal (red tide)	meso	III	M-M	36.6	0.7
Fasham (1995)	0 (1P1Z) ^N	Station P	-	II	disk	6.6	1
Franks and Chen (1996)	2 (1P1Z) ^N	Georges Bank	meso	II	Ivlev	22.9	.5
Franks and Walstad (1997)	2 (1P1Z) ^N	-	meso	II	Ivlev	22.9	.5
Denman and Peña (1999)	1 (1P1Z) ^N	Station P	micro	III	M-M	2.64	1
Edwards et al. (2000)	2 (1P1Z) ^N	coastal upwelling	micro macro	II II	Ivlev Ivlev	15.3 22.9	4 0.5
Franks and Chen (2001)	3 (1P1Z) ^N	Georges Bank	meso	II	Ivlev	22.9	.5
Denman and Peña (2002)	1 (1P2Z) ^N	Station P	micro meso	III III	M-M M-M	4.96 (4.96) 3.96 (3.96)	1 0.5
Leising et al. (2003)	0 (1P1Z) ^N	HNLC equatorial Pacific	micro micro micro micro	II II th II III	M-M M-M M-M M-M	0.66 1.45 3.98 1.45	4 4 4 4
Newberger et al. (2003)	0 (1P1Z) ^N	coastal upwelling	micro	II	Ivlev	76.18	1.5
Spitz et al. (2003)	2 (1P1Z) ^N		macro	II	Ivlev	76.18	0.52
Schartau and Oschlies (2003b)	3 (1P1Z) ^N	N. Atlantic	-	III	disk	6.67	1.58
Aumont and Bopp (2006) (PISCES)	3 (2P2Z) ^C	global	micro meso	II II	M-M M-M	20 (20) 20 (20)	4 0.7
Gentleman and Neuheimer (2008)	0 (1P1Z) ^N	-	-	III, II, II, II th	M-M, M-M Ivlev, M-M	4.68	1.5
Stock et al. (2008)	0 (3P4Z) ^N	Low, Mid, High Productivity	nano(100 μ m) micro(1e4 μ m) meso(1e6 μ m) macro(1e8 μ m)	II II II II	M-M M-M M-M M-M	20 (20) 20 (20) 20 (20) 20 (20)	10 3.3 1.1 0.6
Sinha et al. (2010) (PLANKTOM5.2)	3 (3P2Z) ^C	global	micro meso	II II	M-M M-M	11.6 (15) 0.1 (0.26)	3.5 0.31
T. Anderson et al. (2010)	3 (3P2Z) ^C	global	micro meso	I, II, II, III	M-M, M-M, Ivlev, M-M	1 (1) 3 (3)	4 1
Adjou et al. (2012)	0 (2P1Z) ^N	Station P	-	II, III	M-M, disk	6.6	1
Kriest et al. (2012)	3 (1P1Z) ^P	global	-	III	M-M	9.38	2
Shigemitsu et al. (2012) (MEM)	1 (2P3Z) ^N	N. Pacific	micro meso	II th II th	Ivlev Ivlev	3.38 3.28	.4 0.1, 0.4
Dunne et al. (2013) (TOPAZ)	3 (1P0Z)	global	allometric	-	-	-	0.19
Tjiputra et al. (2013) (NORESM1)	3 (1P1Z) ^P	global	-	II	M-M	4.8	1
Hauck et al. (2013) (REcoM2)	3 (2P1Z) ^N	global	<i>micro</i> <i>meso</i>	III III	M-M M-M	3.9 (3.9) 7.8 (3.9)	2.4 2.4
Moore et al. (2013) (BEC)	3 (3P1Z) ^C	global	<i>micro</i> <i>meso</i>	III III	M-M M-M	1.05 1.05	2.05 2.75
Oke et al. (2013) (WOMBAT)	3 (1P1Z) ^N	global	-	III	disk	9.1	2.1
Dutkiewicz et al. (2015) (Darwin)	3 (8P2Z) ^P	global	micro meso	III III	M-M M-M	2.86 (2.86) 3.01 (2.86)	1 1
Le Quéré et al. (2016) (PlankTOM10)	3 (6P3Z) ^C	global	micro meso macro	II II II	M-M M-M M-M	5 (10) 10 (10) 9 (9)	0.46 0.31 0.03
Law et al. (2017) (WOMBAT)	3 (1P1Z) ^N	global	-	III	disk	6.57	1.58
Totterdell (2019) (diat-HadOCC)	3 (2P1Z) ^N	global	<i>micro</i> <i>meso</i>	II II	M-M M-M	3.3 (3.3) 3.3 (3.3)	0.8 0.8
Stock et al. (2020, 2014) (COBALV2, COBALT)	3 (3P3Z) ^N	global	micro meso macro	II II II	M-M M-M M-M	8.28 (8.28) 8.28 (8.28) 8.28 (8.28)	1.42 0.57 0.23
Christian et al. (2021) (CANOE)	3 (2P2Z) ^C	global	micro meso	II II	Ivlev Ivlev	2.77 2.77 (2.77)	1.75 0.85
Yool et al. (2021, 2013) (MEDUSA2.0)	3 (2P2Z) ^N	global	micro meso	III III	M-M M-M	7.65 (5.3) 3.36 (1.88)	2 0.5
Long et al. (2021) (MARBL)	3 (3P1Z) ^C	global	<i>micro</i> <i>meso</i>	II II	M-M M-M	1.2 1.2	3.3 3.15
Hajima et al. (2020) (MIROC)	3 (2P1Z) ^N	global	<i>micro</i> <i>meso</i>	II II	disk disk	9.36 9.36	2 2
Aumont et al. (2015) (PISCESv2)	3 (2P2Z) ^C	global	micro meso	II II	M-M M-M	20 (20) 20 (20)	3 0.75
Tjiputra et al. (2020) (NORESM2)	3 (1P1Z) ^P	global	-	II	M-M	9.76	1.2

Table 2. The parameterization of the grazing formulation in biogeochemical models. The model currency (C,N, or P) is noted in the superscript in column 1 and units of $K_{1/2}$ are converted to carbon where required using a Redfield ratio of 106:16:1 (C:N:P) if not noted in the study. The $K_{1/2}$ relationship algebraically relates the mathematical half saturation concentration ($g(P) = g_{max}/2$) to the parameters specified in the model when not parameterized explicitly. Different zooplankton size classes have separate rows. Values from a given study separated by commas indicate different simulations. Models with a multiple prey response are highlighted in grey and reported $K_{1/2}$ values refer to the implied single-prey response when grazing exclusively on their most preferred prey. In parentheses is the $K_{1/2}$ prescribed for bulk ingestion on the total preference weighted prey field. Models with one zooplankton tracer that grazes separately on two phytoplankton groups with two distinct single-prey responses (i.e. specific grazing rates on one prey group are not effected by the concentration of the other) are considered to have a single-prey response and two implicit zooplankton groups. Implicit functional groups are italicized.

a) Empirical Estimates: Trait-based Correlation with Size

Size Class	$K_{1/2}$			g_{max}			ϵ		
	p	r^2	b	p	r^2	b	p	r^2	b
All Sizes n=119	0.12	0.02	0.04	10^{-11}	0.31	-0.17	10^{-13}	0.37	-0.21
Nano. & Micro. n = 49	0.06	0.07	-0.10	10^{-7}	0.44	-0.24	0.01	0.12	-0.13
Micro & Meso. n=94	10^{-4}	0.13	0.17	0.01	0.06	-0.11	10^{-8}	0.29	-0.27
Nanozooplankton n=19	0.1	0.15	-0.47	0.41	0.04	-0.18	0.35	0.05	0.30
Microzooplankton n=30	0.68	.008	0.06	10^{-4}	0.33	-0.39	10^{-3}	0.29	-0.046
Mesozooplankton n=64	10^{-6}	0.29	0.47	10^{-5}	0.23	0.34	0.18	0.03	-0.13

b) Empirical Estimates: Sample Statistics by Size Class

Size Class	$K_{1/2}$ (mmolC/m ³)				g_{max} (1/d)				ϵ (m ³ /mmolC/d)			
	mean	med.	range	IQR	mean	med.	range	IQR	mean	med.	range	IQR
All zooplankton n=119	40	16	$8.3e^{-2}$ 500	6.4 43	3.7	1.6	$2.1e^{-2}$ 46	0.46 3.8	0.49	$8.4e^{-2}$	$3.4e^{-3}$ 9.5	$2.1e^{-2}$ 0.27
Nanozooplankton n=19	37	23	1.7 120	10 62	13	10	1.1 46	7.0 19	1.1	0.40	$3.0e^{-2}$ 9.5	0.22 0.85
Microzooplankton n=30	25	8.9	0.41 210	4.5 17	3.6	3.0	0.11 12	2.2 4.1	0.71	0.25	$9.1e^{-3}$ 8.8	$9.0e^{-2}$ 0.78
Mesozooplankton n=64	45	18	$8.0e^{-2}$ 500	5.8 45	1.3	0.77	$2.0e^{-2}$ 8.2	0.29 1.8	0.24	$4.0e^{-2}$	$3.4e^{-3}$ 9.1	$1.0e^{-2}$ 0.10

c) Values Used in Models: Sample Statistics by Size Class

Size Class	$K_{1/2}$ (mmolC/m ³)				g_{max} (1/d)				ϵ (m ³ /mmolC/d) *				ϵ_c (m ³ /mmolC ² /d) **			
	mean	med.	range	IQR	mean	med.	range	IQR	mean	med.	range	IQR	mean	med.	range	IQR
All Zoo. (n=70,47*,23**)	11	6.6	0.1 76	3.3 11.6	1.7	1.1	$3.0e^{-2}$ 10	0.7 2.4	0.56	0.15	$3.3e^{-3}$ 6.1	$3.2e^{-2}$ 0.32	0.50	0.04	$5.0e^{-4}$ 4	$3.3e^{-2}$ 0.14
Uncat. (n=14,5*,9**)	6.3	6.6	3.3 9.4	4.7 7.3	1.5	1.5	1.0 2.4	1.0 2.0	0.19	0.15	0.14 0.32	0.15 0.24	$5.6e^{-2}$	$3.5e^{-2}$	$2.3e^{-4}$ 0.16	$2.5e^{-4}$ 4
Nanozoo. (n=1,1*,0**)	20	20	-	-	10	10	-	-	0.51	0.51	-	-	-	-	-	-
Microzoo. (n=25,18*,7**)	9.1	3.3	0.66 76	1.6 9.9	2.4	2.8	0.40 4.0	1.2 4.0	0.96	0.23	$1.4e^{-2}$ 6.1	0.17 1.0	1.2	0.14	4.0 4.0	$6.1e^{-2}$ 2.3
Mesozoo. (n=24,17*,7**)	10	6.6	0.10 37	3.1 20	1.0	0.78	0.10 3.2	0.5 1.2	0.44	$6.9e^{-2}$	$1.5e^{-2}$ 3.1	$2.9e^{-2}$ 0.22	0.31	$4.4e^{-2}$	$5.0e^{-4}$ 1.9	$3.3e^{-2}$ 0.11
Macrozoo. (n=6,6*,0**)	35	21	8.3 76	9 76	0.37	0.43	$3.0e^{-2}$ 0.52	0.23 0.52	$1.2e^{-2}$	$9.9e^{-3}$	$3.3e^{-3}$ $2.8e^{-2}$	$4.7e^{-3}$ $1.8e^{-2}$	-	-	-	-

d) Values Used in Models: Sample Statistics by Grazing Formulation

Grazing Formulation	$K_{1/2}$ (mmolC/m ³)				g_{max} (1/d)				ϵ (m ³ /mmolC/d) *				ϵ_c (m ³ /mmolC ² /d) **			
	mean	med.	range	IQR	mean	med.	range	IQR	mean	med.	range	IQR	mean	med.	range	IQR
Type III (n=23,0*,23**)	6.0	4.0	1.0 37	3.0 6.7	1.7	1.6	0.5 4.0	1 2.1	-	-	-	-	0.50	$4.4e^{-2}$	$5.0e^{-4}$ 4	$3.3e^{-2}$ 0.14
Type II (Ivlev) (n=35,35*,0**)	8.9	7.3	0.1 20	3.5 11	1.9	1.2	$3.0e^{-2}$ 10	0.8 3.1	0.72	0.20	$3.3e^{-3}$ 6.1	0.10 0.49	-	-	-	-
Ivlev (n=12,12*,0**)	29	23	2.7 76	3.3 50	0.97	0.51	0.1 4.0	0.5 1.2	$8.5e^{-2}$	$1.5e^{-2}$	$4.7e^{-3}$ 0.44	$1.4e^{-2}$ 0.13	-	-	-	-
Michaelis-Menten (n=49,32*,17**)	7.8	5.0	0.10 37	12.8 9.2	1.9	1.2	$3.0e^{-2}$ 10	0.79 3.0	0.77	0.19	$3.3e^{-3}$ 6.1	$8.0e^{-2}$ 0.54	0.66	0.11	$5.0e^{-4}$ 4.0	$3.8e^{-2}$ 0.58
disk (n=9,3*,6**)	7.1	6.6	3.2 9.4	6.6 9.2	1.5	1.6	1.0 2.1	1.0 2.0	0.19	0.21	0.15 0.21	0.17 0.21	0.04	$3.6e^{-2}$	$2.3e^{-2}$ $9.3e^{-2}$	$2.5e^{-2}$ $3.6e^{-2}$
Single Prey (n=40,27*,13**)	13	6.6	0.66 76	2.7 9.8	1.8	1.5	0.1 4.0	1.0 2.4	0.75	0.18	$4.7e^{-3}$ 6.1	$1.6e^{-2}$ 0.55	0.52	$3.6e^{-2}$	$5.0e^{-4}$ 2.5	$2.5e^{-2}$ 0.57
Multiple Prey (n=30,20*,10**)	9.3	7.8	0.1 20	3.3 20	1.6	1.0	$3.0e^{-2}$ 10	0.5 2.4	0.29	0.15	$3.3e^{-3}$ 3.1	$3.6e^{-2}$ 0.23	0.5	$7.0e^{-2}$	$3.3e^{-2}$ 3.1	$3.6e^{-2}$ 0.23

Table 3. Statistics from empirically estimated and modelled grazing parameters. **a.** The p-value (p), coefficient of determination (r^2), and slope (b) are displayed for a linear regression fit between the \log_{10} of zooplankton size (μm^3) and the \log_{10} of $K_{1/2}$, g_{max} , and ϵ . Data included in each model is limited to the size class(es) specified in the left column. Statistically significant relationship ($p < 0.05$) are highlighted in blue for positive correlations ($b > 0$) and red for negative correlations ($b < 0$). **b,c,d.** Sample statistics are shown for **b.** empirical values sorted by size classes and **c,d.** model values sorted by size class and other attributes of the grazing formulation. The IQR refers to the Inter-quartile range (i.e. middle 50%). Statistics for ϵ do not include any type III responses and statistics for ϵ_c do not include any type II or Ivlev response. ϵ_c is not shown for the empirical data as a type II response was always assumed.

631 prey options, we consider the implied $K_{1/2}$ for the single-prey response as it is informa-
 632 tive as to how modellers assume zooplankton behave in optimal conditions, grazing ex-
 633 clusively on their preferred prey.

634 Overall, the full range of grazing parameters used in models varies considerably (**Fig.**
 635 **2; empty red markers**). $K_{1/2}$ and g_{max} both vary by over two orders of magnitude,
 636 from 0.1-76 $mmol\ C/m^3$ and 0.03-10 $1/d$, respectively. When converted into a disk pa-
 637 rameter scheme the range is even larger, with ϵ in type II (and Ivlev) response functions
 638 spanning more than 3 orders of magnitude, from $3.3 \cdot 10^{-3}$ to $6.1 \frac{m^3}{mmolCd}$, and ϵ_c in type
 639 III response functions spanning nearly 4 orders of magnitude, from $5.2 \cdot 10^{-4}$ to $4 \frac{m^6}{mmol^2Cd}$.
 640 Considering that these values are used to represent the mean state of many zooplank-
 641 ton, they might be expected to vary substantially less than empirical estimates, which
 642 should be expected to span a large range of natural variability. However, the range of
 643 model values for each parameter exceeds the interquartile range of empirical estimates
 644 (**Table 3b,c**), suggesting that some models may be using unreasonably high or low pa-
 645 rameter values. This is especially true for model values of ϵ , which exceed the interquar-
 646 tile range of empirical estimates by an order of magnitude in both directions. Moreover,
 647 the mean of model and empirical distributions are not statistically similar ($p > 0.05$; 2-
 648 sample t-test) for any parameter. However, this comparison may be biased by intended
 649 differences in the zooplankton functional groups being modelled.

650 Breaking down the model values by size class gives a better indication of how rep-
 651 resentative model values are of empirically estimates (**Fig. 3d-f; Table 3b,c**). Focus-
 652 ing on microzooplankton and mesozooplankton, the most commonly simulated size classes,
 653 the range of $K_{1/2}$, g_{max} , and ϵ for both size classes falls within the range, but beyond
 654 the interquartile range, of their respective empirical estimates. However, relative differ-
 655 ences between the two size classes are generally consistent with observations. Statisti-
 656 cally, modelled consumption (g_{max} ; **Fig. 3e**) and capture (ϵ , ϵ_c ; **Fig. 3f**) rates both de-
 657 cline with zooplankton size and do so in a manner that increases $K_{1/2}$ (**Fig. 3d**).

658 In particular, variability in g_{max} across the two size classes is well aligned with the
 659 observations (**Fig. 3b,e; Table 3b,c**). The median value (and interquartile range) of
 660 g_{max} decreases from 2.75 (1.2-4) in microzooplankton to 0.78 (0.5-1.15) in mesozooplank-
 661 ton models, compared to from 3.0 (2.2-4) to 0.77 (0.3-1.8) in the empirically measured
 662 values. Moreover, there is no statistical difference between the mean of the model and
 663 empirical distributions of g_{max} in either simulated size class. Unsurprisingly, both sets
 664 of model and empirical values reported here are consistent with values of 2-4 $1/d$ and
 665 1 $1/d$, respectively, reported elsewhere throughout the literature (C. A. Edwards et al.,
 666 2000; Gismervik, 2005; Lancelot et al., 2005; Leising, Gentleman, & Frost, 2003; Strom
 667 & Morello, 1998).

668 However, allometric variability in capture rates, either prescribed directly by ϵ (**Fig.**
 669 **3c,f**) and ϵ_c or indirectly by $K_{1/2}$ (**Fig. 3a,d**), is less consistent with observations. The
 670 median value (and IQR) of ϵ decreases from 0.27 (.17-1.79) to 0.14 (.04-.37) in models,
 671 compared to from 0.25 (.09-0.78) to .04 (.01-.09) in the empirically measured values. This
 672 smaller drop in ϵ between size classes in the models is consistent with a smaller increase
 673 in $K_{1/2}$ than observed. The median value (and IQR) of $K_{1/2}$ increases from 3.3 (1.6-9.9)
 674 to 6.6 (3-9.9) in models, compared to from 8.9 (4.5-17) to 18 (5.8-45) in the empirically
 675 measured values (**Table 3b,c**). In turn, the relative decrease in mesozooplankton graz-
 676 ing at low prey concentrations (where capture rates dominate) may be underestimated
 677 in models. This is likely happening because most models that include micro- and meso-
 678 zooplankton use a Michaelis-Menten parameter scheme and vary g_{max} between size classes
 679 but not $K_{1/2}$ (**Table 2**). While this is consistent with the allometric relationships mea-
 680 sured across the full range of zooplankton, it may not be when focusing explicitly on the
 681 difference between micro- and mesozooplankton (**Sec 4.1; Table 3a**). In turn, models
 682 that vary both g_{max} and $K_{1/2}$ (e.g. T. Anderson et al. (2010)) may be more realistic than
 683 those that fix $K_{1/2}$ across size.

684 While the clearest source of variability between model values is justifiably allomet-
685 ric, we additionally checked for differences associated with attributes of the grazing for-
686 mulation (**Table 3d**). The only statistically significant difference related to the grazing
687 formulation was between capture rates prescribed in Ivlev response types compared to
688 those in Holling type III, or even type II, responses. The mean $K_{1/2}$ used in zooplank-
689 ton simulated with an Ivlev response was nearly 5x larger (29 mmolC/m^3) than that
690 used in a type III response (6.0), and over 3x larger than that used in a qualitatively sim-
691 ilar type II response (8.0). Although a disproportionate number of zooplankton simu-
692 lated with a Ivlev response are described as macrozooplankton (50%), mean $K_{1/2}$ val-
693 ues for micro- (24) and mesozooplankton (15) simulated with an Ivlev response are also
694 much higher than the average value used in non-Ivlev type II response functions (7.8 &
695 9.6, respectively). This suggests that $K_{1/2}$ may be systematically overestimated in Ivlev
696 responses, perhaps because the Ivlev parameter is further abstracted from any mecha-
697 nistically meaningful value or intuitive characteristic of the curve. Finally, there was no
698 statistically significant difference between the mean of any parameter value when compar-
699 ing those used in Michaelis-Menten versus disk parameter schemes or when compar-
700 ing single-prey response types with the implied single prey response from multi-prey re-
701 sponse types.

702 5 Sensitivity of the grazing formulation

703 To isolate the sensitivity of phytoplankton population dynamics to the functional
704 response and its parameterization, we extend the sensitivity analysis conducted by Gen-
705 tleman and Neuheimer (2008). We use an identical, idealized, 0-dimensional Nutrient-
706 Phytoplankton-Zooplankton (NPZ) box model to that of Gentleman and Neuheimer (2008),
707 and earlier Franks et al. (1986). This model assumes that phytoplankton (P) grow via
708 uptake of external inorganic nutrients (N) and are lost to zooplankton (Z) grazing and
709 mortality. Nutrients are returned to the inorganic pool via phytoplankton mortality, zoo-
710 plankton mortality and sloppy grazing. Phytoplankton growth follows nutrient limited
711 Michaelis-Menten kinetics (Michaelis & Menten, 1913) and both phytoplankton and zoo-
712 plankton mortality terms are linear. Mass transfer between N, P and Z pools is described
713 by

$$\begin{aligned}
\frac{dN}{dt} &= (1 - \alpha)g([P])Z - \mu_{max} \frac{N}{K_N + N}P + m_pP + m_zZ, \\
\frac{dP}{dt} &= \mu_{max} \frac{N}{K_N + N}P - g([P])Z - m_pP, \\
\frac{dZ}{dt} &= \alpha g([P])Z - m_zZ,
\end{aligned}
\tag{27}$$

714 where α is the grazing efficiency, μ_{max} is the phytoplankton maximum specific growth
715 rate, K_N is the nutrient uptake half saturation constant, m_p is the phytoplankton mor-
716 tality rate, m_z is the zooplankton mortality rate, and $g([P])$ is the grazing formulation
717 (i.e. **eq. 17, 18, 24, or 25**). The model is not forced with seasonality in light, mixing
718 or other environmental conditions, such that μ_{max} is constant and phytoplankton growth
719 is determined only by nutrient availability. Non-grazing parameters and initial condi-
720 tions (**Table 4b**) are identical to Gentleman and Neuheimer (2008), but converted to
721 carbon units using a stoichiometric ratio of C:N = 106:16.

722 Gentleman and Neuheimer (2008) used this model to assess the change in dynamical
723 stability when switching between a type II and III response or doubling/halving $K_{1/2}$
724 and g_{max} . In addition to testing both response types, we go on to test both parameter
725 schemes (disk, Michaelis-Menten) and a much larger range of grazing parameters. This
726 allows for the comparison of gradients across the parameter space between four differ-
727 ent grazing formulations (i.e. Type II-disk, Type III-disk, Type II-Michaelis-Menten, Type

a. The Grazing Formulation					b. Other Parameters and Initial Conditions				
	Response Type	Parameter Scheme	Parameters	Sensitivity Range		Parameter	Value	Sensitivity Range	
$g([P])$	II	disk	ϵ	0.01 – 10	$\frac{m^3}{mmolCd}$	α	Grazing efficiency	0.7	0.35, 1.0
			g_{max}	0.1 – 45		μ_{max}	Phytoplankton maximum specific growth rate	$2 d^{-1}$	1, 4 d^{-1}
	III	disk	ϵ_c	0.01 – 10	$\frac{m^6}{mmolC^2d}$	m_P	Phytoplankton mortality rate	$0.1 d^{-1}$.05, 0.2 d^{-1}
			g_{max}	0.1 – 45		m_Z	Zooplankton mortality rate	$0.2 d^{-1}$	0.1, 0.4 d^{-1}
II	Michaelis-Menten	$K_{1/2}$	100 – 0.1	$\frac{mmolC}{m^3}$	K_N	Nutrient uptake half-saturation constant	$6.6 \frac{mmolC}{m^3}$	3.3, 13.2 $\frac{mmolCl}{m^3}$	
		g_{max}	0.1 – 45		N_0	Nutrient density initial condition	$10.6 \frac{mmolC}{m^3}$	5.3, 21.2 $\frac{mmolC}{m^3}$	
III	Michaelis-Menten	$K_{1/2}$	100 – 0.1	$\frac{mmolC}{m^3}$	P_0	Phytoplankton density initial condition	$1.3 \frac{mmolC}{m^3}$	0.65, 2.6 $\frac{mmolC}{m^3}$	
		g_{max}	0.1 – 45		Z_0	Zooplankton density initial condition	$1.3 \frac{mmolC}{m^3}$	0.65, 2.6 $\frac{mmolC}{m^3}$	

Table 4. List of **a.** grazing formulations and **b.** other parameters and initial conditions used for the NPZ (eq. 27) sensitivity analysis in **Section 5.**

728 III-Michaelis-Menten; see **Table 4a**). Within each grazing formulation, we consider a
 729 range of \log_{10} -spaced values spanning nearly 3 orders of magnitude for both parameters
 730 (**Table 4a**). These ranges are all within the range of empirical estimates (**Fig. 2; Ta-**
 731 **ble 3b**). Note that corresponding grid cells in each panel of **Figs. 5 & 6** do not equate
 732 to identical functional response curves; identical parameter values used in different re-
 733 sponse types or parameter schemes will yield differently shaped curves and thus differ-
 734 ent dynamics. Instead, when comparing panels, we consider differences in gradients across
 735 the parameter space.

736 All 784 combinations of parameters values for each functional response (i.e. 3136
 737 total tests) were integrated for 5 years, after which the system either reached steady state,
 738 quasi state-state (repeating limit cycles), or numerical instability. Integrating any fur-
 739 ther did not meaningfully change our results. We analyse the final year of each integra-
 740 tion, which was long enough to capture limit cycles that had a period of anywhere from
 741 weeks to months. We then assessed how the choice of response type, parameter scheme,
 742 and parameter values influences prescribed grazing rates (**Section 5.1**) and in turn drives
 743 the size (**Section 5.2**) and stability (**Section 5.3**) of the phytoplankton population. The
 744 sensitivity of our results to non-grazing parameters and initial conditions is also exam-
 745 ined (**Table 4b; Section 5.4**).

746 5.1 Sensitivity of grazing rates

747 Modellers can prescribe faster grazing rates by increasing ϵ , ϵ_c , and/or g_{max} in a
 748 disk parameter scheme, or decreasing $K_{1/2}$ and/or increasing g_{max} in a Michaelis-Menten
 749 parameter scheme. Note that while ϵ and g_{max} modify the curve in the same direction
 750 when using a disk formulation, $K_{1/2}$ and g_{max} modify it in opposite directions when us-
 751 ing a Michaelis-Menten formulation, meaning that modellers must ensure parameter changes
 752 do not inadvertently cancel out if modifying both in the same direction. Moreover, the
 753 sensitivity of the shape of the curve and associated grazing rates to these parameters varies
 754 with the parameter scheme, response type, and the prey density (or location on the curve)
 755 in question. To illustrate this, we have provided a schematic showing how proportional
 756 changes in different parameters modify the curve in different ways at low and high $[P]$
 757 values (**Fig. 4**). We then quantify these changes by computing the mean grazing rates
 758 prescribed at low and high $[P]$ values for all curves defined across the entire parameter
 759 space (**Fig. 5**).

760 When using a disk scheme (**Fig. 4**, green), regardless of response type, grazing rates
 761 are determined almost entirely by prey capture rates when food is scarce (Low $[P]$; **Fig.**
 762 **4**, middle row) and by consumption rates when food is replete (High $[P]$; **Fig. 4**, bot-
 763 tom row). This is a direct consequence of the underlying theory, but not necessarily ob-
 764 vious from the terms ‘attack’ or ‘capture rate’. In turn, g_{max} has almost no bearing on
 765 the shape of the curve at low $[P]$ (**Fig. 4f, h**) and ϵ (or ϵ_c) has little influence on the
 766 shape of the curve at high $[P]$; (**Fig. 4i, k**). Moving from a type II (**Fig. 4**, left side)
 767 to III (**Fig. 4**, right side) response switches the description of prey capture rates from
 768 a linear to quadratic function of $[P]$ (see **Section 2**), which decreases the sensitivity of
 769 grazing rates to ϵ_c (relative to ϵ), especially at low $[P]$ (**Fig. e, g**).

770 When using a Michaelis-Menten parameter scheme (**Fig. 4**, magenta), grazing rates
 771 are proportionally, but inversely, affected by changes in $K_{1/2}$ compared to ϵ in a disk scheme
 772 (**Fig. 4a, e, i**), leading to the dark green overlapping curves in the left-most panel of
 773 **Fig. 4**. This occurs because $K_{1/2}$ is equal to $\frac{g_{max}}{\epsilon}$, or equivalently $\frac{1}{\epsilon h}$ (see **Sec. 2.3**),
 774 and g_{max} (and its reciprocal, h) are held constant. However, in a type III response, graz-
 775 ing rates are substantially more sensitive to $K_{1/2}$ than ϵ_c , (**Fig. 4c, g, k**), particularly
 776 at low prey densities (**Fig. 4g**). Moreover, in both a type II and III response, the Michaelis-
 777 Menten scheme is dramatically more sensitive to g_{max} at low prey densities (**Fig. 4f,**
 778 **h**). This is because faster (slower) prey capture rates and thus a larger prey capture ef-
 779 ficiency are implicitly required for the curve to saturate at a faster (slower) grazing rate
 780 with the same half saturation concentration.

781 Computing the mean grazing rate across low ($0-0.5 \frac{mmolC}{m^3}$) and high ($10-15 \frac{mmolC}{m^3}$)
 782 phytoplankton concentrations ($[P]$) for all grazing formulations considered in our sensi-
 783 tivity analysis (**Table 4**) confirms these trends (**Fig. 5**). In a type II disk formulation,
 784 grazing rates at low $[P]$ are almost entirely unaffected by g_{max} , especially when ϵ is low
 785 (**Fig. 5a**), whereas grazing rates at high $[P]$ are almost entirely driven by g_{max} , espe-
 786 cially when ϵ is large (**Fig. 5b**). Introducing the concavity of a Type III response in-
 787 creases this disparity. In turn, the mean grazing pressure at low $[P]$ increases with ϵ_c but
 788 is effectively invariant across 3 orders of magnitude change in g_{max} (**Fig. 5c**). Alterna-
 789 tively, mean grazing rates at high $[P]$ are almost entirely described by g_{max} unless ϵ_c is
 790 so low that our definition of ‘high $[P]$ ’ no longer falls above the half saturation point of
 791 the curve (**Fig. 5d**).

792 Using a Michaelis-Menten scheme increases the sensitivity of grazing rates to both
 793 parameters (**Fig. 5e-h**), such that g_{max} has much more influence at low $[P]$ (**Fig. 5e,**
 794 **g**) and $K_{1/2}$ has more influence at high $[P]$ (**Fig. 5f, h**). However, in a type III response,
 795 grazing rates are still more sensitive to $K_{1/2}$ than g_{max} at low $[P]$ (**Fig. 5g**) and more
 796 sensitive to g_{max} than $K_{1/2}$ at high $[P]$ (**Fig. 5h**). Increased parameter sensitivity in
 797 the Michaelis-Menten scheme means that a greater variety of curve shapes and associ-
 798 ated grazing rates can be described with an equivalent range of parameter values, albeit
 799 with lower resolution. This means that there should be more variability in model out-
 800 put derived from equivalent changes in Michaelis-Menten versus disk parameters.

801 In other words, in a Michaelis-Menten scheme a smaller range of parameters can
 802 test the same range of curves, but many intermediate options will be skipped.

803 5.2 Sensitivity of phytoplankton population size

804 The mean size of the phytoplankton population, $\overline{[P]}$, (**Fig. 6**, left column) is largely
 805 driven by the shape of the functional response at low phytoplankton concentrations and
 806 unaffected by the curve as it begins to saturate at high phytoplankton concentrations.
 807 For example, $\overline{[P]}$ is 14% lower in type II than analogously parameterized type III responses
 808 (i.e. same $K_{1/2}$ and g_{max}), despite the fact that a type II response takes much longer
 809 to reach maximum grazing rates (i.e. saturation), and prescribes slower grazing at all
 810 prey concentrations above $K_{1/2}$. This disparity increases to 58% when only considering

SCHMATIC OF THE FUNCTIONAL RESPONSE CURVE

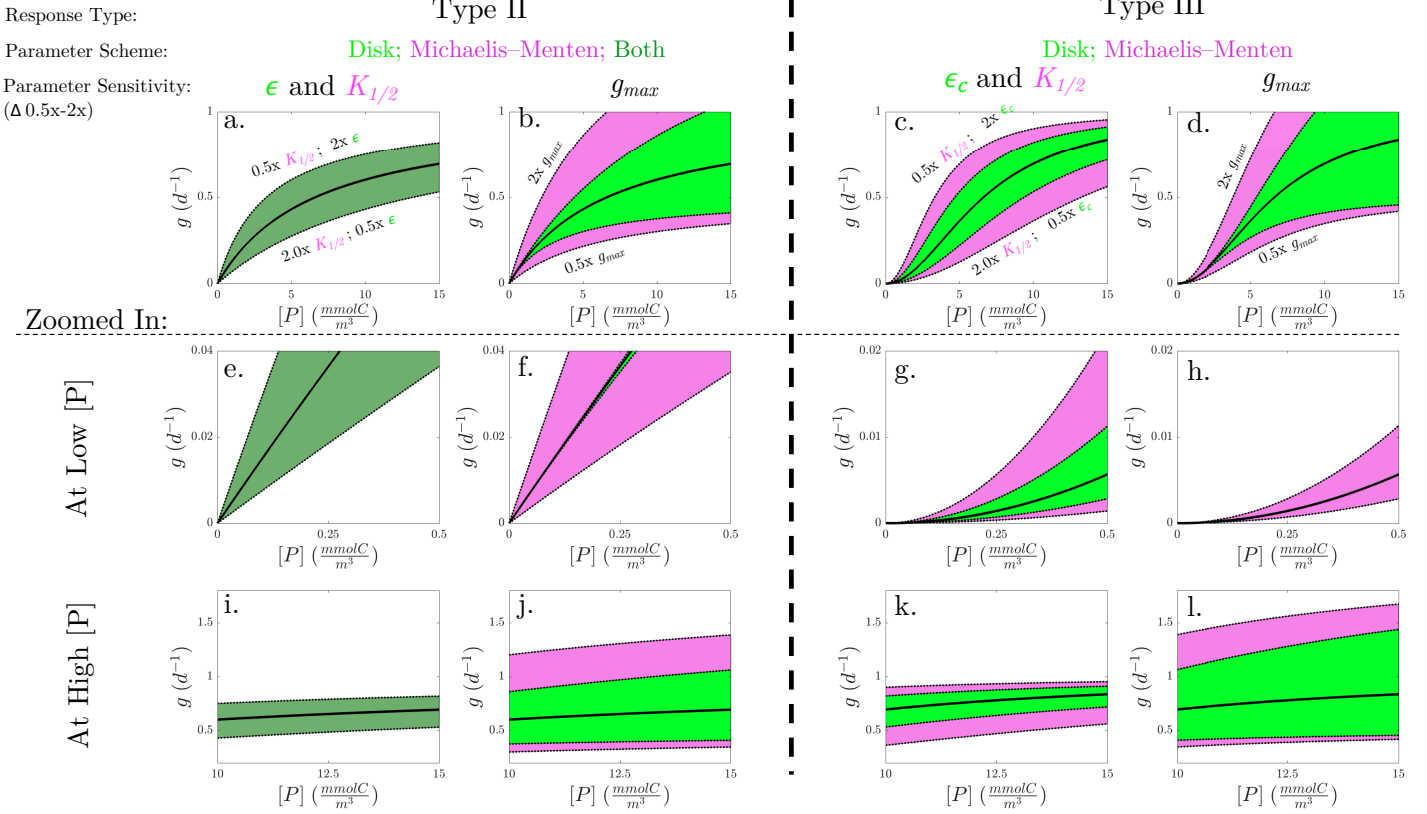


Figure 4. Schematic of the functional response curve. A type II (a,b) and III (c,d) response curve is plotted in black with colored windows depicting how the curve varies with proportional changes to its parameters. Initial parameters were chosen such that the disk and Michaelis-Menten parameter schemes yield mathematical identical curves ($g_{max} = 1$, $K_{1/2} = 6.625$). Colored windows show how the curve varies when its parameters are individually halved (0.5x) or doubled (2x) within a disk (green) or Michaelis-Menten (magenta) parameter scheme. The shaded region depicts the range of curves encompassing a 0.5x-2x change in the associated parameter. Close ups of the same curves are shown below for (e-h) low and (i-l) high phytoplankton concentrations. Annotations in Row 1 show which curves correspond to which parameter modification. Note the dark green shading in (a,e & i) indicates a complete overlap in the variability window for both parameter schemes.

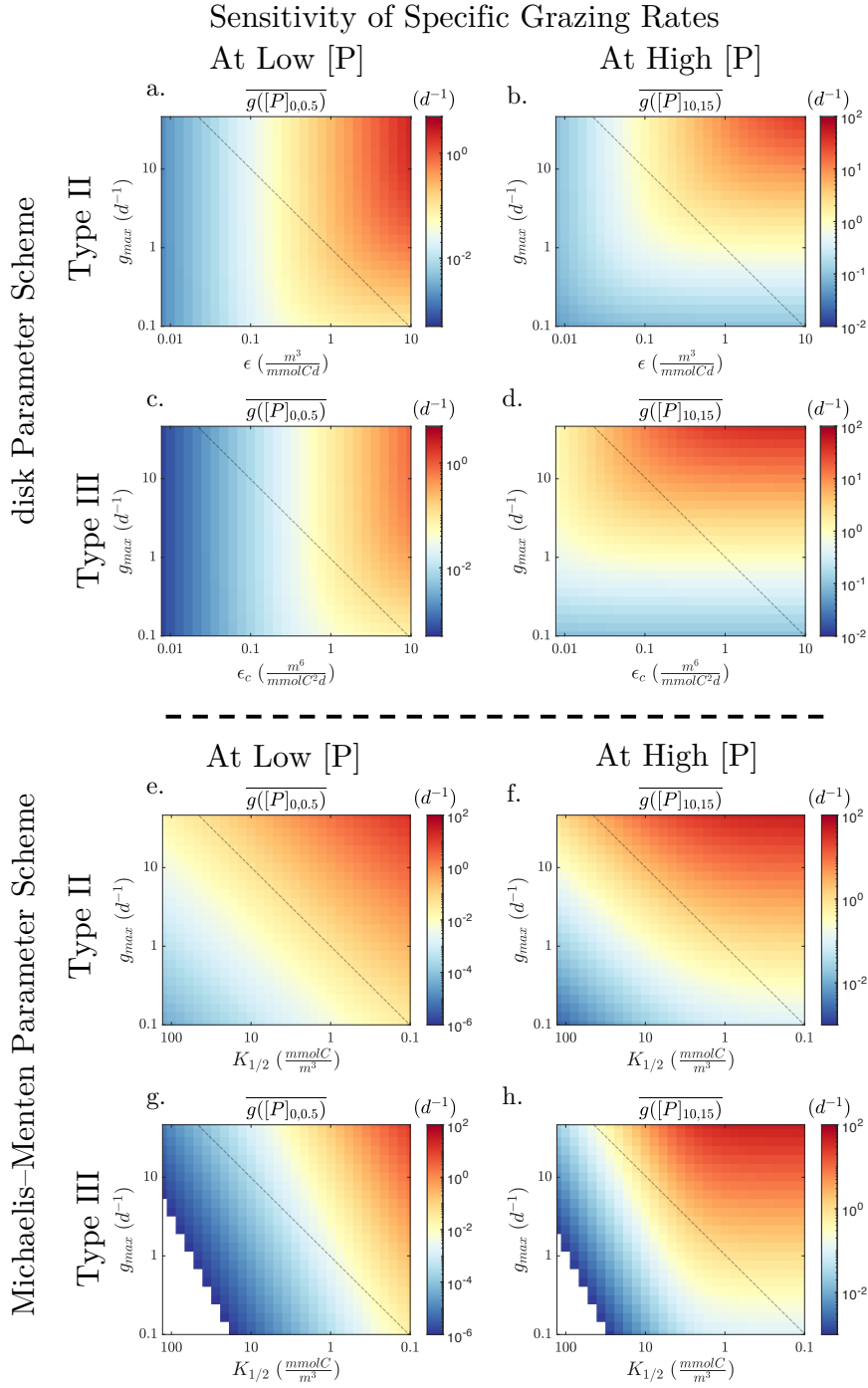


Figure 5. Sensitivity of specific grazing rates. Variability in the mean zooplankton specific grazing rate averaged across (a, c, e, g) low ($[P] < 0.5 \frac{\text{mmolC}}{\text{m}^3}$) and (b, d, f, h) high ($10 < [P] < 15 \frac{\text{mmolC}}{\text{m}^3}$) phytoplankton concentrations ($[P]$) is shown as a function of the parameters of the functional response curve using a (a, b, e, f) Type II and (c, d, g, h) Type III response type, as well as a (a-d) disk and (e-h) Michaelis-Menten parameter scheme. The range of low and high $[P]$ correspond to the zoomed in panels of the schematic in **Fig. 4**. A dashed log 1:1 line is included to assess the relative parameter sensitivity.

Sensitivity of Phytoplankton Population Dynamics

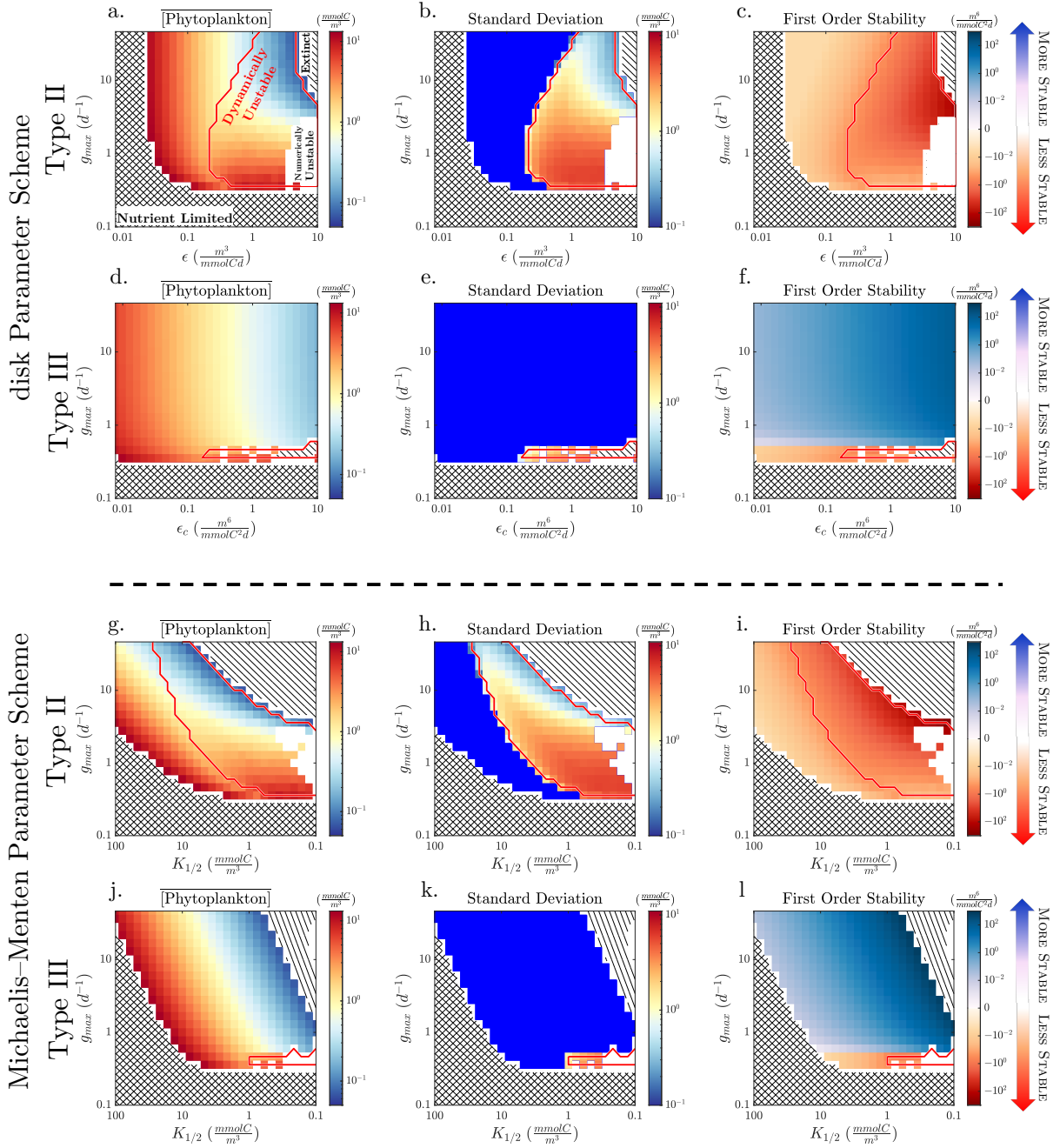


Figure 6. Sensitivity of phytoplankton population dynamics. Variability in the (a, d, g, j. mean annual phytoplankton concentration, (b, e, h, k. standard deviation, and (c, f, i, l. First Order Stability of the solution are plotted against the parameterization of the functional response curve using a (a-c, g-j. Type II and (d-f, j-l. Type III response type as well as a (a-f. disk and (g-l. Michaelis-Menten parameter scheme. Parameter schemes that yield complete nutrient utilization or phytoplankton extinction are hatched out with cross or single lines, respectively. Dynamically unstable regions are bounded with a red contour, while dynamically stable solutions have a near-zero standard deviation and appear blue in b, e, h, k. Numerically unstable regions are plotted in white. Note that the dynamics and stability of the disk and Michaelis-Menten parameter schemes are identical when their parameters overlap (i.e. $\epsilon_c = g_{max}/K_{1/2}$ or $\epsilon_c = g_{max}/K_{1/2}^2$)

811 stable solutions that have neither gone extinct nor reached complete nutrient limitation
 812 (see **Section 5.3**). This occurs because $\overline{[P]}$ dynamics are more sensitive to grazing when
 813 prey $[P]$ is low and a type II response imposes faster grazing than its type III analogue
 814 below $K_{1/2}$.

815 The out-sized importance of the grazing rates at low $[P]$ is even more noticeable
 816 in the type III response. Considering all dynamically solutions, $\overline{[P]}$ has a much stronger
 817 correlation with mean grazing rates at low $[P]$ ($r^2 = 0.97$) than high $[P]$ ($r^2 = -0.53$).
 818 Accordingly, the sensitivity of $\overline{[P]}$ to the grazing formulation qualitatively mirrors the
 819 sensitivity of mean grazing rates at low $[P]$ to the grazing formulation (**Fig. 5, 6**, left
 820 columns). Ecologically, this implies that the size of phytoplankton populations is lim-
 821 ited by zooplankton capture rates, which dominate when prey is scarce, not consump-
 822 tion rates, which dominate when prey is abundant and the zooplankton community is
 823 more likely to be larger and capable of exerting strong grazing pressure, regardless of the
 824 speed of zooplankton specific grazing rates.

825 In turn, $\overline{[P]}$ is most sensitive to the parameterization of the response curve when
 826 the response type and parameter scheme allow for those parameters to most efficiently
 827 describe the bottom of the response curve. This means $\overline{[P]}$ is less sensitive to the param-
 828 eterization of the functional response in a disk than Michaelis-Menten parameter scheme.
 829 For example, phytoplankton in a type III disk scheme only experienced extinction or com-
 830 plete nutrient utilization in 20% of the tested parameter space (**Fig. 6d**), compared to
 831 40% when using a type III Michaelis-Menten scheme (**Fig. 6j**). The size of the inter-
 832 mediate solution space will vary with other parameter choices and the size of the nutri-
 833 ent pool; however, the fact remains that a smaller range of parameters is needed to span
 834 from extinction to complete nutrient utilization in a Michaelis-Menten than disk scheme.
 835 Similarly, when using a type III response, $\overline{[P]}$ is more sensitive to $K_{1/2}$ and ϵ_c than g_{max}
 836 in both parameter schemes because they more directly define the shape of the response
 837 curve when prey is scarce (**Fig. 4g, h**). The value g_{max} has almost no influence on the
 838 size of the phytoplankton population in a type III disk scheme.

839 **5.3 Sensitivity of phytoplankton population stability**

840 In the simplified NPZ model, with no seasonal forcing, phytoplankton populations
 841 tend to quickly reach a seasonally invariant steady state. However, if the destabilizing
 842 influence of the functional response is large enough, dynamically unstable oscillations (i.e.
 843 limit cycles) in the phytoplankton population can emerge. The magnitude of the desta-
 844 bilizing (or stabilizing) influence of the grazing formulation is determined by both the
 845 curvature the functional response as well as the prognostic feedback of grazing on the
 846 phytoplankton population, which determines its the position on the curve. We approx-
 847 imate the magnitude of this stabilizing influence with the First Order Stability (**Fig. 6c,**
 848 **f, i, l**), defined as the first derivative of clearance rates (see **Sec. 3**) calculated at the
 849 mean phytoplankton concentration in year 5 of the solution. Larger negative values, for
 850 example, mean that the grazing formulation has a more destabilizing influence on the
 851 mean phytoplankton population, but does not necessarily determine if the system is dy-
 852 namically unstable, as other stabilizing processes could dominate.

853 To determine if the system is dynamically unstable, we investigated whether os-
 854 cillations emerged. The strength of these oscillations was approximated by the standard
 855 deviation of the phytoplankton population (**Fig. 6b, e, h, k**). The system was deemed
 856 stable if it reached roughly steady state by year five of the integration and exhibited a
 857 near-0 standard deviation (plotted in blue). The system was deemed dynamically un-
 858 stable if the standard deviation in year 5 is greater than 0.5% of the total nutrient pool.
 859 The system was further deemed numerically unstable if Matlab's ode45 solver, a stan-
 860 dard non-stiff integration technique, was unable to meet the integration tolerance with-
 861 out reducing the integration time-step below the smallest allowed. This occurs when the

862 initial slope of the functional response curve is exceedingly steep (i.e. high ϵ), allowing
 863 for large changes in grazing, even at slow integration time-steps, causing the solution to
 864 explode toward negative or positive infinity. Such solutions are theoretically attainable
 865 using a smaller time-step or more sophisticated stiff integration technique but are not
 866 necessary for our purposes. Here, we only flag the numerically parameter combinations
 867 as too stiff to be solved with a standard non-stiff integration technique at a reasonable
 868 time-step.

869 The phytoplankton population remains dynamically stable, with a near zero stan-
 870 dard deviation (**Fig. 6b, e, h, k**, blue shading), when First Order Stability is positive
 871 or slightly negative (**Fig. 6c, f, i, l**). However, the phytoplankton population begins to
 872 oscillate, exhibiting much larger standard deviations, once First Order Stability becomes
 873 sufficiently negative. It is possible for a dynamically stable solution with negative First
 874 Order Stability to emerge if other stabilizing factors dominate the destabilizing influenc-
 875 ing of the grazing formulation. First Order Stability, as defined here, is only a measure
 876 of the stabilizing (or destabilizing) influence of the grazing formulation and other factors
 877 can provide a stabilizing feedback on the phytoplankton population. In this model,
 878 these factors include nutrient limitation and the size of the zooplankton community, which
 879 both increasingly dampen phytoplankton population growth as phytoplankton biomass
 880 accumulates, even if specific grazing rates decline. In more complicated NPZ models other
 881 factors, including more complex closure schemes such as quadratic zooplankton mortal-
 882 ity, can provide stability as well (A. M. Edwards & Yool, 2000; J. H. Steele & Hender-
 883 son, 1992). Conversely, in this simple model, oscillations never occur when First Order
 884 Stability is positive, even when initial conditions are varied by 0.5-2x (**Table 4b**). How-
 885 ever, it is possible that in longer simulations of more complex models with other desta-
 886 bilizing factors, they may.

887 When using a type II response (**Fig. 6**; rows 1 & 3), First Order Stability is al-
 888 ways negative and the phytoplankton population in 53% of tested solutions was either
 889 dynamically unstable (37.5%, red contour), numerically unstable (5.5%, white), or ex-
 890 tinct (10%, diagonal hash). Increasing g_{max} and decreasing $K_{1/2}$ both decrease stabil-
 891 ity; however, when using a Michaelis-Menten parameter scheme, the First Order Stabili-
 892 ty is, on average, ~ 5 times more sensitive to changes in $K_{1/2}$ than g_{max} due to its greater
 893 influence on the curvature of the functional response. In a disk scheme, however, First
 894 Order Stability is only 0.25 times more sensitive to ϵ than g_{max} , because both param-
 895 eters influence the location of $K_{1/2}$. Because the stability of the population is much more
 896 sensitive to g_{max} than the size of the population, relatively small changes in g_{max} could
 897 trigger sudden instabilities with little warning.

898 When using a type III response (**Fig. 6**; rows 2 & 4), First Order Stability is rarely
 899 negative. Only 5.5% of tested solutions were dynamically (1.7%) or numerically (3.8%)
 900 unstable and less than 4% led to phytoplankton extinction. First Order Stability becomes
 901 increasingly stable with increasing g_{max} and decreasing $K_{1/2}$ because increasing graz-
 902 ing pressure drives $[P]$ below $K_{1/2}$, where the upward concavity of the response curve
 903 provides stability and protects against extinction. This holds even though decreasing $K_{1/2}$
 904 simultaneously lowers the threshold for instability. There is only negative First Order
 905 Stability and oscillations in the phytoplankton population when both $K_{1/2}$ and g_{max} are
 906 very low. This occurs because as the g_{max} approaches the zooplankton mortality rate,
 907 zooplankton net population growth slows, decoupling $[P]$ and $[Z]$ and allowing $[P]$ to es-
 908 cape grazing pressure and exceed a low $K_{1/2}$ value.

909 5.4 Influence of other parameters

910 The sensitivity of phytoplankton population size to the grazing formulation does
 911 not appear to be qualitatively influenced by the selection of other non-grazing param-
 912 eters or initial conditions (see **Table 4b**); however, these choices influence the size of the

913 stable solution space. Nutrient limitation is described by a type II Michaelis-Menten curve
 914 and thus has similar, but qualitatively opposite, stabilizing properties to the grazing for-
 915 mulation. The difference is that the saturation of nutrient uptake provides a negative,
 916 rather than positive, feedback on phytoplankton population growth. In turn, increas-
 917 ing the maximum phytoplankton specific division rates (μ_{max}) or decreasing the half sat-
 918 uration concentration for nutrient uptake (K_N) both increase the stability of the sys-
 919 tem and reduce the number of unstable solutions. On the other hand, our results agree
 920 with previous work that limiting zooplankton community growth by either increasing
 921 zooplankton mortality (m_Z) or reducing grazing efficiency (α) can increase the desta-
 922 bilizing influence of a type II (or Ivlev) response (Edwards et al., 2000a, b, GN08) (C. Ed-
 923 wards, Powell, & Batchelder, 2000; C. A. Edwards et al., 2000; Gentleman & Neuheimer,
 924 2008). We go on to show that this can even occur in a type III response if $m_Z > \alpha g_{max}$
 925 (**Fig. 6e,k**), thereby decoupling specific grazing rates from bulk grazing pressure (i.e.
 926 $g[Z]$). Reallocating the initial distribution of nutrients between the $[N]$, $[P]$, and $[Z]$ pools
 927 had little influence on stability. However, as similiarly shown by Franks and Chen (1996,
 928 2001), increasing the total nutrient pool increases the number of unstable solutions by
 929 diminishing the stabilizing influence of nutrient limitation.

930 6 Sensitivity to sub-grid scale heterogeneity

931 Mechanistic derivations (**Sec. 2**) and empirical approximations (**Sec. 4**) of the func-
 932 tional response are based on communities that are spatially well-mixed. Therefore, the
 933 shape and sensitivity of the functional response is predicated on the assumption that a
 934 homogeneously distributed zooplankton community is grazing on a homogeneously dis-
 935 tributed phytoplankton population. However, the ocean is notoriously patchy, with global
 936 plankton distributions highly heterogeneous at scales well below the typical resolution
 937 of even eddy-resolving ocean models (Ohman, 1990; Raymont, 2014). Phytoplankton and
 938 zooplankton communities are often log-normally distributed (J. Campbell, 1995; Druon
 939 et al., 2019), such that an increase in the mean plankton concentration is associated with
 940 a disproportionate increase in smaller areas of high productivity, surrounded by large
 941 swaths of lower productivity. In turn, the functional response used in global, or even coarse
 942 regional models, is likely to be implicitly averaged over substantial sub-grid scale het-
 943 erogeneity.

944 Ideally, coarse models should strive to prescribe how mean specific grazing rates,
 945 \bar{g} , averaged across a grid-cell, vary with the grid-cell mean phytoplankton population,
 946 $[P]$. However, this apparent mean functional response ($\bar{g}([P])$) can differ substantially
 947 from the local response of individual zooplankton ($g([P])$) when averaged across sufficient
 948 sub-grid scale heterogeneity. Notably, Morozov and Arashkevich (2008, 2010) have shown
 949 the emergence of upward concavity in $\bar{g}([P])$ when averaged across a 1-D water column
 950 model, even though $g([P])$ was prescribed with a type II response. These modelling stud-
 951 ies were further supported by field work (Morozov et al., 2008) and led Morozov to ad-
 952 vocate for the emergence of the type III response as a more appropriate representation
 953 of dynamics integrated vertically across the water column (Morozov, 2010). Critical to
 954 this finding were the conditions that: 1) The vertical distribution of prey becomes more
 955 heterogeneous as the mean state increases due to nonlinear effects of light attenuation
 956 and self-shading (Herman & Platt, 1983); and 2) Zooplankton can take advantage of this
 957 disparity through active vertical migration (Giske, Rosland, Berntsen, & Fiksen, 1997;
 958 Herman & Platt, 1983; Lampert, 2005). In turn, increasing the mean prey field coincides
 959 with: 1) An increase in the discrepancy between the depth-averaged prey concentration
 960 and that of high density layers; and 2) An increase in the relative proportion of zooplank-
 961 ton grazing in those high density layers. Together, this is capable of yielding an expo-
 962 nential increase in the mean grazing rate with the mean prey concentration (i.e. Type
 963 III), even if the local response is linear (i.e. Type II).

964 We further generalize these results by examining a simple non-dimensional system
 965 (or grid cell) composed of just two regimes: one fraction of high productivity water, and
 966 one fraction with low productivity water. Unlike Morozov and Arashkevich (2008), in
 967 which the biological rates in each vertical layer are explicitly linked via the active mi-
 968 gration of zooplankton and the attenuation of light due to shelf-shading, our two frac-
 969 tions can be considered independent. This has the advantage of considering the effect
 970 of averaging across two distinct ecological niches in a coarse grid cell, rather than one
 971 tightly coupled system. This is an important distinction because because uncoupling the
 972 system decreases the degree of inherent non-linearity (e.g. in Morozov and Arashkevich
 973 (2008) increasing phytoplankton growth rates in one layer necessarily decrease growth
 974 rates in the layer below via shelf-shading). Further, general circulation models have much
 975 higher vertical (10 m) than horizontal resolution (10-100s km), most biogeochemical mod-
 976 els already resolve self-shading, and future generation models may include active verti-
 977 cal migration as well (Archibald, Siegel, & Doney, 2019). Thus, future models may ex-
 978 plicitly account for the mechanisms that lead to the emergence of a type III response in
 979 the vertical, but still implicitly average across a great deal of ecological heterogeneity hor-
 980 izontally. In this way our generalized 0-D representation may be a more useful analogue
 981 to a 3D grid-cell, as it is not tied to specific mechanisms that operate vertically. Our re-
 982 sults show that averaging across a spatially patchy ocean fundamentally changes the shape
 983 of the apparent mean functional response, even without direct interaction between the
 984 oligotrophic and eutrophic parts of the grid cell. We show how this averaging can increase
 985 apparent mean capture rates, induce upward concavity at low $\overline{[P]}$, and increase the sen-
 986 sitivity of mean specific grazing rates to local consumption rates.

987 We assume a generic model grid cell is divided into two regimes, one fraction with
 988 high productivity eutrophic water, f_{eu} and one fraction with low productivity oligotrophic
 989 water, f_{ol} ($f_{eu} + f_{ol} = 1$). All zooplankton are assumed to graze according to the same
 990 local functional response, $g([P])$, but the sub-grid scale distributions of phytoplankton
 991 ($[P]_{eu}$, $[P]_{ol}$) and zooplankton ($[Z]_{eu}$, $[Z]_{ol}$) biomass are assumed to be heterogeneous
 992 and allowed to vary in time. The phytoplankton population is assumed to grow expo-
 993 nentially with a different growth rate in each region (μ_{ol} , μ_{eu}).

994 The concentration of zooplankton biomass in either region is assumed to be pro-
 995 portional to the distribution of phytoplankton. This is a similar assumption to that made
 996 by Morozov and Arashkevich (2010), who assume that zooplankton biomass co-varies
 997 with prey abundance across the water column. In the vertical, this assumption is well
 998 supported by observations of zooplankton aggregating in food-rich layers (Giske et al.,
 999 1997; Herman & Platt, 1983; Lampert, 2005). While it is difficult to observe individual
 1000 lateral migration in the open ocean (Pearre, 2003), it is plausible that zooplankton, known
 1001 to forage vertically between different depths based on the balance between predation risk
 1002 and hunger (Pearre, 2003; Pierson, Frost, & Leising, 2013), may drift with currents for
 1003 longer at depth between unsuccessful forays to the surface, before vertically migrating
 1004 less and staying closer to the surface once they find food (Bandara, Varpe, Wijewardene,
 1005 Tverberg, & Eiane, 2021). This would lead to a similar consolidation of zooplankton around
 1006 horizontally distributed high-density prey patches. More importantly, active individual
 1007 migration of zooplankton is not a necessary assumption here. In the work of Morozov
 1008 and Arashkevich (2010) and Morozov and Arashkevich (2008), active migration was re-
 1009 quired to account for shifts in the zooplankton distribution because the short time scale
 1010 considered precluded substantial population growth (note that many zooplankton - es-
 1011 pecially microzooplankton and some mesozooplankton and macrozooplankton - exhibit
 1012 very little vertical migration). However, by considering two distinct ecological niches, as-
 1013 sumed to exist in the same grid cell but implicitly averaged over larger space and time
 1014 scales, the population of zooplankton needs only to be assumed to increase faster in re-
 1015 gions with higher prey abundance (and thus higher grazing and growth rates) for the re-
 1016 lative distribution of zooplankton to shift towards more eutrophic patches as the grid cell

1017 mean prey concentration increases. Therefore, no assumptions regarding active migra-
 1018 tion are required.

1019 The concentration of phytoplankton and zooplankton in either fraction of the grid
 1020 cell ($R = eu, ol$) can then be computed at a given time as

$$[P]_R = [P]_{R,t=0}(1 + \mu_R)^t \quad (28)$$

$$[Z]_R = \theta \frac{[P]_R}{[P]}, \quad (29)$$

1021 where $[P]_{R,t=0}$ is the initial concentration and θ is the proportionality constant for zoo-
 1022 plankton biomass. Finally, the apparent grid cell mean specific grazing rate, \bar{g} , and phy-
 1023 toplankton concentration, $\overline{[P]}$, can be calculated as

$$\overline{[P]} = (f_{eu}[P]_{eu} + f_{ol}[P]_{ol}) \quad (30)$$

$$\bar{g} = g([P]_{eu}) \frac{[Z]_{eu}f_{eu}}{Z_{tot}} + g([P]_{ol}) \frac{[Z]_{ol}f_{ol}}{Z_{tot}}, \quad (31)$$

1024 where Z_{tot} is the sum of all zooplankton in the grid cell (i.e. $Z_{tot} = [Z]_{eu}*[f]_{eu} + [Z]_{ol}*$
 1025 f_{ol}). Note that θ cancels out in **eq. 31**. The spatially-averaged, apparent mean func-
 1026 tional response, $\bar{g}(\overline{[P]})$, can then be examined by plotting all values of $\overline{[P]}$ against \bar{g} (**Fig.**
 1027 **7**).

1028 We consider two scenarios. In the first scenario (**Fig. 7a, b**), all biology is assumed
 1029 to be consolidated in the eutrophic fraction of the grid cell (i.e. $[P]_{ol,t=0}$, μ_{ol} , $[P]_{ol}$ and
 1030 $[Z]_{ol}$ all equal 0). In this scenario it does not matter what the initial concentration or
 1031 growth rate of phytoplankton in the euphotic region is because the relative distribution
 1032 is constant (i.e. $[P]_{eu}f_{eu}/[P]_{Tot} = 1$) and the grid-cell mean specific grazing rate, \bar{g} ,
 1033 reduces to the local response, $g([P]_{eu})$. However, $\overline{[P]}$ is less than $[P]_{eu}$ as it is diluted
 1034 by the oligotrophic fraction. We consider a local type II (**Fig. 7a**) and type III (**Fig.**
 1035 **7b**) response. In both cases, the qualitative shape of $\bar{g}(\overline{[P]})$ is consistent with the local
 1036 response; however, there is a decrease in the half saturation concentration of $\bar{g}(\overline{[P]})$ which
 1037 is proportional to the size of the euphotic fraction of the grid cell, such that $\bar{K}_{1/2} = f_{eu}K_{1/2}$.
 1038 This occurs because all zooplankton are actually grazing on a phytoplankton concentra-
 1039 tion ($[P]_{eu}$) that is $1/f_{eu}$ larger than the grid cell mean. In turn, as biological produc-
 1040 tivity is consolidated into a smaller fraction of the grid cell, the apparent capture rate
 1041 appears to increase (i.e. the initial slope of the curve steepens). However, this occurs not
 1042 because local capture rates increase, but because zooplankton are grazing at saturation
 1043 in a smaller area.

1044 Note that unlike the results of Morozov and Arashkevich (2008) and Morozov and
 1045 Arashkevich (2010), this deformation of the mean response does not require any assump-
 1046 tions about how the distribution of phytoplankton or zooplankton biomass varies with
 1047 the mean concentration. This is not necessarily inconsistent with their findings that such
 1048 conditions are required for the emergence of a type III mean response because here it
 1049 is only the apparent parameters of the mean response, not the response type itself, that
 1050 changes. However, it is clear that a much simpler set of assumptions, only that the ocean
 1051 is patchy and a given grid-cell likely includes some swaths of relatively oligotrophic wa-
 1052 ter, can lead to dramatic differences between the local and mean functional response.

1053 In the second scenario (**Fig. 7c-f**) we assume that all water contains at least some
 1054 biomass, but that phytoplankton population growth is faster in the eutrophic fraction.
 1055 Here, phytoplankton biomass begins uniformly distributed with an initial concentration

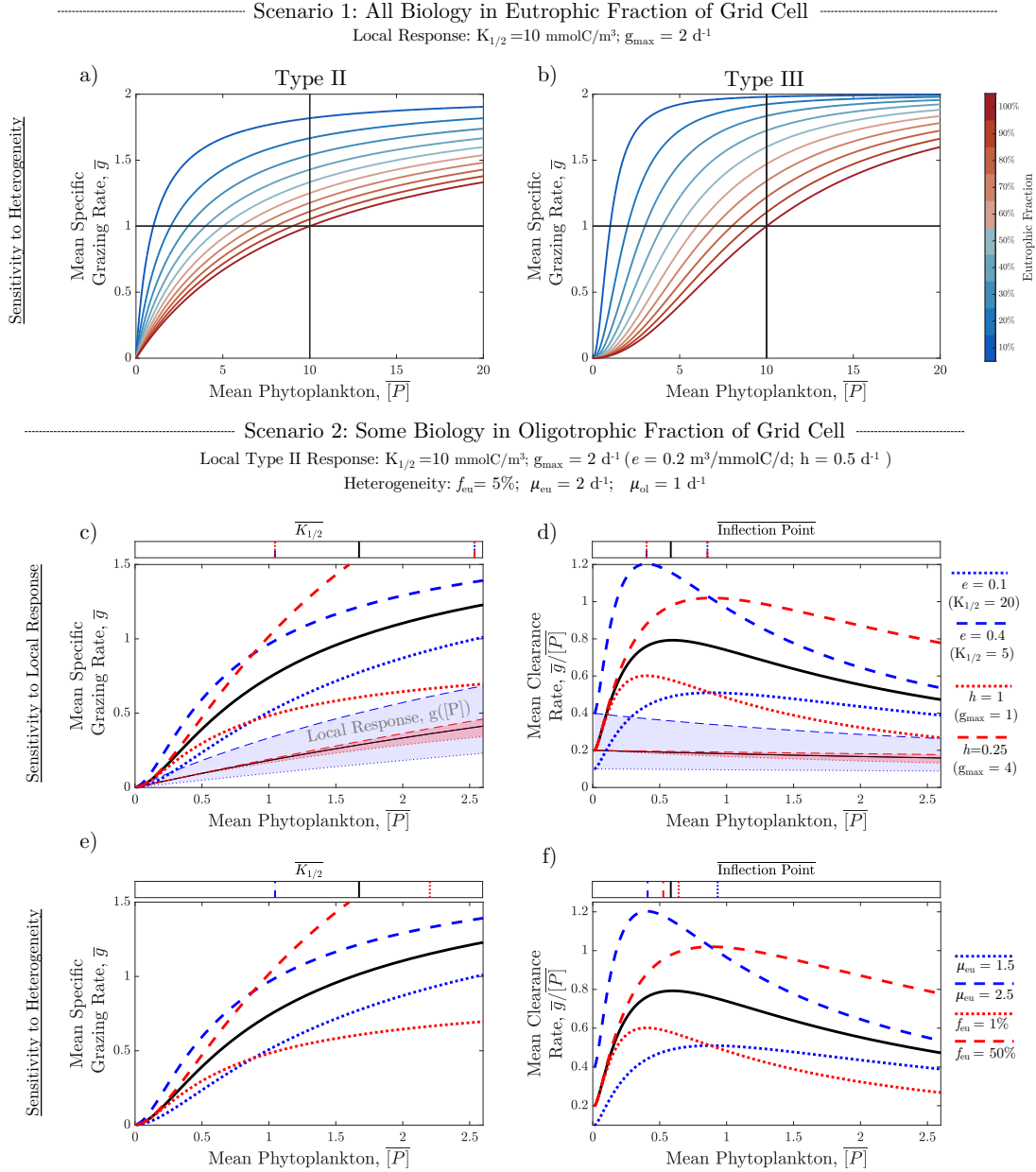


Figure 7. Influence of sub-grid scale heterogeneity. The spatially-averaged, apparent mean functional response is plotted for several simple examples of sub-grid scale heterogeneity. **a,b.** shows what happens if a **a.** type II or **b.** III local functional response is used but biological activity is consolidated in some fraction (see colorbar) of the grid cell, with nothing in the remaining fraction. Note, the darkest red line ($f_{eu}=1$) is equivalent to the local response. **c-f.** show what happens to **c,e.** the mean functional response and **d,f.** mean clearance rates (solid black lines) when the same local type II response is used but some phyto- and zooplankton growth is permitted in the oligotrophic fraction of the grid cell, but at a slower rate. Red and blue lines show the sensitivity of the mean functional response to changes in **c,d.** the local response parameters and **e,f.** degree of sub-grid scale heterogeneity. The sensitivity of the local response is shaded in the background of **c & d.** Above each subplot, the location of the half saturation concentration and inflection point of the mean response is noted with the corresponding line style.

1056 of $0.01 \text{ mmolC}/m^3$, then grows exponentially at a rate of $2 d^{-1}$ in the eutrophic frac-
 1057 tion and $1 d^{-1}$ in the oligotrophic fraction. Zooplankton biomass is still assumed pro-
 1058 portional to phytoplankton. The eutrophic fraction of the grid cell is now assumed to
 1059 be 5% and the local grazing response is a Type II disk response with $K_{1/2} = 10$ and
 1060 $g_{max} = 2$. We find that even though all zooplankton graze locally with a type II re-
 1061 sponse (**Fig. 7c; thin black line**), $\overline{g([P])}$ exhibits upward concavity at low $\overline{[P]}$ (**Fig.**
 1062 **7c; solid black line**), akin to a type III response. This is even clearer when looking at
 1063 mean clearance rates ($\overline{g}/\overline{[P]}$). Unlike local clearance rates (**Fig. 7d; thin black line**)
 1064 which decreases monotonically, mean clearance rates (**Fig. 7d; solid black line**) ini-
 1065 tially increase, providing the same stabilizing influence as the type III response (**Sec.**
 1066 **3**). Note, however, $\overline{g([P])}$ is a fundamentally different mathematical curve than the stan-
 1067 dard type III response. Its apparent mean half saturation constant ($\overline{K}_{1/2} = 1.7$) is sub-
 1068 stantially lower than that of the local response ($K_{1/2} = 10$) and unlike the standard type
 1069 III response, $\overline{K}_{1/2}$ is no longer the location of the inflection point of the curve (i.e. tran-
 1070 sition from upward to downward concavity) which occurs before $\overline{K}_{1/2}$ in $\overline{g([P])}$ (**Fig. 7b,c**)

1071 Still, it is important that the mean of many individual type II responses can yield
 1072 the upward concavity associated with a type III response when averaged across hetero-
 1073 geneously distributed plankton populations. Similar to the conditions described by Mo-
 1074 rozov (2010), the reason for this is that phytoplankton growth is associated with a shift
 1075 in the relative distribution of zooplankton into the eutrophic region where they can graze
 1076 faster. This hinges on the assumption that more predators are likely to reside where there
 1077 is more prey, but is agnostic to the specific mechanisms for how they get there (i.e. pop-
 1078 ulation growth vs. migration) or their time scales. In turn, as the mean grid cell phy-
 1079 toplankton concentration increases, the mean specific grazing rate will increase multi-
 1080 plicatively with an increasing proportion of zooplankton grazing at increasingly fast spe-
 1081 cific rates, leading to an exponential increase at low $\overline{[P]}$. Note that there was no upward
 1082 concavity in Scenario 1, despite sub-grid scale heterogeneity. This is because the pro-
 1083 portion of zooplankton grazing in the eutrophic region did not increase with $\overline{[P]}$. There-
 1084 fore, for upward concavity to exist in the mean state, we must assume that zooplank-
 1085 ton are more likely to aggregate where there is more prey, either because they are grow-
 1086 ing faster locally or because they are actively migrating. This is ecologically and numeri-
 1087 cally important because it can provide dynamical stability and refuge for low phytoplank-
 1088 ton concentrations without invoking any associated change in the assumptions about the
 1089 foraging behavior of individual zooplankton.

1090 The exact shape of $\overline{g([P])}$ is a function of the local response (**Fig. 7c,d**) and the
 1091 evolution of sub-grid scale plankton distributions (**Fig. 7e,f**). Alterations to the local
 1092 capture rate (**Fig. 7c,d; blue lines**) and consumption time (red lines) show how mod-
 1093 ifications to the local response (thin lines; shaded area) do not directly translate to the
 1094 mean response (thick lines). As with the local response, increasing (decreasing) capture
 1095 rates (ϵ) or decreasing consumption times (h) both decrease the half saturation concen-
 1096 tration, $\overline{K}_{1/2}$, of the mean response. However, $\overline{g([P])}$ is much more sensitive to changes
 1097 in the consumption time compared to the local response. For the most part, \overline{g} is more
 1098 sensitive to changes in h (thick red lines) than ϵ (thick blue lines) at low $\overline{[P]}$, despite hardly
 1099 any change to \overline{g} at low $\overline{[P]}$ (thin, shaded lines). This is possible because even at low $\overline{[P]}$,
 1100 heterogeneously distributed zooplankton are predominately grazing at or near satura-
 1101 tion in small patches, where rates of consumption, not capture, drive grazing.

1102 Altering the distribution of plankton (**Fig. 7e,f**), either by increasing population
 1103 growth rates in the eutrophic fraction (blue lines) or by changing the size of the eutrophic
 1104 fraction (red lines) also has a pronounced effect on the shape of $\overline{g([P])}$. Increasing (de-
 1105 creasing) μ_{eu} has a qualitatively similar effect to decreasing (increasing) $K_{1/2}$ because
 1106 it increases the disparity between eutrophic and oligotrophic plankton populations. Re-
 1107 ducing sub-grid scale heterogeneity by increasing (decreasing) the size of f_{eu} lowers the
 1108 inflection point and decreases (increases) the extent of upward concavity. At $f_{eu} = 50\%$,

1109 $\overline{g([P])}$ begins to qualitatively resemble $g([P])$, but $\overline{K_{1/2}}$ is still 45% lower than $K_{1/2}$. Even
 1110 when we reduced heterogeneity to 20% of the grid cell growing just 10% faster, $\overline{g([P])}$
 1111 still exhibited increasing clearance rates at very low $[P]$. Together, it is clear that the
 1112 shape of $\overline{g([P])}$ can dramatically diverge from $g([P])$ but the degree to which it does is
 1113 sensitive to the degree of sub-grid scale heterogeneity.

1114 Considering that the evolution of natural plankton distributions is much more com-
 1115 plex than modelled here, a more sophisticated analysis is required to understand which
 1116 curve best represents their mean state and how varying degrees of patchiness would mod-
 1117 ify the concavity and parameters of the apparent response. However, provided there is
 1118 sufficient heterogeneity, when compared to the local response, it appears that $\overline{g([P])}$ should
 1119 have faster capture rates, be more sensitive to consumption rates at low $[P]$, and exhibit
 1120 a larger degree of upward concavity at low $[P]$, than does $g([P])$.

1121 7 Recommendations for modellers

1122 7.1 Functional Response Choice for Single-Prey Grazing

1123 Biogeochemical models are largely split in their use of a type II (or Ivlev) or type
 1124 III functional response (**Table 3**). Of all 70 surveyed grazing formulations, 23 use a type
 1125 III and 35 use a type II (12 used an Ivlev). Of those that graze with a single-prey re-
 1126 sponse the split is 13, 16, and 14 for type III, II and Ivlev, respectively. Mathematically,
 1127 when parameterized with analogous parameters (i.e. the same $K_{1/2}$ and g_{max}), a type
 1128 II response is more likely to exert stronger grazing pressure (**Sec. 5.2**) and produce dy-
 1129 namically unstable solutions (**Sec. 3, 5.3**) due to its downward concavity at low prey
 1130 concentrations. Ecologically, the most realistic option likely depends on the model con-
 1131 figuration and the system being simulated.

1132 Models that use a type III response typically benefit from its stabilizing proper-
 1133 ties (Gentleman & Neuheimer, 2008). For example, many models require a type III re-
 1134 sponse to produce realistic blooms rather than unstable oscillations (Hernández-García
 1135 & López, 2004; Malchow et al., 2005; Morozov, 2010; Truscott & Brindley, 1994; Truscott
 1136 et al., 1994). This is because the stabilizing properties of a type III response prevent the
 1137 extinction of a very small wintertime phytoplankton seed population, while starving the
 1138 zooplankton community, subsequently permitting a bloom at the onset of rapid changes
 1139 in bottom-up growth conditions during spring stratification (Behrenfeld et al., 2013; Evans
 1140 & Parslow, 1985).

1141 However, stability is not a sufficient justification to use a type III response. Nat-
 1142 ural systems have been observed to exhibit dynamical instabilities (McCauley & Mur-
 1143 doch, 1987) and even when they do not, there are many plausible stabilizing factors that
 1144 could dominate unstable predator-prey dynamics to dampen limit cycles and stabilize
 1145 the system (C. A. Edwards et al., 2000; Gentleman & Neuheimer, 2008). For example,
 1146 only half the parameter combinations tested here actually produced a dynamically un-
 1147 stable solution when using a type II response (**Fig. 6a,g**). This was because the desta-
 1148 bilizing influence of the predator-prey dynamics (i.e. the First Order Stability; **Fig. 6c,i**)
 1149 was weak enough to be dominated by the stabilizing influence of nutrient limitation, which
 1150 buffers changes in the phytoplankton population by decreasing (increasing) division rates
 1151 when the population is large (small). Similarly, other factors such as quadratic zooplank-
 1152 ton mortality can create a negative feedback loop which stabilizes population dynam-
 1153 ics despite the destabilizing influence of the grazing formulation. Selecting a response
 1154 type that does not represent the true destabilizing (or stabilizing) influence of natural
 1155 predator-prey dynamics could lead parameter optimization schemes to underestimating
 1156 (or overestimating) the influence other stabilizing processes. Thus, the stabilizing influ-
 1157 ence of a type III response is only preferable if it is ecologically representative of the predator-
 1158 prey dynamics it seeks to represent.

1159 Ecologically, there is disagreement on whether a type II (Hansen et al., 1997; Hirst
 1160 & Bunker, 2003; Jeschke et al., 2004) or type III (Chow-Fraser & Sprules, 1992; Frost,
 1161 1975; Gismervik & Andersen, 1997; Sarnelle & Wilson, 2008) response is more appro-
 1162 priate to represent the grazing behavior of individual zooplankton. Laboratory dilution
 1163 experiments are often better fit empirically by a type II response (Hansen et al., 1997;
 1164 Hirst & Bunker, 2003), while a type III response is typically justified by more complex
 1165 behavior, such as changes in prey refugia, (Wang, Morrison, Singh, & Weiss, 2009), preda-
 1166 tor learning (Holling, 1965; van Leeuwen, Jansen, & Bright, 2007), predator effort, (Gis-
 1167 mervik, 2005), or prey switching (Gentleman et al., 2003; Oaten & Murdoch, 1975; Uye,
 1168 1986). Unfortunately, this behavior is difficult to replicate in a lab (Leising et al., 2003)
 1169 and large-scale field experiments are challenging and rare.

1170 However, despite uncertainty in the true behavior of individual zooplankton in their
 1171 natural environment, it is possible that a type III response is more representative of their
 1172 mean state, even if individuals are assumed to exhibit a sub-grid scale type II response
 1173 (**Sec. 6**). If plankton are assumed to be heterogeneously distributed and the relative dis-
 1174 tribution of the zooplankton community is assumed to co-vary with the phytoplankton
 1175 population, then the mean grazing rate should generally exhibit some degree of upward
 1176 concavity (**Fig. 6c,e**) and exert an associated stabilizing influence on mean population
 1177 dynamics (**Fig. 6d, f**). Morozov (2010) found similar upward concavity in the mean dy-
 1178 namics of vertically distributed plankton and argued for a Holling type III response. How-
 1179 ever, it should be clarified that while the mean behavior of heterogeneous systems likely
 1180 does exhibit some upward concavity, the function is not exactly sigmoidal in shape and
 1181 is mathematically distinct from a type III disk response. Importantly, the mean response
 1182 becomes destabilizing (i.e. downwardly concave) well before the half-saturation concen-
 1183 tration of the local response (**Fig. 6a,b**) and varies with the degree of sub-grid scale het-
 1184 erogeneity (**Fig. 6c,d**).

1185 In turn, the most ecologically justifiable response type may depend on the resolu-
 1186 tion of the model in question. For high resolution, small scale models, or those repre-
 1187 senting systems known to be well-mixed, a type II response is likely to be the most ap-
 1188 propriate. Even though laboratory incubations are unlikely to translate directly to zoo-
 1189 plankton feeding behavior in the ocean (Dutkiewicz et al., 2015), there are insufficient
 1190 observations of individual zooplankton grazing with type III dynamics to justify ignor-
 1191 ing the many empirical estimates of a type II response (Hansen et al., 1997; Hirst & Bunker,
 1192 2003). However, a type III response may be a more ecologically realistic representation
 1193 of the mean state of many zooplankton grazing locally with a type II response on a highly
 1194 heterogeneous phytoplankton population. Therefore, for coarse-resolution, large-scale mod-
 1195 els (e.g. global earth system models) a type III response may be more appropriate.

1196 **7.2 Parameter Scheme for Single-Prey Grazing**

1197 Throughout the literature, the type II and type III functional responses appear in
 1198 two distinct, but mathematically equivalent, forms (**Table 2**): the disk parameter scheme
 1199 (**eq. 17, 24**) (Adjou et al., 2012; Fasham, 1995; Law et al., 2017; Oke et al., 2013; Schar-
 1200 tau & Oschlies, 2003b) and the Michaelis–Menten parameter scheme (**eq. 19, 25**) (Au-
 1201 mont & Bopp, 2006; Dutkiewicz et al., 2015; Hauck et al., 2013; Le Quéré et al., 2016;
 1202 Moore et al., 2013; Stock, Dunne, & John, 2014; Totterdell, 2019; Vichi et al., 2007). Both
 1203 schemes can describe identical response curves given the right parameterization, but use
 1204 different information to do so. The disk scheme uses ecologically meaningful quantities
 1205 to mechanistically determine how grazing rates vary in well-mixed systems. On the other
 1206 hand, the Michaelis–Menten scheme is an empirical description of the shape of the curve,
 1207 with no theoretical basis.

1208 This distinction would be irrelevant if we had infinite computational power to sam-
 1209 ple all parameter combinations and a complete set of observations with which to eval-

1210 uate their skill. In this scenario, the optimized cost function (i.e. the agreement between
 1211 model output and observations) would converge on a mathematically and dynamically
 1212 identical functional response curve, regardless of whether a Michaelis–Menten or disk scheme
 1213 was used. However, modern biogeochemical models include dozens of different param-
 1214 eters, many with a large spread of plausible values (e.g. **Section 4**), and computational
 1215 limitations exist (Matear, 1995; Neelin, Bracco, Luo, McWilliams, & Meyerson, 2010).
 1216 Therefore, it is not practical (or often possible) to test all parameter combinations. More-
 1217 over, these models are heavily under constrained (Doney, 1999; Matear, 1995; Schartau
 1218 et al., 2017; Ward et al., 2010), meaning there are insufficient observations to identify
 1219 a unique parameter set as optimal. Instead, parameter optimization routines must use
 1220 limited information to decide which parameter sets to test to converge on the optimal
 1221 solution. Unfortunately, these routines can yield the right result for the wrong reason
 1222 (T. R. Anderson, 2005) and/or identify local rather than global minima/maxima (Ward
 1223 et al., 2010), meaning that they do not always converge on the ‘true’ optimal solution.

1224 Whether or not a specific search routine is successful (or computationally efficient)
 1225 is often determined by the path it uses to search the parameter space. Often the direc-
 1226 tion of this path is determined by back-computing the partial derivatives of the cost func-
 1227 tion with respect to each parameter and then moving down the steepest gradient in pa-
 1228 rameter space (Kane et al., 2011). In other algorithms, movement across parameter space
 1229 is more stochastic, mimicking the evolutionary process by selecting for optimal genomes
 1230 (i.e. parameter sets) from a population of initial estimates and passing on their param-
 1231 eters (sometimes with mutations) to future ‘generations’ (Falls et al., 2022). Either way,
 1232 if search schemes are ‘pointed’ in the wrong direction, say by a partial with a large mag-
 1233 nitude or a mutation with strong fitness, then they may take much longer to compute
 1234 or, worse, never converge on the ‘true’ optimal solution. It is therefore important to con-
 1235 sider the influence of individual parameters on the model solution, as they can help steer
 1236 parameter search routines.

1237 Although g_{max} and $K_{1/2}$ in a Michaelis–Menten scheme and g_{max} and ϵ (or ϵ_c) in
 1238 a disk scheme form the same basis, they are fundamentally different parameters. Thus,
 1239 their partials with respect to the functional response, model solution, and cost function
 1240 will be different, meaning they could point search algorithms in different directions. There-
 1241 fore, even though it is plausible for an optimization scheme to converge on the same func-
 1242 tional response regardless of parameter scheme (particularly in simpler models), it would
 1243 be prudent to use the parameter scheme with partials that most accurately represent real-
 1244 ity. This would presumably be more likely to ‘point’ in the ‘right’ direction and thus
 1245 converge on the ‘true’ optimal solution in the most efficient manner. Thus it is useful
 1246 to consider how the partials of both parameter schemes compare with what we would
 1247 expect ecologically.

1248 The most notable difference between the influence of the individual parameters of
 1249 the functional response is that independent changes to g_{max} have a much more pronounced
 1250 influence on the shape of $g([P])$ at low $[P]$ in the Michaelis–Menten scheme (**Section**
 1251 **5.1, 5.2**). This is because changing g_{max} in a Michaelis–Menten scheme implicitly changes
 1252 the initial slope of the response curve (i.e. ϵ), while changing g_{max} in a disk scheme con-
 1253 serves the value of ϵ , but instead modifies the half saturation concentration (i.e. $K_{1/2}$)
 1254 (**Section 2**). In turn, phytoplankton population growth, which is most sensitive to graz-
 1255 ing at low concentrations, is much more responsive to changes to g_{max} in a Michaelis–Menten
 1256 scheme than in a disk scheme, leading to entirely different model dynamics (**Section 5.3**).
 1257 Therefore, the partial derivative of the cost function with respect to g_{max} could point
 1258 the search algorithm in entirely different directions depending on which parameter scheme
 1259 is used. The question is which direction is most ecologically realistic, or more specifically,
 1260 should zooplankton specific grazing rates at saturation be related to those when food is
 1261 scarce? We suggest that the answer depends on the system being simulated.

1262 If the system in question is well-mixed, then it is reasonable to assume it gener-
 1263 ally conforms to the assumptions that underlie the disk parameter scheme and classic
 1264 Holling-style predator-prey dynamics. In this case there should be no relationship
 1265 between grazing rates at very low and very high prey concentrations. This is because
 1266 grazing is limited by capture rates (ϵ) when food is scarce versus consumption times ($h =$
 1267 $1/g_{max}$) when food is replete and these are assumed to be two physiologically distinct
 1268 processes. Thus, a disk scheme will yield the theoretically correct partial with respect
 1269 to g_{max} , in that it has fairly little influence on the model solution, particularly in oligo-
 1270 trophic (i.e low $[P]$) regions. The disk scheme has the added advantage of a strong theo-
 1271 retical basis, which allows modellers to directly prescribe biologically meaningful quan-
 1272 tities. In general, this is the simplest way to reduce confusion amongst biologists and mod-
 1273 ellers and ensure that trait-based relationships are correctly parameterized between func-
 1274 tional groups (see **Section 4**).

1275 However, the theoretical integrity of the disk response may be limited to well-mixed
 1276 systems and not necessarily represent the mean state of a patchy ocean, which coarse
 1277 global models must implicitly average over. In **Section 6**, we demonstrated how when
 1278 averaged across a patchy grid cell, decreasing local zooplankton consumption times can
 1279 substantially increase the grid cell mean grazing rate at low mean $[P]$, without actually
 1280 influencing how zooplankton graze locally at low local $[P]$, where grazing rates remain
 1281 dominated by capture rates (**Fig. 7c**). This is possible because a greater proportion of
 1282 zooplankton are grazing at a prey density closer to saturation than the grid cell mean,
 1283 which is diluted by large swaths of oligotrophic water, would suggest. In other words,
 1284 the partial derivative of the apparent mean functional response with respect to g_{max} is
 1285 qualitatively more consistent with that of a Michaelis–Menten rather than disk param-
 1286 eter scheme. In this case, the empirical nature of the Michaelis–Menten scheme is ad-
 1287 vantageous, as it is not constrained by mechanistic underpinning of the disk response, al-
 1288 lowing the individual influence of each parameter to capture a combination of the local
 1289 grazing dynamics (as governed by the disk parameters) as well as the time-evolving sub-
 1290 grid scale distribution of zooplankton and phytoplankton. Therefore, when modelling
 1291 the mean state of a sufficiently heterogeneous region, it may be more appropriate to use
 1292 a Michaelis–Menten parameter scheme.

1293 Additionally, another potential advantage of the Michaelis–Menten scheme is that
 1294 population dynamics are more sensitive to proportional changes in its parameters, com-
 1295 pared to the disk parameters, particularly for a type III response (**Section 5.2**). This
 1296 is predominately because ϵ_c implicitly varies with the square of $K_{1/2}$ in a Michaelis-Menten
 1297 scheme ($\epsilon_c = \frac{g_{max}}{K_{1/2}^2}$). In turn, the disk scheme is less sensitive to its parameterization,
 1298 meaning it requires a larger range of parameters to be tested to cover the same range
 1299 of solutions. For example, a conservative range of observed ϵ_c values, from $.0001-1 \frac{m^6}{mmolC^2d}$,
 1300 can span $K_{1/2} \frac{mmolC}{m^3}$ values from 1-100 at a fixed g_{max} (see contours on **Fig. 2**). The
 1301 trade off is increased precision in the disk scheme; however, the overwhelming lack of con-
 1302 sensus on what these parameters actually are (**Section 4**), especially for the mean state
 1303 of the entire ocean (Moriarty et al., 2013; Moriarty & O’Brien, 2012), suggests that it
 1304 is more valuable to consider a wider, but lower resolution, set of parameters to avoid in-
 1305 advertently constraining the parameter space, rather than trying to focus on an impos-
 1306 sibly exact value. For example, the parameter search used by Schartau and Oschlies (2003a),
 1307 who use a disk scheme to represent the mean state of relatively coarse grid cells, chose
 1308 both parameter values at the boundary of their search space, suggesting a wider range
 1309 might have found a better solution. Practically speaking, this problem could be addressed
 1310 by careful conversion. Modellers using a disk scheme could sub sample a wider set of coarser
 1311 resolution ϵ_c values in optimization search schemes; however, modellers must select a search
 1312 range for dozens, if not hundreds, of parameters, and are less likely to mistakenly con-
 1313 strain the parameter space if using a Michaelis-Menten scheme, which has a narrower
 1314 range of realistic parameters and more intuitive units.

1315 Together, the mechanistic and empirical nature of the disk and Michaelis-Menten
 1316 parameter schemes respectively can be used intentionally to the modellers' advantage,
 1317 depending on whether they are trying to represent mechanistically the behavior of zoo-
 1318 plankton in a well-mixed system or represent empirically the mean state of grazing at
 1319 the mean phytoplankton concentration of a patchy grid cell. Thus a disk scheme can be
 1320 used in smaller-scale, higher-resolution models, in which the biological attributes of zoo-
 1321 plankton are relatively well understood. This allows known, measured values, of ϵ and
 1322 h to be directly prescribed and reduces the chance of inadvertently mis-parameterizing
 1323 their relationship in a Michaelis-Menten scheme. However, a Michaelis-Menten scheme
 1324 may be more appropriate to represent the mean state of a patchy ocean in larger-scale,
 1325 lower-resolution models, in which the true parameter values are not well known. This
 1326 affords the empirical flexibility to account for differences in the system as a whole, not
 1327 just the local dynamics. This may allow parameter optimization routines to search more
 1328 efficiently for the 'true' apparent mean response, which is necessarily an empirical re-
 1329 lationship averaged over the effects of many distinct processes, including local grazing
 1330 behavior rates and any processes that modify plankton distributions (e.g. zooplankton
 1331 migration, sub-mesoscale nutrient enhancement).

1332 7.3 Parameter Search Range for Single-Prey Grazing

1333 Given the uncertainty in empirically estimated parameter values, it is necessary to
 1334 select what range of parameters to test in optimization routines. Although there is a high
 1335 degree of variability in all parameter values (**Fig. 3; Table 3**), there is more uncertainty
 1336 in the correct value of $K_{1/2}$, or associated attack rates in a disk scheme. Compared to
 1337 $K_{1/2}$, the value of g_{max} is better constrained by size (**Sec. 4.1**), more consistent between
 1338 models and observations (**Sec. 4.2**), and less influential on driving phytoplankton pop-
 1339 ulation dynamics (**Section 5.2**). In turn, parameter search schemes should favor test-
 1340 ing a larger range of $K_{1/2}$ values than g_{max} values when resource limited. However, it
 1341 is reasonable to ask how large a range is appropriate, lest implicitly imposing ecologi-
 1342 cally unrealistic prey capture rates or selecting values of fringe functional groups to rep-
 1343 resent the mean state. However, there are insufficient empirical, ecological, and math-
 1344 ematical arguments to heavily restrict the range of grazing parameters, and $K_{1/2}$ val-
 1345 ues as low as $0.1 \left(\frac{mmolC}{m^3}\right)$ and as high as $100 \left(\frac{mmolC}{m^3}\right)$ should be considered.

1346 Empirically, reported estimates of $K_{1/2}$ and g_{max} fit to a type II response function
 1347 by Hansen et al. (1997) and Hirst and Bunker (2003) combine to yield a range of ϵ that
 1348 spans 4 orders of magnitude, from .003 to $10 \frac{m^3}{mmolC d}$ (**Section 3.1; Fig. 2**). Moreover,
 1349 if a type III response had been assumed, $K_{1/2}$ estimates would remain similar while the
 1350 range of ϵ_c would increase to nearly 7 orders of magnitude, from .00001 to $21 \frac{m^6}{mmolC^2 d}$,
 1351 or roughly 1 order of magnitude slower and 3 orders of magnitude faster than the range
 1352 tested in the parameter optimization search of Schartau and Oschlies (2003a) ($0.00056 <$
 1353 $\epsilon_c < .0364$). At the species level, the range of plausible $K_{1/2}$ values appears largely un-
 1354 constrained by empirical estimates of ϵ_c .

1355 Ecologically, we do not have a firm understanding of how a myriad of complex in-
 1356 teractions combine across innumerable zooplankton species and evolve over time to yield
 1357 a reasonable approximation of the mean state. For instance, juvenile zooplankton have
 1358 faster metabolic rates (Clerc, Aumont, & Bopp, 2021) and graze with $K_{1/2}$ an order of
 1359 magnitude smaller than adults (Hirst & Bunker, 2003; Richardson & Verheye, 1998), sug-
 1360 gesting the apparent $K_{1/2}$ of the community could be substantially lower during spawn-
 1361 ing. On the other hand, most applications of the functional response assume an instan-
 1362 taneous response between increasing prey and faster grazing rates, while in reality there
 1363 is likely a longer acclimation time as predators adapt to new conditions (Mayzaud & Poulet,
 1364 1978). Explicitly including acclimation times can destabilize the response in even the most
 1365 stable configurations (i.e. type III, quadratic mortality; Gentleman and Neuheimer (2008)).
 1366 However, one might consider implicitly including them by using larger $K_{1/2}$ values than

1367 found in dilution experiments, suggesting that the zooplankton community is always adapted
 1368 to a lower prey density than present. This could be useful for modelling bloom initia-
 1369 tion, where time scales of prey accumulation are similar to that of predator acclimation
 1370 (1-6 days), but fails to capture dynamics accurately at steady state or during bloom de-
 1371 cline. Additionally, filter feeding meso- and macrozooplankton, such as salps and larvaceans,
 1372 are typically common in low chlorophyll waters and have a much smaller $K_{1/2}$ than eu-
 1373 phausiids and copepods that graze in high chlorophyll waters (Hansen et al., 1997; Hirst
 1374 & Bunker, 2003). If species with slower $K_{1/2}$ values dominate in more productive ecosys-
 1375 tems, such that $K_{1/2}$ increases with chlorophyll (Chen et al., 2014), that would effectively
 1376 raise the apparent global mean $K_{1/2}$ value. In turn, the community-wide $K_{1/2}$ value prob-
 1377 ably varies spatially and temporally depending on the zooplankton community present
 1378 and whether it is dominated by juveniles or adults, such that the mean state of a pop-
 1379 ulation with shifting age and species distributions could have an apparent $K_{1/2}$ value
 1380 much different than any individual within.

1381 Mathematically, it is not just the ecosystem complexity that is poorly resolved in
 1382 models, but also its spatial heterogeneity. If the phytoplankton density the average zoo-
 1383 plankton experiences is larger than the grid cell mean, which is averaged across many
 1384 square kilometers of implicitly less productive water (J. Campbell, 1995; Druon et al.,
 1385 2019) then the $K_{1/2}$ value of the mean response will appear much lower than the actual
 1386 grazing rate of the zooplankton (**Fig. 7a, b**). This further increases the range of pos-
 1387 sible $K_{1/2}$ values below even the fastest prey capture rates inferred from dilution exper-
 1388 iments with homogeneous phytoplankton concentrations.

1389 Although the full range of empirically observed $K_{1/2}$ values ($0.1\text{-}71\text{ mmolC}/\text{m}^3$)
 1390 is likely to be larger than the range of plausible values to represent the mean state, this
 1391 only applies to the mean value of individuals in well-mixed incubation experiments. Un-
 1392 certain ecological complexities and spatial heterogeneity both work to expand the range
 1393 of $K_{1/2}$ values that plausibly could represent the mean state of myriad dynamics across
 1394 a patchy ocean. We thus recommend testing a broad range of $K_{1/2}$ values, particularly
 1395 on the lower end, in parameter optimization routines.

1396 **7.4 Recommendations for future models**

1397 Biogeochemical models are evolving to include an increasingly complex represen-
 1398 tation of phytoplankton, including dozens of functional groups (Follows & Dutkiewicz,
 1399 2011), variable composition (Smith et al., 2015), and the flexibility to adapt to chang-
 1400 ing environments (Anugerahanti, Kerimoglu, & Smith, 2021). With these changes should
 1401 come similar advances in the representation of zooplankton and zooplankton grazing. No-
 1402 tably, it is essential that the mean parameterization of the zooplankton field be able to
 1403 respond to the evolving phytoplankton field to reflect that different zooplankton eat dif-
 1404 ferent things and do so at different rates. Already, many modern models include mul-
 1405 tiple zooplankton functional groups (Le Qu  r   et al., 2016; Stock et al., 2020) and multiple-
 1406 prey grazing response (Aumont et al., 2015; Yool et al., 2021). Moving forward, it is im-
 1407 portant to consider how insights into the single-prey response extend to more complex
 1408 grazing schemes.

1409 One concern is that the Michaelis-Menten form of the multi-prey response is over
 1410 parameterized, requiring an extra parameter to describe the same equation as the cor-
 1411 responding disk form (Gentleman et al., 2003). In turn, the parameterization of the im-
 1412 plied single-prey response cannot be prescribed directly, but becomes a function of prey
 1413 preference and the preference weighted $K_{1/2}$ used for bulk ingestion. If not careful, this
 1414 could confuse the interpretation of parameter values and lead modellers to prescribe un-
 1415 intended single-prey dynamics that may imply inappropriate relationships between func-
 1416 tional groups. Despite recommendations to parameterize the attributes of the multi-prey
 1417 response directly with a disk scheme (Gentleman et al., 2003), 29 of 30 multi-prey graz-

1418 ing formulations surveyed here used a Michaelis-Menten scheme, and none used a disk
 1419 (**Table 2**). To help assess if this has influenced their parameterization, we compared the
 1420 implied single-prey response of micro- and meso-zooplankton grazing on their preferred
 1421 prey and compared them to those directly parameterized in single-prey formulations. In
 1422 multi-prey formulations the median implied single-prey $K_{1/2}$ value decreases from 7.7
 1423 in microzooplankton to 4.0 in mesozooplankton. This is qualitatively inconsistent with
 1424 the observed relationship (**Table 3**) as well as single-prey formulations in which the median
 1425 $K_{1/2}$ value increases from 2.4 in microzooplankton to 9.1 in mesozooplankton. This
 1426 suggests the models using a Michaelis-Menten multi-prey response may be implying un-
 1427 intended allometric relationships between functional groups grazing in their optimal con-
 1428 ditions and highlights that modeller’s who select a Michaelis-Menten multi-prey response
 1429 must carefully consider the implied relationships between parameter values.

1430 Finally, future work is needed to better assess the shape of the apparent mean func-
 1431 tional response, both in-situ and in models. Higher resolution general circulation mod-
 1432 els are known to modify local biogeochemical distributions via their representation of nu-
 1433 trient transport (Harrison, Long, Lovenduski, & Moore, 2018). While it is intractable
 1434 to estimate the apparent mean functional response exactly, it would be useful to better
 1435 understand its attributes with deliberate experiments designed to empirically average
 1436 across high resolution biogeochemical models into coarser grid-cells representative of stan-
 1437 dard global earth system models. This may help constrain the functional response curve
 1438 and range of parameter values beyond what has been observed for individual well-mixed
 1439 zooplankton, and lead to a better understanding of how to represent unresolved processes
 1440 across the entire system that could influence sub-grid scale heterogeneity.

1441 7.5 Implications for other models

1442 We focus on grazing in marine biogeochemical models, but these recommendations
 1443 apply to a much broader range of marine and terrestrial ecological models. Most mod-
 1444 els in marine and terrestrial systems that involve predator-prey interactions use type I,
 1445 type II or type III functional responses. We found that when trying to implicitly repre-
 1446 sent sub-grid scale heterogeneity, a type III (**Section 6.1**) Michaelis-Menten response
 1447 (**Section 6.2**) parameterized with a lower than-expected $K_{1/2}$ value (**Section 6.3**) may
 1448 be a more ecologically realistic way to describe the mean state of patchy predator and
 1449 prey populations, even if individual interactions are best described by a type II disk re-
 1450 sponse, parameterized with higher $K_{1/2}$ values. In the ocean, this would apply to most
 1451 higher trophic levels simulated in size spectrum (Blanchard, Heneghan, Everett, Trebilco,
 1452 & Richardson, 2017; Heneghan et al., 2020), population (Alver et al., 2016), ecosystem
 1453 (Audzijonyte et al., 2019; Butenschön et al., 2016) and fisheries models (Maury, 2010;
 1454 Tittensor et al., 2018, 2021). Fish, for instance aggregate in schools and feed on sparse,
 1455 but consolidated, prey patches. These distributions are in turn reflected in global fish-
 1456 ing effort (Kroodsma et al., 2018). On land, plants and animals are also patchy in time
 1457 and space, with high prey concentrations rare. Most abundance data for marine and ter-
 1458 restrial species are overdispersed and/or have an excess of zeros, implying there is a long
 1459 tail to the right of low abundances (H. Campbell, 2021). The mean state of any of these
 1460 systems is likely best represented by a low- $K_{1/2}$, type III, Michael-Menten response; how-
 1461 ever, the range of possible $K_{1/2}$ considered should increase with the number of unique
 1462 species, interactions, and stages of life history being averaged into individual pools.

1463 On the other hand, well understood interactions in well mixed systems, may be bet-
 1464 ter represented by a type II disk response, provided there is a low amount of implicit av-
 1465 eraging at the species and spatial level. At the species level, this may include models of
 1466 simple systems with fewer species, such as lakes or polar regions rather than rainforests
 1467 or coral reefs, or models of more complex systems, but with many explicitly resolved preda-
 1468 tor groups. At the spatial level, this may include the oligotrophic gyres in the ocean and
 1469 grasslands or boreal forests on the land. Still, modellers should consider how much im-

1470 plicit averaging is baked into their model and consider if it warrants a more empirical
 1471 approach before choosing a mechanistic framework (disk) or response type (II) better
 1472 suited for homogeneously distributed systems.

1473 8 Conclusions

1474 In marine biogeochemical and ecological modelling, the transfer of carbon and nu-
 1475 trients between trophic groups, particularly from phytoplankton to zooplankton via graz-
 1476 ing, is typically represented with one of two functional response curves. However, we find
 1477 that there is little consensus across biogeochemical models regarding: **I**) which response
 1478 type to use (II vs. III); **II**) whether to describe that curve with mechanistic (disk scheme)
 1479 or empirical parameters (Michaelis-Menten scheme); and **III**) what parameter values to
 1480 use.

1481 We examine the single-prey formulation of the functional response in systematic
 1482 detail to provide theoretical clarity, assess the agreement between observed parameters
 1483 and those used in models, examine the sensitivity of the response to its parameteriza-
 1484 tion, and explore how the shape of the curve changes when averaged explicitly over sub-
 1485 grid scale heterogeneity. Considering these issues collectively, we recommend using a type
 1486 II disk response in models with smaller scales, finer resolution, and or well understood
 1487 ecological interactions. However, we suggest that a type III Michaelis-Menten response
 1488 may be more appropriate for models with larger scales, coarser resolution, and more com-
 1489 plex ecological and physical processes implicitly being averaged across. In both scenar-
 1490 ios, a large range of parameter values should be tested in parameter optimization schemes
 1491 as the interquartile range of empirically observed values spans roughly an order of mag-
 1492 nitude for all parameters, and the full range spans 3-4. Moreover, averaging across sub-
 1493 grid scale heterogeneity could lead to $K_{1/2}$ values well below the mean of empirically es-
 1494 timated values obtained from experiments in well-mixed solutions. These recommenda-
 1495 tions are specifically tailored to the single-prey grazing formulation in marine biogeochem-
 1496 ical models, but also apply to any effort to describe the mean state of multiple interac-
 1497 tions across coarse grid cells with populations assumed to have heterogeneous sub-grid
 1498 cell distributions.

1499 Data Access

1500 All Matlab code required to run all four NPZ models and compute the relevant di-
 1501 agnostics from **Section 5** (PO_Rohr_NPZ_Models.m) and run the theoretical experiments
 1502 on sub-grid scale heterogeneity from **Section 6** (PO_Rohr_Subgrid_Heterogeneity.m) is
 1503 hosted on the CSIRO data portal and can be found at <https://doi.org/10.25919/cmn7-1j48>. Please contact tyler.rohr@csiro.au for any further data access inquiries.

1505 Acknowledgments

1506 This research was supported by the Centre for Southern Hemisphere Oceans Research
 1507 (CSHOR), a partnership between the Commonwealth Scientific and Industrial Research
 1508 Organisation (CSIRO) and the Qingdao National Laboratory for Marine Science, and
 1509 the Australian Antarctic Program Partnership through the Australian Government's Antarc-
 1510 tic Science Collaboration Initiative.

1511 References

- 1512 Adjou, M., Bendtsen, J., & Richardson, K. (2012, January). Modeling the influence
 1513 from ocean transport, mixing and grazing on phytoplankton diversity. *Ecologi-
 1514 cal Modelling*, 225, 19–27. doi: 10.1016/j.ecolmodel.2011.11.005
 1515 Aksnes, D., & EGGE, J. (1991, February). A Theoretical Model for Nutrient Uptake

- 1516 in Phytoplankton. *Marine Ecology-Progress Series*, 70, 65–72. doi: 10.3354/
1517 meps070065
- 1518 Aldebert, C., & Stouffer, D. (2018, December). Community dynamics and sensi-
1519 tivity to model structure: towards a probabilistic view of process-based model
1520 predictions. *Journal of The Royal Society Interface*, 15, 20180741. doi:
1521 10.1098/rsif.2018.0741
- 1522 Alver, M. O., Broch, O. J., Melle, W., Bagoien, E., & Slagstad, D. (2016). Val-
1523 idation of an Eulerian population model for the marine copepod *Calanus*
1524 *finmarchicus* in the Norwegian Sea. *Journal of Marine Systems*, C(160),
1525 81–93. Retrieved 2021-08-10, from [https://www.infona.pl//resource/
1526 bwmeta1.element.elsevier-ccc8cb9c-f8aa-31bb-9e36-b87db0d09727](https://www.infona.pl//resource/bwmeta1.element.elsevier-ccc8cb9c-f8aa-31bb-9e36-b87db0d09727) doi:
1527 10.1016/j.jmarsys.2016.04.004
- 1528 Anderson, T., Gentleman, W. C., & Sinha, B. (2010, October). Influence of graz-
1529 ing formulations on the emergent properties of a complex ecosystem model
1530 in a global ocean general circulation model. *Progress In Oceanography*, 87,
1531 201–213. doi: 10.1016/j.pocean.2010.06.003
- 1532 Anderson, T. R. (2005, November). Plankton functional type modelling: Running
1533 before we can walk? *Journal of Plankton Research*, 27(11), 1073–1081. (Pub-
1534 lisher: Oxford Academic) doi: 10.1093/plankt/fbi076
- 1535 Anugerahanti, P., Kerimoglu, O., & Smith, S. (2021, July). Enhancing Ocean Bio-
1536 geochemical Models With Phytoplankton Variable Composition. *Frontiers in*
1537 *Marine Science*, 8. doi: 10.3389/fmars.2021.675428
- 1538 Archibald, K. M., Siegel, D. A., & Doney, S. C. (2019). Modeling the Impact of Zoo-
1539 plankton Diel Vertical Migration on the Carbon Export Flux of the Biological
1540 Pump. *Global Biogeochemical Cycles*, 33(2), 181–199. Retrieved 2022-02-03,
1541 from <https://onlinelibrary.wiley.com/doi/abs/10.1029/2018GB005983>
1542 doi: 10.1029/2018GB005983
- 1543 Audzijonyte, A., Pethybridge, H., Porobic, J., Gorton, R., Kaplan, I., & Fulton,
1544 E. A. (2019). Atlantis: A spatially explicit end-to-end marine ecosystem model
1545 with dynamically integrated physics, ecology and socio-economic modules.
1546 *Methods in Ecology and Evolution*, 10(10), 1814–1819. Retrieved 2021-11-
1547 09, from [https://onlinelibrary.wiley.com/doi/abs/10.1111/2041-210X
1548 .13272](https://onlinelibrary.wiley.com/doi/abs/10.1111/2041-210X.13272) (eprint: [https://onlinelibrary.wiley.com/doi/pdf/10.1111/2041-
1549 210X.13272](https://onlinelibrary.wiley.com/doi/pdf/10.1111/2041-210X.13272)) doi: 10.1111/2041-210X.13272
- 1550 Aumont, O., & Bopp, L. (2006). Globalizing Results from Ocean in Situ Iron Fertil-
1551 ization Studies. *Global Biogeochemical Cycles*, 20(2). (tex.copyright: Copyright
1552 2006 by the American Geophysical Union.) doi: 10.1029/2005GB002591
- 1553 Aumont, O., Ethé, C., Tagliabue, A., Bopp, L., & Gehlen, M. (2015, August).
1554 PISCES-v2: An ocean biogeochemical model for carbon and ecosystem studies.
1555 *Geoscientific Model Development*, 8. doi: 10.5194/gmd-8-2465-2015
- 1556 Bandara, K., Varpe, , Wijewardene, L., Tverberg, V., & Eiane, K. (2021).
1557 Two hundred years of zooplankton vertical migration research. *Biolog-
1558 ical Reviews*, 96(4), 1547–1589. Retrieved 2021-11-09, from [https://
1559 onlinelibrary.wiley.com/doi/abs/10.1111/brv.12715](https://onlinelibrary.wiley.com/doi/abs/10.1111/brv.12715) (eprint:
1560 <https://onlinelibrary.wiley.com/doi/pdf/10.1111/brv.12715>) doi: 10.1111/
1561 brv.12715
- 1562 Beardsell, A., Gravel, D., Berteaux, D., Gauthier, G., Clermont, J., Careau, V., ...
1563 Bêty, J. (2021). Derivation of Predator Functional Responses Using a Mech-
1564 anistic Approach in a Natural System. *Frontiers in Ecology and Evolution*, 9,
1565 115. Retrieved 2021-09-23, from [https://www.frontiersin.org/article/
1566 10.3389/fevo.2021.630944](https://www.frontiersin.org/article/10.3389/fevo.2021.630944) doi: 10.3389/fevo.2021.630944
- 1567 Behrenfeld, M. J., Doney, S. C., Lima, I., Boss, E. S., & Siegel, D. A. (2013).
1568 Annual cycles of ecological disturbance and recovery underlying the
1569 subarctic Atlantic spring plankton bloom. *Global Biogeochemi-
1570 cal Cycles*, 27(2), 526–540. Retrieved 2022-03-08, from <https://>

- 1571 onlinelibrary.wiley.com/doi/abs/10.1002/gbc.20050 (_eprint:
1572 <https://onlinelibrary.wiley.com/doi/pdf/10.1002/gbc.20050>) doi: 10.1002/
1573 gbc.20050
- 1574 Blanchard, J. L., Heneghan, R. F., Everett, J. D., Trebilco, R., & Richardson, A. J.
1575 (2017, March). From Bacteria to Whales: Using Functional Size Spectra to
1576 Model Marine Ecosystems. *Trends in Ecology & Evolution*, 32(3), 174–186.
1577 doi: 10.1016/j.tree.2016.12.003
- 1578 Brander, K. M. (2007, December). Global fish production and climate change. *Pro-
1579 ceedings of the National Academy of Sciences*, 104(50), 19709–19714. doi: 10
1580 .1073/pnas.0702059104
- 1581 Butenschön, M., Clark, J., Aldridge, J. N., Allen, J. I., Artioli, Y., Blackford, J.,
1582 ... Torres, R. (2016, April). ERSEM 15.06: a generic model for marine
1583 biogeochemistry and the ecosystem dynamics of the lower trophic levels.
1584 *Geoscientific Model Development*, 9(4), 1293–1339. Retrieved 2021-08-
1585 10, from <https://gmd.copernicus.org/articles/9/1293/2016/> doi:
1586 10.5194/gmd-9-1293-2016
- 1587 Campbell, H. (2021). The consequences of checking for zero-inflation
1588 and overdispersion in the analysis of count data. *Methods in Ecology
1589 and Evolution*, 12(4), 665–680. Retrieved 2021-11-09, from [https://
1590 onlinelibrary.wiley.com/doi/abs/10.1111/2041-210X.13559](https://onlinelibrary.wiley.com/doi/abs/10.1111/2041-210X.13559) (_eprint:
1591 <https://onlinelibrary.wiley.com/doi/pdf/10.1111/2041-210X.13559>) doi:
1592 10.1111/2041-210X.13559
- 1593 Campbell, J. (1995, August). The lognormal distribution as a model for bio-optical
1594 variability in the sea. *Journal of Geophysical Research Atmospheres*, 100. doi:
1595 10.1029/95JC00458
- 1596 Caperon, J. (1967). Population Growth in Micro-Organisms Limited by
1597 Food Supply. *Ecology*, 48(5), 715–722. Retrieved 2022-04-01, from
1598 <https://onlinelibrary.wiley.com/doi/abs/10.2307/1933728> (_eprint:
1599 <https://onlinelibrary.wiley.com/doi/pdf/10.2307/1933728>) doi: 10.2307/
1600 1933728
- 1601 Chen, B., Laws, E. A., Liu, H., & Huang, B. (2014). Estimating microzooplank-
1602 ton grazing half-saturation constants from dilution experiments with non-
1603 linear feeding kinetics. *Limnology and Oceanography*, 59(3), 639–644. doi:
1604 10.4319/lo.2014.59.3.0639
- 1605 Chenillat, F., Rivière, P., & Ohman, M. D. (2021, May). On the sensitivity of plank-
1606 ton ecosystem models to the formulation of zooplankton grazing. *PLOS ONE*,
1607 16(5), e0252033. Retrieved 2021-05-27, from [https://journals.plos.org/
1608 plosone/article?id=10.1371/journal.pone.0252033](https://journals.plos.org/plosone/article?id=10.1371/journal.pone.0252033) doi: 10.1371/journal
1609 .pone.0252033
- 1610 Chow-Fraser, P., & Sprules, W. G. (1992, April). Type-3 functional response in lim-
1611 netic suspension-feeders, as demonstrated by in situ grazing rates. *Hydrobiolo-
1612 gia*, 232(3), 175–191. doi: 10.1007/BF00013703
- 1613 Christian, J. R., Denman, K. L., Hayashida, H., Holdsworth, A. M., Lee, W. G.,
1614 Riche, O. G. J., ... Swart, N. C. (2021, October). Ocean biogeochemistry in
1615 the Canadian Earth System Model version 5.0.3: CanESM5 and CanESM5-
1616 CanOE. *Geoscientific Model Development Discussions*, 1–68. Retrieved
1617 2022-01-05, from [https://gmd.copernicus.org/preprints/gmd-2021-327/
1618 doi: 10.5194/gmd-2021-327](https://gmd.copernicus.org/preprints/gmd-2021-327/)
- 1619 Clerc, C., Aumont, O., & Bopp, L. (2021, July). Should we account for mesozoo-
1620 plankton reproduction and ontogenetic growth in biogeochemical modeling?
1621 *Theoretical Ecology*. Retrieved 2021-07-20, from [https://doi.org/10.1007/
1622 s12080-021-00519-5](https://doi.org/10.1007/s12080-021-00519-5) doi: 10.1007/s12080-021-00519-5
- 1623 Denny, M. (2014). Buzz Holling and the Functional Response. *The Bulletin of the
1624 Ecological Society of America*, 95(3), 200–203. Retrieved 2021-09-23, from
1625 <https://onlinelibrary.wiley.com/doi/abs/10.1890/0012-9623-95.3.200>

- (eprint: <https://esajournals.onlinelibrary.wiley.com/doi/pdf/10.1890/0012-9623-95.3.200>) doi: 10.1890/0012-9623-95.3.200
- 1626
1627
1628 Doney, S. C. (1999). Major challenges confronting marine biogeochemical modeling.
1629 *Global Biogeochemical Cycles*, 13(3), 705–714. doi: 10.1029/1999GB900039
- 1630 Druon, J.-N., Hélaouët, P., Beaugrand, G., Fromentin, J.-M., Palialexis, A., &
1631 Hoepffner, N. (2019, March). Satellite-based indicator of zooplankton dis-
1632 tribution for global monitoring. *Scientific Reports*, 9(1), 4732. Retrieved
1633 2021-11-09, from <https://www.nature.com/articles/s41598-019-41212-2>
1634 (Bandiera_abtest: a Cc_license_type: cc_by Cg_type: Nature Research Jour-
1635 nals Number: 1 Primary_atype: Research Publisher: Nature Publishing Group
1636 Subject_term: Ecological modelling;Ecosystem ecology;Marine biology Sub-
1637 ject_term_id: ecological-modelling;ecosystem-ecology;marine-biology) doi:
1638 10.1038/s41598-019-41212-2
- 1639 Dunn, R. P., & Hovel, K. A. (2020, January). Predator type influences the fre-
1640 quency of functional responses to prey in marine habitats. *Biology Letters*,
1641 16(1), 20190758. (Publisher: Royal Society) doi: 10.1098/rsbl.2019.0758
- 1642 Dutkiewicz, S., Hickman, A. E., Jahn, O., Gregg, W. W., Mouw, C. B., & Follows,
1643 M. J. (2015, July). Capturing optically important constituents and properties
1644 in a marine biogeochemical and ecosystem model. *Biogeosciences*, 12(14),
1645 4447–4481. doi: 10.5194/bg-12-4447-2015
- 1646 Edwards, A. M., & Yool, A. (2000, June). The role of higher predation in plank-
1647 ton population models. *Journal of Plankton Research*, 22(6), 1085–1112. Re-
1648 trieved 2022-04-04, from <https://doi.org/10.1093/plankt/22.6.1085> doi:
1649 10.1093/plankt/22.6.1085
- 1650 Edwards, C., Powell, T., & Batchelder, H. (2000, January). The stability of an
1651 NPZ model subject to realistic levels of vertical mixing. *Journal of Marine Re-*
1652 *search*, 58. doi: 10.1357/002224000321511197
- 1653 Edwards, C. A., Batchelder, H. P., & Powell, T. M. (2000, September). Modeling
1654 microzooplankton and macrozooplankton dynamics within a coastal upwelling
1655 system. *Journal of Plankton Research*, 22(9), 1619–1648. (Publisher: Oxford
1656 Academic) doi: 10.1093/plankt/22.9.1619
- 1657 Evans, G. T., & Parslow, J. S. (1985, January). A Model of Annual Plankton Cy-
1658 cles. *Biological Oceanography*, 3(3), 327–347. (Publisher: Taylor & Francis)
1659 doi: 10.1080/01965581.1985.10749478
- 1660 Eyring, V., Bony, S., Meehl, G. A., Senior, C. A., Stevens, B., Stouffer, R. J., &
1661 Taylor, K. E. (2016, May). Overview of the Coupled Model Intercomparison
1662 Project Phase 6 (CMIP6) experimental design and organization. *Geoscientific*
1663 *Model Development*, 9(5), 1937–1958. (Publisher: Copernicus GmbH) doi:
1664 10.5194/gmd-9-1937-2016
- 1665 Falls, M., Bernardello, R., Castrillo, M., Acosta, M., Lloret, J., & Galí, M. (2022,
1666 July). Use of genetic algorithms for ocean model parameter optimisation: a
1667 case study using PISCES-v2_rc for North Atlantic particulate organic carbon.
1668 *Geoscientific Model Development*, 15(14), 5713–5737. Retrieved 2022-08-08,
1669 from <https://gmd.copernicus.org/articles/15/5713/2022/> (Publisher:
1670 Copernicus GmbH) doi: 10.5194/gmd-15-5713-2022
- 1671 Fasham, M. J. R. (1995, July). Variations in the seasonal cycle of biological pro-
1672 duction in subarctic oceans: A model sensitivity analysis. *Deep Sea Research*
1673 *Part I: Oceanographic Research Papers*, 42(7), 1111–1149. doi: 10.1016/0967-
1674 -0637(95)00054-A
- 1675 Fasham, M. J. R., Ducklow, H. W., & McKelvie, S. M. (1990, August). A nitrogen-
1676 based model of plankton dynamics in the oceanic mixed layer. *Journal of Ma-*
1677 *rine Research*, 48(3), 591–639. doi: 10.1357/002224090784984678
- 1678 Flato, G., Marotzke, J., Abiodun, B., Braconnot, P., Chou, S. C., Collins, W., . . .
1679 Rummukainen, M. (2013). *Evaluation of climate models*. Cambridge University
1680 Press. (Pages: 741) doi: 10.1017/CBO9781107415324.020

- 1681 Flynn, K. J., & Mitra, A. (2016). Why Plankton Modelers Should Reconsider Using
1682 Rectangular Hyperbolic (Michaelis-Menten, Monod) Descriptions of Predator-
1683 Prey Interactions. *Frontiers in Marine Science*, 3. (Publisher: Frontiers) doi:
1684 10.3389/fmars.2016.00165
- 1685 Follows, M. J., & Dutkiewicz, S. (2011). Modeling Diverse Communities of Marine
1686 Microbes. *Annual Review of Marine Science*, 3(1), 427–451. Retrieved 2022-
1687 04-28, from <https://doi.org/10.1146/annurev-marine-120709-142848>
1688 (_eprint: <https://doi.org/10.1146/annurev-marine-120709-142848>) doi:
1689 10.1146/annurev-marine-120709-142848
- 1690 Franks, P., & Chen, C. (1996, July). Plankton production in tidal fronts: A model of
1691 Georges Bank in summer. *Journal of Marine Research*, 54(4), 631–651. doi: 10
1692 .1357/0022240963213718
- 1693 Franks, P., & Chen, C. (2001, January). A 3-D prognostic numerical model study of
1694 the Georges bank ecosystem. Part II: Biological–Physical model. *Deep Sea Re-
1695 search Part II: Topical Studies in Oceanography*, 48(1), 457–482. doi: 10.1016/
1696 S0967-0645(00)00125-9
- 1697 Franks, P., Wroblewski, J. S., & Flierl, G. R. (1986, April). Behavior of a sim-
1698 ple plankton model with food-level acclimation by herbivores. *Marine Biology*,
1699 91(1), 121–129. doi: 10.1007/BF00397577
- 1700 Frost, B. W. (1972). Effects of Size and Concentration of Food Particles on the
1701 Feeding Behavior of the Marine Planktonic Copepod *Calanus Pacificus*1. *Lim-
1702 nology and Oceanography*, 17(6), 805–815. (tex.copyright: © 1972, by the As-
1703 sociation for the Sciences of Limnology and Oceanography, Inc.) doi: 10.4319/
1704 lo.1972.17.6.0805
- 1705 Frost, B. W. (1975). A threshold feeding behavior in *Calanus pacificus*1. *Limnology
1706 and Oceanography*, 20(2), 263–266. (tex.copyright: © 1975, by the Association
1707 for the Sciences of Limnology and Oceanography, Inc.) doi: 10.4319/lo.1975.20
1708 .2.0263
- 1709 Fussmann, G. F., & Blasius, B. (2005, March). Community response to enrichment
1710 is highly sensitive to model structure. *Biology Letters*, 1(1), 9–12. (Publisher:
1711 Royal Society) doi: 10.1098/rsbl.2004.0246
- 1712 Gentleman, W. C., Leising, A., Frost, B., Strom, S., & Murray, J. (2003, November).
1713 Functional responses for zooplankton feeding on multiple resources: A review
1714 of assumptions and biological dynamics. *Deep Sea Research Part II: Topical
1715 Studies in Oceanography*, 50(22), 2847–2875. doi: 10.1016/j.dsr2.2003.07.001
- 1716 Gentleman, W. C., & Neuheimer, A. B. (2008, November). Functional responses
1717 and ecosystem dynamics: How clearance rates explain the influence of satia-
1718 tion, food-limitation and acclimation. *Journal of Plankton Research*, 30(11),
1719 1215–1231. doi: 10.1093/plankt/fbn078
- 1720 Giske, J., Rosland, R., Berntsen, J., & Fiksen, (1997, February). Ideal free dis-
1721 tribution of copepods under predation risk. *Ecological Modelling*, 95(1), 45–
1722 59. Retrieved 2022-08-04, from [https://www.sciencedirect.com/science/
1723 article/pii/S0304380096000270](https://www.sciencedirect.com/science/article/pii/S0304380096000270) doi: 10.1016/S0304-3800(96)00027-0
- 1724 Gismervik, I. (2005, September). Numerical and functional responses of choreo- and
1725 oligotrich planktonic ciliates. *Aquatic Microbial Ecology*, 40(2), 163–173. doi:
1726 10.3354/ame040163
- 1727 Gismervik, I., & Andersen, T. (1997, October). Prey switching by *Acartia
1728 clausi*: Experimental evidence and implications of intraguild predation as-
1729 sessed by a model. *Marine Ecology Progress Series*, 157, 247–259. doi:
1730 10.3354/meps157247
- 1731 Gross, T., Ebenhöf, W., & Feudel, U. (2004, April). Enrichment and foodchain sta-
1732 bility: The impact of different forms of Predator–Prey interaction. *Journal of
1733 Theoretical Biology*, 227(3), 349–358. doi: 10.1016/j.jtbi.2003.09.020
- 1734 Hajima, T., Watanabe, M., Yamamoto, A., Tatebe, H., Noguchi, M. A., Abe, M.,
1735 ... Kawamiya, M. (2020, May). Development of the MIROC-ES2L Earth

- 1736 system model and the evaluation of biogeochemical processes and feedbacks.
 1737 *Geoscientific Model Development*, 13(5), 2197–2244. Retrieved 2022-03-10,
 1738 from <https://gmd.copernicus.org/articles/13/2197/2020/> (Publisher:
 1739 Copernicus GmbH) doi: 10.5194/gmd-13-2197-2020
- 1740 Hansen, P. J., Bjørnsen, P. K., & Hansen, B. W. (1997). Zooplankton grazing and
 1741 growth: Scaling within the 2-2-Mm body size range. *Limnology and Oceanog-*
 1742 *raphy*, 42(4), 687–704. doi: 10.4319/lo.1997.42.4.0687
- 1743 Hansen, P. J., Bjørnsen, P. K., & Hansen, B. W. (2014, August). Maximum
 1744 ingestion and maximum clearance rate of Zooplankton determined ex-
 1745 perimentally. Retrieved 2021-05-11, from [https://doi.pangaea.de/](https://doi.pangaea.de/10.1594/PANGAEA.834800)
 1746 10.1594/PANGAEA.834800 (Publisher: PANGAEA type: dataset) doi:
 1747 10.1594/PANGAEA.834800
- 1748 Harrison, C. S., Long, M. C., Lovenduski, N. S., & Moore, J. K. (2018, April).
 1749 Mesoscale Effects on Carbon Export: A Global Perspective. *Global Biogeo-*
 1750 *chemical Cycles*, 0(0). doi: 10.1002/2017GB005751
- 1751 Hauck, J., Völker, C., Wang, T., Hoppema, M., Losch, M., & Wolf-Gladrow, D. A.
 1752 (2013). Seasonally different carbon flux changes in the Southern Ocean in
 1753 response to the southern annular mode. *Global Biogeochemical Cycles*, 27(4),
 1754 1236–1245. (tex.copyright: © 2013 The Authors. Global Biogeochemical Cy-
 1755 cles published by Wiley on behalf of the American Geophysical Union.) doi:
 1756 10.1002/2013GB004600
- 1757 Heneghan, R. F., Everett, J. D., Sykes, P., Batten, S. D., Edwards, M., Takahashi,
 1758 K., ... Richardson, A. J. (2020, November). A functional size-spectrum
 1759 model of the global marine ecosystem that resolves zooplankton composition.
 1760 *Ecological Modelling*, 435, 109265. Retrieved 2021-08-10, from [https://](https://www.sciencedirect.com/science/article/pii/S0304380020303355)
 1761 www.sciencedirect.com/science/article/pii/S0304380020303355 doi:
 1762 10.1016/j.ecolmodel.2020.109265
- 1763 Herman, A. W., & Platt, T. (1983, January). Numerical modelling of diel carbon
 1764 production and zooplankton grazing on the Scotian shelf based on observa-
 1765 tional data. *Ecological Modelling*, 18(1), 55–72. Retrieved 2022-08-04, from
 1766 <https://www.sciencedirect.com/science/article/pii/0304380083900753>
 1767 doi: 10.1016/0304-3800(83)90075-3
- 1768 Hernández-García, E., & López, C. (2004, September). Sustained plankton blooms
 1769 under open chaotic flows. *Ecological Complexity*, 1(3), 253–259. doi: 10.1016/
 1770 j.ecocom.2004.05.002
- 1771 Hirst, A. G., & Bunker, A. J. (2003). Growth of marine planktonic cope-
 1772 pods: Global rates and patterns in relation to chlorophyll a, temperature,
 1773 and body weight. *Limnology and Oceanography*, 48(5), 1988–2010. doi:
 1774 10.4319/lo.2003.48.5.1988
- 1775 Holling, C. S. (1959a, May). The Components of Predation as Revealed by a Study
 1776 of Small-Mammal Predation of the European Pine Sawfly1. *The Canadian Ent-*
 1777 *omologist*, 91(5), 293–320. (Publisher: Cambridge University Press) doi: 10
 1778 .4039/Ent91293-5
- 1779 Holling, C. S. (1959b, July). Some Characteristics of Simple Types of Predation
 1780 and Parasitism. *The Canadian Entomologist*, 91(7), 385–398. doi: 10.4039/
 1781 Ent91385-7
- 1782 Holling, C. S. (1965). The Functional Response of Predators to Prey Density and its
 1783 Role in Mimicry and Population Regulation. *The Memoirs of the Entomologi-*
 1784 *cal Society of Canada*, 97(S45), 5–60. doi: 10.4039/entm9745fv
- 1785 Ivlev, V. (1961). *Experimental ecology of the feeding of fishes*. New Haven: Yale Uni-
 1786 versity Press.
- 1787 Jeschke, J. M., Kopp, M., & Tollrian, R. (2004). Consumer-food systems: Why type
 1788 I functional responses are exclusive to filter feeders. *Biological Reviews*, 79(2),
 1789 337–349. doi: 10.1017/S1464793103006286
- 1790 Kane, A., Moulin, C., Thiria, S., Bopp, L., Berrada, M., Tagliabue, A., ... Bad-

- 1791 ran, F. (2011, June). Improving the parameters of a global ocean biogeo-
 1792 chemical model via variational assimilation of in situ data at five time series
 1793 stations. *Journal of Geophysical Research*, *116*(C6), C06011. Retrieved
 1794 2022-08-08, from <http://doi.wiley.com/10.1029/2009JC006005> doi:
 1795 10.1029/2009JC006005
- 1796 Kroodsma, D. A., Mayorga, J., Hochberg, T., Miller, N. A., Boerder, K., Fer-
 1797 retti, F., . . . Worm, B. (2018, February). Tracking the global foot-
 1798 print of fisheries. *Science*, *359*(6378), 904–908. Retrieved 2021-06-01,
 1799 from <https://science.sciencemag.org/content/359/6378/904> doi:
 1800 10.1126/science.aao5646
- 1801 Lampert, W. (2005, April). Vertical distribution of zooplankton: density dependence
 1802 and evidence for an ideal free distribution with costs. *BMC Biology*, *3*(1), 10.
 1803 Retrieved 2022-08-04, from <https://doi.org/10.1186/1741-7007-3-10> doi:
 1804 10.1186/1741-7007-3-10
- 1805 Lancelot, C., Spitz, Y., Gypens, N., Ruddick, K., Becquevort, S., Rousseau, V., . . .
 1806 Billen, G. (2005, March). Modelling diatom and Phaeocystis blooms and nutri-
 1807 ent cycles in the Southern Bight of the North Sea: The MIRO model. *Marine*
 1808 *Ecology Progress Series*, *289*, 63–78. doi: 10.3354/meps289063
- 1809 Laufkötter, C., Vogt, M., Gruber, N., Aita-Noguchi, M., Aumont, O., Bopp, L., . . .
 1810 Völker, C. (2015, December). Drivers and Uncertainties of Future Global Ma-
 1811 rine Primary Production in Marine Ecosystem Models. *Biogeosciences*, *12*(23),
 1812 6955–6984. doi: 10.5194/bg-12-6955-2015
- 1813 Law, R. M., Ziehn, T., Matear, R. J., Lenton, A., Chamberlain, M. A., Stevens,
 1814 L. E., . . . Vohralik, P. F. (2017, July). The carbon cycle in the Australian
 1815 Community Climate and Earth System Simulator (ACCESS-ESM1) – Part 1:
 1816 Model description and pre-industrial simulation. *Geoscientific Model Develop-*
 1817 *ment*, *10*(7), 2567–2590. doi: 10.5194/gmd-10-2567-2017
- 1818 Laws, E. A., Falkowski, P. G., Smith, W. O., Ducklow, H., & McCarthy, J. J.
 1819 (2000). Temperature Effects on Export Production in the Open Ocean. *Global*
 1820 *Biogeochemical Cycles*, *14*(4), 1231–1246. (tex.copyright: Copyright 2000 by
 1821 the American Geophysical Union.) doi: 10.1029/1999GB001229
- 1822 Leising, A. W., Gentleman, W. C., & Frost, B. W. (2003, November). The thresh-
 1823 old feeding response of microzooplankton within Pacific high-nitrate low-
 1824 chlorophyll ecosystem models under steady and variable iron input. *Deep Sea*
 1825 *Research Part II: Topical Studies in Oceanography*, *50*(22), 2877–2894. doi:
 1826 10.1016/j.dsr2.2003.07.002
- 1827 Le Quéré, C., Buitenhuis, E. T., Moriarty, R., Alvain, S., Aumont, O., Bopp, L., . . .
 1828 Vallina, S. M. (2016, July). Role of Zooplankton Dynamics for Southern Ocean
 1829 Phytoplankton Biomass and Global Biogeochemical Cycles. *Biogeosciences*,
 1830 *13*(14), 4111–4133. doi: 10.5194/bg-13-4111-2016
- 1831 Long, M. C., Moore, J. K., Lindsay, K., Levy, M., Doney, S. C., Luo, J. Y., . . .
 1832 Sylvester, Z. T. (2021). Simulations With the Marine Biogeochemistry Li-
 1833 brary (MARBL). *Journal of Advances in Modeling Earth Systems*, *13*(12),
 1834 e2021MS002647. Retrieved 2022-01-05, from [https://onlinelibrary.wiley](https://onlinelibrary.wiley.com/doi/abs/10.1029/2021MS002647)
 1835 [.com/doi/abs/10.1029/2021MS002647](https://onlinelibrary.wiley.com/doi/abs/10.1029/2021MS002647) doi: 10.1029/2021MS002647
- 1836 Lotka, A. J. (1910, March). Contribution to the Theory of Periodic Reactions. *The*
 1837 *Journal of Physical Chemistry*, *14*(3), 271–274. (Publisher: American Chemi-
 1838 cal Society) doi: 10.1021/j150111a004
- 1839 Malchow, H., Hilker, F. M., Sarkar, R. R., & Brauer, K. (2005, November). Spa-
 1840 tiotemporal patterns in an excitable plankton system with lysogenic viral
 1841 infection. *Mathematical and Computer Modelling*, *42*(9), 1035–1048. doi:
 1842 10.1016/j.mcm.2004.10.025
- 1843 Matear, R. J. (1995, July). Parameter optimization and analysis of ecosystem mod-
 1844 els using simulated annealing: A case study at Station P. *Journal of Marine*
 1845 *Research*, *53*(4), 571–607. doi: 10.1357/0022240953213098

- 1846 Maury, O. (2010, January). An overview of APECOSM, a spatialized mass balanced
1847 “Apex Predators ECOSystem Model” to study physiologically structured tuna
1848 population dynamics in their ecosystem. *Progress in Oceanography*, 84(1),
1849 113–117. doi: 10.1016/j.pocean.2009.09.013
- 1850 Mayzaud, P., & Poulet, S. A. (1978). The importance of the time factor in the re-
1851 sponse of zooplankton to varying concentrations of naturally occurring particu-
1852 late matter 1. *Limnology and Oceanography*, 23(6), 1144–1154. (textcopyright:
1853 © 1978, by the Association for the Sciences of Limnology and Oceanography,
1854 Inc.) doi: 10.4319/lo.1978.23.6.1144
- 1855 Mayzaud, P., Tirelli, V., Bernard, J. M., & Roche-Mayzaud, O. (1998, June).
1856 The influence of food quality on the nutritional acclimation of the cope-
1857 pod *Acartia clausi*. *Journal of Marine Systems*, 15(1), 483–493. doi:
1858 10.1016/S0924-7963(97)00039-0
- 1859 McCauley, E., & Murdoch, W. W. (1987, January). Cyclic and Stable Populations:
1860 Plankton as Paradigm. *The American Naturalist*, 129(1), 97–121. Retrieved
1861 2021-08-20, from [https://www.journals.uchicago.edu/doi/abs/10.1086/](https://www.journals.uchicago.edu/doi/abs/10.1086/284624)
1862 [284624](https://www.journals.uchicago.edu/doi/abs/10.1086/284624) (Publisher: The University of Chicago Press) doi: 10.1086/284624
- 1863 Menden-Deuer, S., & Lessard, E. J. (2000). Carbon to volume relationships
1864 for dinoflagellates, diatoms, and other protist plankton. *Limnology and*
1865 *Oceanography*, 45(3), 569–579. Retrieved 2022-04-18, from [https://](https://onlinelibrary.wiley.com/doi/abs/10.4319/lo.2000.45.3.0569)
1866 onlinelibrary.wiley.com/doi/abs/10.4319/lo.2000.45.3.0569 (_eprint:
1867 <https://onlinelibrary.wiley.com/doi/pdf/10.4319/lo.2000.45.3.0569>) doi:
1868 10.4319/lo.2000.45.3.0569
- 1869 Michaelis, L., & Menten, M. (1913). Die Kinetik der Invertinwirkung. *Biochem Z*,
1870 49, 333–369.
- 1871 Moloney, C. L., & Field, J. G. (1989). General allometric equations
1872 for rates of nutrient uptake, ingestion, and respiration in plank-
1873 ton organisms. *Limnology and Oceanography*, 34(7), 1290–1299.
1874 Retrieved 2021-04-09, from [https://aslopubs.onlinelibrary](https://aslopubs.onlinelibrary.wiley.com/doi/abs/10.4319/lo.1989.34.7.1290)
1875 [.wiley.com/doi/abs/10.4319/lo.1989.34.7.1290](https://aslopubs.onlinelibrary.wiley.com/doi/abs/10.4319/lo.1989.34.7.1290) (_eprint:
1876 <https://aslopubs.onlinelibrary.wiley.com/doi/pdf/10.4319/lo.1989.34.7.1290>)
1877 doi: <https://doi.org/10.4319/lo.1989.34.7.1290>
- 1878 Monod, J. (1949, October). The growth of bacterial cultures. *Annual Review of Mi-*
1879 *crobiology*, 3(1), 371–394. (Publisher: Annual Reviews) doi: 10.1146/annurev
1880 .mi.03.100149.002103
- 1881 Moore, J. K., Lindsay, K., Doney, S. C., Long, M. C., & Misumi, K. (2013, August).
1882 Marine Ecosystem Dynamics and Biogeochemical Cycling in the Community
1883 Earth System Model [CESM1(BGC)]: Comparison of the 1990s with the 2090s
1884 under the RCP4.5 and RCP8.5 Scenarios. *Journal of Climate*, 26(23), 9291–
1885 9312. doi: 10.1175/JCLI-D-12-00566.1
- 1886 Moriarty, R., Buitenhuis, E. T., Le Quéré, C., & Gosselin, M.-P. (2013, July).
1887 Distribution of known macrozooplankton abundance and biomass in the
1888 global ocean. *Earth System Science Data*, 5(2), 241–257. doi: 10.5194/
1889 [essd-5-241-2013](https://doi.org/10.5194/essd-5-241-2013)
- 1890 Moriarty, R., & O’Brien, T. (2012, September). Mesozooplankton biomass in the
1891 global ocean. *Earth System Science Data Discussions*, 5, 893–919. doi: 10
1892 [.5194/essdd-5-893-2012](https://doi.org/10.5194/essdd-5-893-2012)
- 1893 Morozov, A. (2010). Emergence of Holling type III zooplankton functional response:
1894 Bringing together field evidence and mathematical modelling. *Journal of Theo-*
1895 *retical Biology*, 265(1), 45–54. doi: 10.1016/j.jtbi.2010.04.016
- 1896 Morozov, A., & Arashkevich, E. (2008). Patterns of Zooplankton Functional Re-
1897 sponse in Communities with Vertical Heterogeneity: a Model Study. *Mathe-*
1898 *matical Modelling of Natural Phenomena*, 3(3), 131–148. Retrieved 2022-08-
1899 04, from [https://www.mnnp-journal.org/articles/mnnp/abs/2008/03/](https://www.mnnp-journal.org/articles/mnnp/abs/2008/03/mnnp20083p131/mnnp20083p131.html)
1900 [mnnp20083p131/mnnp20083p131.html](https://www.mnnp-journal.org/articles/mnnp/abs/2008/03/mnnp20083p131/mnnp20083p131.html) (Number: 3 Publisher: EDP Sciences)

- doi: 10.1051/mmnp:2008061
- 1901
1902 Morozov, A., & Arashkevich, E. (2010, January). Towards a correct description
1903 of zooplankton feeding in models: Taking into account food-mediated unsyn-
1904 chronized vertical migration. *Journal of Theoretical Biology*, 262(2), 346–360.
1905 Retrieved 2022-04-21, from [https://www.sciencedirect.com/science/
1906 article/pii/S0022519309004536](https://www.sciencedirect.com/science/article/pii/S0022519309004536) doi: 10.1016/j.jtbi.2009.09.023
- 1907 Morozov, A., Arashkevich, E., Reigstad, M., & Falk-Petersen, S. (2008, Oc-
1908 tober). Influence of spatial heterogeneity on the type of zooplankton
1909 functional response: A study based on field observations. *Deep Sea Re-
1910 search Part II: Topical Studies in Oceanography*, 55(20), 2285–2291. doi:
1911 <https://doi.org/10.1016/j.dsr.2008.05.008>
- 1912 Neelin, J. D., Bracco, A., Luo, H., McWilliams, J. C., & Meyerson, J. E. (2010, De-
1913 cember). Considerations for parameter optimization and sensitivity in climate
1914 models. *Proceedings of the National Academy of Sciences*, 107(50), 21349–
1915 21354. Retrieved 2021-10-13, from [https://www.pnas.org/content/107/50/
1916 21349](https://www.pnas.org/content/107/50/21349) (Publisher: National Academy of Sciences Section: Physical Sciences)
1917 doi: 10.1073/pnas.1015473107
- 1918 Oaten, A., & Murdoch, W. W. (1975, May). Functional Response and Stability in
1919 Predator-Prey Systems. *The American Naturalist*, 109(967), 289–298. (Pub-
1920 lisher: The University of Chicago Press) doi: 10.1086/282998
- 1921 Ohman, M. D. (1990). The Demographic Benefits of Diel Vertical Migration by Zoo-
1922 plankton. *Ecological Monographs*, 60(3), 257–281. (tex.copyright: © 1990 by
1923 the Ecological Society of America) doi: 10.2307/1943058
- 1924 Oke, P. R., Griffin, D. A., Schiller, A., Matear, R. J., Fiedler, R., Mansbridge,
1925 J., ... Ridgway, K. (2013, May). Evaluation of a near-global eddy-
1926 resolving ocean model. *Geoscientific Model Development*, 6, 591–615. doi:
1927 10.5194/gmd-6-591-2013
- 1928 Pearre, S. (2003, February). Eat and run? The hunger/satiation hypothesis in
1929 vertical migration: history, evidence and consequences. *Biological Reviews*,
1930 78(1), 1–79. Retrieved 2022-08-04, from [https://www.cambridge.org/
1931 core/journals/biological-reviews/article/abs/eat-and-run-the
1932 -hungersatiation-hypothesis-in-vertical-migration-history-evidence
1933 -and-consequences/50A1C5DC5D56B93197B31BB386B72CC6](https://www.cambridge.org/core/journals/biological-reviews/article/abs/eat-and-run-the-hungersatiation-hypothesis-in-vertical-migration-history-evidence-and-consequences/50A1C5DC5D56B93197B31BB386B72CC6) (Publisher:
1934 Cambridge University Press) doi: 10.1017/S146479310200595X
- 1935 Peters, R. H., & Downing, J. A. (1984). Empirical analysis of zooplankton
1936 filtering and feeding rates1. *Limnology and Oceanography*, 29(4), 763–
1937 784. Retrieved 2021-04-09, from [https://aslopubs.onlinelibrary
1938 .wiley.com/doi/abs/10.4319/lo.1984.29.4.0763](https://aslopubs.onlinelibrary.wiley.com/doi/abs/10.4319/lo.1984.29.4.0763) (eprint:
1939 <https://aslopubs.onlinelibrary.wiley.com/doi/pdf/10.4319/lo.1984.29.4.0763>)
1940 doi: <https://doi.org/10.4319/lo.1984.29.4.0763>
- 1941 Pierson, J. J., Frost, B. W., & Leising, A. W. (2013, February). Foray foraging
1942 behavior: seasonally variable, food-driven migratory behavior in two calanoid
1943 copepod species. *Marine Ecology Progress Series*, 475, 49–64. Retrieved 2022-
1944 08-04, from <https://www.int-res.com/abstracts/meps/v475/p49-64/> doi:
1945 10.3354/meps10116
- 1946 Ray, S., Sandip, M., Mukherjee, J., M, R., Mandal, S., & Saikia, S. (2011, January).
1947 Body Size versus Rate Parameters of Zooplankton and Phytoplankton: Effects
1948 on Aquatic Ecosystems. In *Zooplankton and Phytoplankton: Types, Charac-
1949 teristics and Ecology* (pp. 219–228). (Journal Abbreviation: Zooplankton and
1950 Phytoplankton: Types, Characteristics and Ecology)
- 1951 Raymont, J. E. G. (2014). *Plankton & Productivity in the Oceans: Volume 1: Phyto-
1952 plankton*. Elsevier.
- 1953 Real, L. A. (1977, March). The Kinetics of Functional Response. *The American Nat-
1954 uralist*, 111(978), 289–300. (Publisher: The University of Chicago Press) doi:
1955 10.1086/283161

- 1956 Real, L. A. (1979). Ecological Determinants of Functional Response. *Ecology*, *60*(3),
1957 481–485. (Publisher: Ecological Society of America) doi: 10.2307/1936067
- 1958 Richardson, A. J., & Verheye, H. M. (1998, January). The relative importance of
1959 food and temperature to copepod egg production and somatic growth in the
1960 southern Benguela upwelling system. *Journal of Plankton Research*, *20*(12),
1961 2379–2399. Retrieved 2021-07-05, from [https://doi.org/10.1093/plankt/](https://doi.org/10.1093/plankt/20.12.2379)
1962 [20.12.2379](https://doi.org/10.1093/plankt/20.12.2379) doi: 10.1093/plankt/20.12.2379
- 1963 Saiz, E., & Calbet, A. (2007). Scaling of feeding in marine calanoid
1964 copepods. *Limnology and Oceanography*, *52*(2), 668–675. Re-
1965 trieved 2021-04-09, from [https://aslopubs.onlinelibrary](https://aslopubs.onlinelibrary.wiley.com/doi/abs/10.4319/lo.2007.52.2.0668)
1966 [.wiley.com/doi/abs/10.4319/lo.2007.52.2.0668](https://aslopubs.onlinelibrary.wiley.com/doi/abs/10.4319/lo.2007.52.2.0668) (eprint:
1967 <https://aslopubs.onlinelibrary.wiley.com/doi/pdf/10.4319/lo.2007.52.2.0668>)
1968 doi: <https://doi.org/10.4319/lo.2007.52.2.0668>
- 1969 Sarnelle, O., & Wilson, A. E. (2008). Type III Functional Response in Daphnia.
1970 *Ecology*, *89*(6), 1723–1732. (text copyright: © 2008 by the Ecological Society
1971 of America) doi: 10.1890/07-0935.1
- 1972 Schartau, M., & Oschlies, A. (2003a, November). Simultaneous data-based opti-
1973 mization of a 1D-Ecosystem model at three locations in the North Atlantic:
1974 Part II—Standing stocks and nitrogen fluxes. *Journal of Marine Research*, *61*,
1975 794–820. doi: 10.1357/002224003322981156
- 1976 Schartau, M., & Oschlies, A. (2003b, November). Simultaneous data-based opti-
1977 mization of a 1D-Ecosystem model at three locations in the North Atlantic:
1978 Part I—Method and parameter estimates. *Journal of Marine Research*, *61*,
1979 765–793. doi: 10.1357/002224003322981147
- 1980 Schartau, M., Wallhead, P., Hemmings, J., Löptien, U., Kriest, I., Krishna, S., ...
1981 Oschlies, A. (2017, March). Reviews and syntheses: Parameter identification in
1982 marine planktonic ecosystem modelling. *Biogeosciences*, *14*(6), 1647–1701. doi:
1983 10.5194/bg-14-1647-2017
- 1984 Scherrer, K. J. N., Harrison, C. S., Heneghan, R. F., Galbraith, E., Bardeen,
1985 C. G., Coupe, J., ... Xia, L. (2020, November). Marine wild-capture
1986 fisheries after nuclear war. *Proceedings of the National Academy of Sci-*
1987 *ences*. (Publisher: National Academy of Sciences Section: Biological Sci-
1988 ences text copyright: Copyright © 2020 the Author(s). Published by PNAS.
1989 <https://creativecommons.org/licenses/by-nc-nd/4.0/>This open access ar-
1990 ticle is distributed under Creative Commons Attribution-NonCommercial-
1991 NoDerivatives License 4.0 (CC BY-NC-ND).) doi: 10.1073/pnas.2008256117
- 1992 Shigemitsu, M., Okunishi, T., Nishioka, J., Sumata, H., Hashioka, T., Aita, M. N.,
1993 ... Yamanaka, Y. (2012). Development of a one-dimensional ecosys-
1994 tem model including the iron cycle applied to the Oyashio region, west-
1995 ern subarctic Pacific. *Journal of Geophysical Research: Oceans*, *117*(C6).
1996 (text copyright: ©2012. American Geophysical Union. All Rights Reserved.)
1997 doi: 10.1029/2011JC007689
- 1998 Smith, S., Pahlow, M., Merico, A., Acevedo-Trejos, E., Yoshikawa, C., Sasai, Y., ...
1999 Honda, M. (2015, April). Flexible Phytoplankton Functional Type (FlexPFT)
2000 model: Size-scaling of traits and optimal growth. *Journal of Plankton Re-*
2001 *search*, *38*, 977–992.
- 2002 Solomon, M. E. (1949). The Natural Control of Animal Populations. *Journal of*
2003 *Animal Ecology*, *18*(1), 1–35. Retrieved 2021-09-23, from [https://www.jstor](https://www.jstor.org/stable/1578)
2004 [.org/stable/1578](https://www.jstor.org/stable/1578) (Publisher: [Wiley, British Ecological Society]) doi: 10
2005 .2307/1578
- 2006 Steele, J. (1974). Stability of plankton ecosystems. In M. B. Usher &
2007 M. H. Williamson (Eds.), *Ecological Stability* (pp. 179–191). Boston, MA:
2008 Springer US. doi: 10.1007/978-1-4899-6938-5_12
- 2009 Steele, J. H., & Henderson, E. W. (1992, January). The role of predation in plank-
2010 ton models. *Journal of Plankton Research*, *14*(1), 157–172. Retrieved 2022-04-

- 2011 04, from [https://doi.org/10.1093/plankt/](https://doi.org/10.1093/plankt/14.1.157)
 2012 14.1.157 doi: 10.1093/plankt/
 2013 Stock, C. A., Dunne, J. P., Fan, S., Ginoux, P., John, J., Krasting, J. P., ... Zadeh,
 2014 N. (2020). Ocean Biogeochemistry in GFDL's Earth System Model 4.1 and
 2015 Its Response to Increasing Atmospheric CO₂. *Journal of Advances in Mod-*
 2016 *eling Earth Systems*, 12(10), e2019MS002043. Retrieved 2022-01-05, from
 2017 <https://onlinelibrary.wiley.com/doi/abs/10.1029/2019MS002043> doi:
 2018 10.1029/2019MS002043
- 2019 Stock, C. A., Dunne, J. P., & John, J. G. (2014, January). Global-scale carbon
 2020 and energy flows through the marine planktonic food web: An analysis with a
 2021 coupled Physical–Biological model. *Progress in Oceanography*, 120, 1–28. doi:
 2022 10.1016/j.pocean.2013.07.001
- 2023 Stock, C. A., Powell, T. M., & Levin, S. A. (2008, November). Bottom–up and
 2024 Top–down forcing in a simple size-structured plankton dynamics model. *Jour-*
 2025 *nal of Marine Systems*, 74(1), 134–152. doi: 10.1016/j.jmarsys.2007.12.004
- 2026 Strom, S. L., & Morello, T. (1998, January). Comparative growth rates and yields of
 2027 ciliates and heterotrophic dinoflagellates. *Journal of Plankton Research*, 20(3),
 2028 571–584. Retrieved 2021-04-09, from <https://doi.org/10.1093/plankt/20.3>
 2029 .571 doi: 10.1093/plankt/20.3.571
- 2030 Taylor, K. E., Stouffer, R. J., & Meehl, G. A. (2012, April). An Overview of CMIP5
 2031 and the Experiment Design. *Bulletin of the American Meteorological Society*,
 2032 93(4), 485–498. (Publisher: American Meteorological Society) doi: 10.1175/
 2033 BAMS-D-11-00094.1
- 2034 Tittensor, D. P., Eddy, T. D., Lotze, H. K., Galbraith, E. D., Cheung, W., Barange,
 2035 M., ... Walker, N. D. (2018, April). A protocol for the intercomparison of
 2036 marine fishery and ecosystem models: Fish-MIP v1.0. *Geoscientific Model*
 2037 *Development*, 11(4), 1421–1442. doi: 10.5194/gmd-11-1421-2018
- 2038 Tittensor, D. P., Novaglio, C., Harrison, C. S., Heneghan, R. F., Barrier, N.,
 2039 Bianchi, D., ... Blanchard, J. L. (2021, October). Next-generation ensemble
 2040 projections reveal higher climate risks for marine ecosystems. *Nature*
 2041 *Climate Change*, 1–9. Retrieved 2021-10-25, from [https://www.nature.com/](https://www.nature.com/articles/s41558-021-01173-9)
 2042 [articles/s41558-021-01173-9](https://www.nature.com/articles/s41558-021-01173-9) doi: 10.1038/s41558-021-01173-9
- 2043 Tjiputra, J. F., Schwinger, J., Bentsen, M., Morée, A. L., Gao, S., Bethke, I., ...
 2044 Schulz, M. (2020, May). Ocean biogeochemistry in the Norwegian Earth Sys-
 2045 tem Model version 2 (NorESM2). *Geoscientific Model Development*, 13(5),
 2046 2393–2431. Retrieved 2022-03-08, from [https://gmd.copernicus.org/](https://gmd.copernicus.org/articles/13/2393/2020/)
 2047 [articles/13/2393/2020/](https://gmd.copernicus.org/articles/13/2393/2020/) doi: 10.5194/gmd-13-2393-2020
- 2048 Totterdell, I. J. (2019, October). Description and evaluation of the Diat-HadOCC
 2049 model v1.0: The ocean biogeochemical component of HadGEM2-ES. *Geoscientific Model Development*, 12(10), 4497–4549. (Publisher: Copernicus GmbH)
 2050 doi: 10.5194/gmd-12-4497-2019
- 2051 Truscott, J. E., & Brindley, J. (1994, September). Ocean plankton populations as
 2052 excitable media. *Bulletin of Mathematical Biology*, 56(5), 981–998. doi: 10
 2053 .1016/S0092-8240(05)80300-3
- 2054 Truscott, J. E., Brindley, J., Brindley, J., & Gray, P. (1994, June). Equilibria,
 2055 stability and excitability in a general class of plankton population models.
 2056 *Philosophical Transactions of the Royal Society of London. Series A: Physical*
 2057 *and Engineering Sciences*, 347(1685), 703–718. (Publisher: Royal Society) doi:
 2058 10.1098/rsta.1994.0076
- 2059 Uye, S. (1986, July). Impact of copepod grazing on the red-tide flagellate *Chat-*
 2060 *tonella antiqua*. *Marine Biology*, 92(1), 35–43. doi: 10.1007/BF00392743
- 2061 van Leeuwen, E., Jansen, V. a. A., & Bright, P. W. (2007). How Population Dy-
 2062 namics Shape the Functional Response in a One-Predator–Two-Prey System.
 2063 *Ecology*, 88(6), 1571–1581. (tex.copyright: © 2007 by the Ecological Society
 2064 of America) doi: 10.1890/06-1335

- 2066 Vichi, M., Pinardi, N., & Masina, S. (2007, January). A generalized model of pelagic
2067 biogeochemistry for the global ocean ecosystem. Part I: Theory. *Journal of*
2068 *Marine Systems*, *64*(1), 89–109. doi: 10.1016/j.jmarsys.2006.03.006
- 2069 Volterra, V. (1927). *Variazioni e fluttuazioni del numero d'individui in specie ani-*
2070 *mali conviventi*. C. Ferrari. (tex.googlebooks: 1ai9PgAACAAJ)
- 2071 Wang, H., Morrison, W., Singh, A., & Weiss, H. H. (2009, June). Modeling inverted
2072 biomass pyramids and refuges in ecosystems. *Ecological Modelling*, *220*(11),
2073 1376–1382. doi: 10.1016/j.ecolmodel.2009.03.005
- 2074 Ward, B. A., Friedrichs, M. A. M., Anderson, T. R., & Oschlies, A. (2010, April).
2075 Parameter optimisation techniques and the problem of underdetermination in
2076 marine biogeochemical models. *Journal of Marine Systems*, *81*(1), 34–43. doi:
2077 10.1016/j.jmarsys.2009.12.005
- 2078 Wirtz, K. W. (2013, January). How fast can plankton feed? Maximum ingestion
2079 rate scales with digestive surface area. *Journal of Plankton Research*, *35*(1),
2080 33–48. Retrieved 2021-04-09, from <https://doi.org/10.1093/plankt/fbs075>
2081 doi: 10.1093/plankt/fbs075
- 2082 Yool, A., Palmiéri, J., Jones, C. G., de Mora, L., Kuhlbrodt, T., Popova, E. E.,
2083 ... Sellar, A. A. (2021, June). Evaluating the physical and biogeochemical
2084 state of the global ocean component of UKESM1 in CMIP6 historical sim-
2085 ulations. *Geoscientific Model Development*, *14*(6), 3437–3472. Retrieved
2086 2022-01-05, from <https://gmd.copernicus.org/articles/14/3437/2021/>
2087 doi: 10.5194/gmd-14-3437-2021